Survey of DC-DC Non-Isolated Topologies for Unidirectional Power Flow in Fuel Cell Vehicles

MAHAJAN SAGAR BHASKAR[1], (Senior Member, IEEE),
VIGNA K. RAMACHANDARAMURTHY[2], (Senior Member, IEEE),
SANJEEVIKUMAR PADMANABAN[3], (Senior Member, IEEE),
FREDE BLAABJERG[4], (Fellow, IEEE), DAN M. IONEL[5], (Fellow, IEEE),
MASSIMO MITOLO[6], (Fellow, IEEE), AND DHAFER ALMAKHLES[1], (Senior Member, IEEE)

[1]Renewable Energy Laboratory (REL), Department of Communications and Networks Engineering, College of Engineering, Prince Sultan University (PSU), Riyadh 11586, Saudi Arabia
[2]Department of Electrical Power Engineering, College of Engineering, Institute of Power Engineering, Universiti Tenaga Nasional, Selangor 43000, Malaysia
[3]Department of Energy Technology, Aalborg University, 6700 Esbjerg, Denmark
[4]Department of Energy Technology, Centre of Reliable Power Electronics (CORPE), Aalborg University, 9220 Aalborg, Denmark
[5]Department of Electrical and Computer Engineering, Power and Energy Institute Kentucky (PEIK), University of Kentucky, Lexington, KY 40506-0046, USA
[6]School of Integrated Design, Engineering and Automation, Irvine Valley College, Irvine, CA 92618, USA

Corresponding authors: Mahajan Sagar Bhaskar (sagar25.mahajan@gmail.com) and Vigna K. Ramachandaramurthy (vigna@uniten.edu.my)

ABSTRACT The automobile companies are focusing on recent technologies such as growing Hydrogen (H_2) and Fuel Cell (FC) Vehicular Power Train (VPT) to improve the Tank-To-Wheel (TTW) efficiency. Benefits, the lower cost, 'Eco' friendly, zero-emission and high-power capacity, etc. In the power train of fuel cell vehicles, the DC-DC power converters play a vital role to boost the fuel cell stack voltage. Hence, satisfy the demand of the motor and transmission in the vehicles. Several DC-DC converter topologies have proposed for various vehicular applications like fuel cell, battery, and renewable energy fed hybrid vehicles etc. Most cases, the DC-DC power converters are viable and cost-effective solutions for FC-VPT with reduced size and increased efficiency. This article describes the state-of-the-art in unidirectional non-isolated DC-DC Multistage Power Converter (MPC) topologies for FC-VPT application. The paper presented the comprehensive review, comparison of different topologies and stated the suitability for different vehicular applications. This article also discusses the DC-DC MPC applications more specific to the power train of a small vehicle to large vehicles (bus, trucks etc.). Further, the advantages and disadvantages pointed out with the prominent features for converters. Finally, the classification of the DC-DC converters, its challenges, and applications for FC technology is presented in the review article as state-of-the-art in research.

INDEX TERMS DC-DC converter, fuel cell vehicles, multistage power converter, non-isolated, power electronics, unidirectional converters, vehicular power train.

I. INTRODUCTION

These days, the fossil fuel system, dwindling to excessive utilization and burning of fossil fuels for the vehicular application, which leads to emission of Green House Gases (CHG) [1]–[6]. Many researchers claim that the Pure Electric Vehicles (PEVs) and the Hybrid Electric Vehicles (HEVs) are the alternative solutions to Internal Combustion Engine (ICE) due to lesser utilization of fossil fuel. However, the PEVs and

The associate editor coordinating the review of this manuscript and approving it for publication was Eklas Hossain.

HEVs are less 'eco' friendly when compared to ICE vehicles if the electricity is generated from coal and other resources to charge the battery. In such cases, CHG emission is high compared to ICE vehicles. Hence, the fuel cell becomes an alternative solution to power electric train vehicles. Both the Fuel Cell Vehicles (FCVs) and HEVs technologies are gaining more attention in research, and they are going to play a vital role for the next decades [7]–[11]. The average temperature of the earth is increasing slowly due to human activities, by transportation, deforestation, etc., responsible for the emission of CHG [12]–[14]. The statistic presented

by the International Energy Agency (IEA) in 2016 states that 37% of the Total Energy Consumption (TEC) of the world is from petroleum, 29% from natural gases, 15% from coal, 9% from nuclear and 10% via renewable energy sources [15]. Estimated that the temperature of the earth's surface increases as early as 2050 if no initiatives were taken to control the present emission rate of CHG. The Energy Information Administration (EIA) anticipated that the transportation sector contributed 55% of the TEC of the world and reported in 2016 [16]. Various policies and schemes like energy taxes on fuel are initiated by many nations to reduce the emission of CHG and to maintain a clean environment. This reason for many researchers throughout the world to find new strategies for power train and develop new energy sources to reduce CHG and to improve the performance of power train of the vehicles [17]–[21]. The power train of Battery Electric Vehicles (BEVs), Hybrid Electric Vehicles (HEVs) and Fuel Cell Vehicles (FCVs) provide a feasible solution to overcome the drawback of ICE power train [22]–[27]. The Fuel Cell Vehicles (FCVs) not only helps to maintain a healthy environment but also reduces the service and operating cost of the vehicles compared to ICE vehicles [28]–[34].

The FCV's and HVEs technologies are overgrowing due to the advancement in Power Electronics (PE) [35]–[38]. Both the FCVs and HEVs offer the cleaner and less emission of CHG, which are the alternative to conventional ICE for the future generation. Both technologies utilize electric energy and PE to drive vehicles [39]–[42]. Onboard fuel cell, hydrogen storage and reformer utilized to drive the FCVs instead of the battery. Whereas, the Fuel Cell Hybrid Electric Vehicles (FCHEVs) are driven by fuel cells along with the batteries.

The power electronic circuits are responsible for the conversion of energy, circulation, control of energy within the power train and as a prime mover for efficient, cost-effective vehicles [43]–[47]. Generation of electrical power from the fuel cell is dependent on the type of fuel cells, the number of stack and size of the fuel cells. The critical working temperature of fuel cells and the type of electrolyte plays the critical parameters to select suitable fuel cells. Because of the characteristics and performance of the fuel cells depend on the operating temperature [48], [49]. Fig. 1 depicts the classification of available fuel cells based on the electrolyte, the power and the working temperature. The Polymer Exchange Membrane or Proton Exchange Membrane Fuel Cell (PEM-FC) are the leading fuel cell technology. These fuel cells generate the electricity by utilizing hydrogen directly from the fuel tank and oxygen from the air, emit only water and heat as the byproduct—the fuel cell vehicles documented as a zero-emission vehicle due to absence of tailpipe pollutant. PEM-FC, Alkaline Fuel Cell (AFC), Zinc-air battery, Phosphoric acid Fuel Cell (PFC), Methanol Fuel Cell (MFC) is suitable for vehicular applications. Among the types of the fuel cell, PEM-FC gaining more popularity due to its high-power density, moderate temperature, low corrosion, regular storage, and robustness against shock and vibration [50]–[58].

Initially, the fuel cells are adapted for slow speed vehicles such as submarine, forklift and industrial handling vehicles. However, nowadays, the fuel cells are also used for high-speed vehicles due to advancement in the power train of FCVs [59]–[61]. Based on the structure of power train, FCVs are classifying into two types; Fuel Cell Electric Vehicles (FCEVs) and Fuel Cell Hybrid Electric Vehicles (FCHEVs). Fig. 2(a) and Fig. 2(b) illustrates the Power train of the FCEVs and FCHEVs with a typical efficiency of each unit. In the power train of FCEVs, batteries or ultra-capacitors are not employing to store the energy and the vehicle operated by only with fuel cells. In case of FCHEVs, the suitable batteries or ultra-capacitors (also called super-capacitor) are being employed by modifying the power train for soft start of the vehicle and improving the performance [61]–[63]. Batteries and super-capacitors are adopted as an auxiliary energy source to support the fuel cell and to satisfy the power demand and supply requirement of the Vehicle Power Train (VPT) [63], [64]. Transfer of energy from the Tank to Wheel (TTW) is dependent on the efficiency of the Power Electronics Converters (PEC) for the VPT [64]. Numerous DC-DC converter topologies proposed for various vehicles (FCEVs, FCHEVs, HEVs and PEVs), renewable energy and electric drive applications [65]–[71]. Most of the DC-DC power converters proposed for renewable energy and electric drive applications also provided an effective solution for FC-VPT technology with the cost, size and efficiency. Thus, the selection of the suitable fuel cells and DC-DC power converters are essential and crucial stage to design efficient, low cost and high-power Fuel Cell Vehicular Power Train (FC-VPT) [72]–[76].

The objective of this article is to present, the state-of-art review of unidirectional non-isolated DC-DC Multistage Power Converter (MPC) topologies for FC-VPT by comparison and application. This paper is organized as sections as follows: The responsibility of power electronics in VPT discussed in the section-II. This section also deals with the classification of DC-DC converter topologies. The conventional multistage DC-DC converter explained in the section-III. Recently proposed MPCs discuss in the section-IV to section-X. Comparison of DC-DC MPC along with its applications, for the low and high-power train, is given by section-XI. The future scenario of a DC-DC converter for the vehicular application elaborated in the section-XII. Finally, the conclusions provided in section-XIII.

II. RESPONSIBILITY OF POWER ELECTRONICS IN FUEL CELL POWER TRAIN AND CLASSIFICATION OF DC-DC CONVERTERS

All the mechanical and hydraulic loads are replaced by electrical loads, to adopt advanced features like air conditioning, power steering, power window, brakes, etc. To achieve, the high efficiency, smart, the highly flexible vehicle with zero-emission along with the flexibility of fuel, safety requirement and for driver comforts, [77]–[80]. Therefore, the power electronics technology plays a viable role in circulating current,
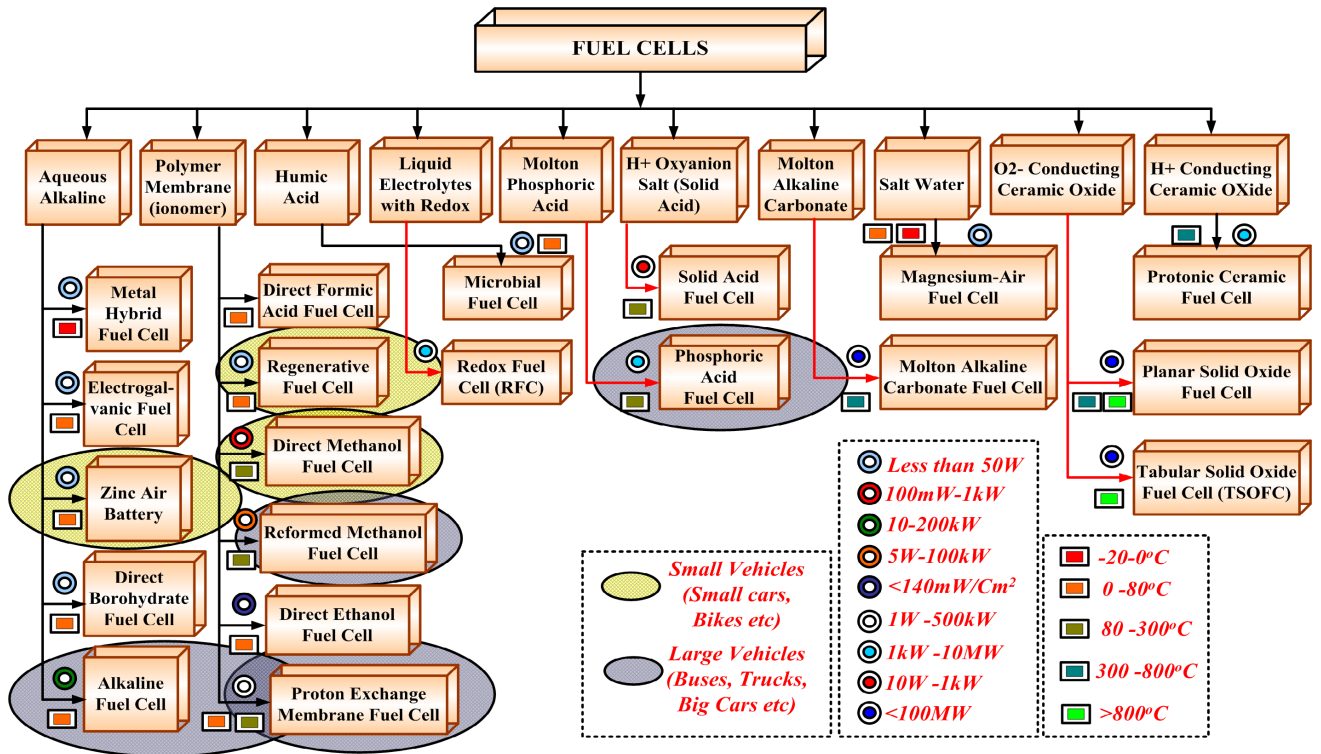
FIGURE 1. Classification of Fuel Cell (based on type of electrolyte, power and working temperature).
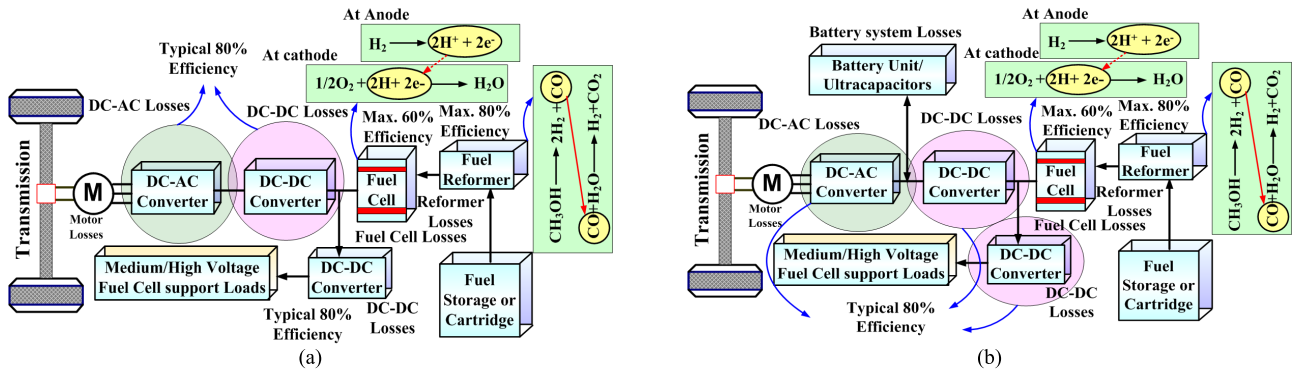

FIGURE 2. Power train of FCVs with efficiency of each unit (a) Fuel cell Electric vehicles (FCEVs) (b) Fuel cell Hybrid Electric vehicles (FCHEVs).

power in VPT and to employ the advanced functionality and luxurious loads in vehicles [81]. In FCVs, the power train and high-power loads supplied by high voltage bus; whereas the low voltage, the bus utilized to supply low power loads. In maximum cases, the battery or ultra-capacitor are using to feed low power loads. For charge and discharge the battery; bidirectional DC-DC converter between the DC-bus and battery is another option. The output voltage of the fuel cell is few, and the number of stacking more fuel cell is not the optimal solution to increase the terminal voltage, to satisfy the demand of power train and luxurious electrical loads [19], [81]. The electrical system of the vehicle becomes more complex and costly due to more electrical

loads. In such cases, the power electronics are the reliable solutions to implement numerous control methods to control, adjustable drives, power electric-mechanical brakes, and electro-hydraulics etc. Apart from this, numerous high power electric actuation and dynamics are adopted to add an extra luxurious feature to the vehicles. Power converter technologies are responsible for managing and for controlling the power flow within the VPT [81].

The Power Electronics Converters (PEC) has classified into four types; DC-DC, DC-AC, AC-DC and AC-AC converters. In fuel cell vehicles, the DC-DC converter used to boost the terminal voltage of the fuel cell and the obtain voltage supply to DC-AC converter to drive the traction

motor. High voltage DC-DC power converter is required with the vehicular application to feed high voltage loads. In literature, various unidirectional multi-stages DC-DC converters addressed with the high gain conversion for various applications including, the hybrid vehicles, renewable energy, battery, and electric drives. These DC-DC converters are also suitable to achieve higher voltage demand of power train [65]–[71].

Fig. 3 shows the classification of PEC to focus on DC-DC converter. DC-DC converters, classified into two main categories; Non-isolated and isolated. A non-isolated converter shares a common ground between input and load or with the floating load. Whereas, in the isolated converter, input and load terminal are electrically isolated [65]. Based on the direction of power flow through the converter, non-isolated and isolated converters classified into two sub-categories; one is unidirectional, and another is bidirectional converters. To provide isolation; the transformer and coupled inductors employed in the power converter. Which increase the conversion ratio of the converter, but also increases the cost, size and losses. Thus, the high frequency is the superior option to reduce the transformer and coupled inductor size. Inside unidirectional converters, the power flow only Input to Output (I to O) direction. However, in case of bidirectional converters, the power flow will be both the direction I to O and O to I [65], [69]. Furthermore, both the unidirectional and bidirectional sub-categories of non-isolated DC-DC converter classified into two sub-categories; one category is a Common Grounded Unidirectional/ Bidirectional Converter (CGUC/CGBC) and Floating Output Unidirectional/Bidirectional Converter (FOUC/FOBC). Further, both the CGUC and FOUC classified into a single stage, multistage and multiphase DC-DC converters.

Fig. 4(a)-(d), the concept of unidirectional non-isolated and isolated with grounded and floating output single-stage DC-DC converters explained in detail. Similarly, in Fig. 4(e)-(h), the concept of unidirectional non-isolated and isolated with grounded and floating output multistage DC-DC converters explained in detail. Magnetic components and energy storing elements used in DC-DC converter along with controlled/ uncontrolled power semiconductor devices and the functionality of the converter depending on the position of elements.

III. STAGES OF MULTISTAGE POWER CONVERTER (CONVENTIONAL DC-DC CONVERTER)

The primary stages of Multistage Power Converter (MPC) classified into three categories; buck, boost and buck-boost converters [82], [83]. The Cuk, Single Ended Primary Inductance Converter (SEPIC) and ZETA converters derived from the hybridization of two conventional converters (addition of two conventional converters). Thus the Cuk, SEPIC and ZETA converter are categorized into MPC [84]–[87]. The conventional DC-DC, Cuk, SEPIC and ZETA converters are not suitable to achieve a high conversion ratio due to

the requirement of high rating components and high duty cycle [88].

The power circuit of the conventional unidirectional common grounded boost, buck and buck-boost converters, depicted in Fig. 5(a)-(c). Whereas the floating output boost, buck, and buck-boost converters, depicted in Fig. 5(d)-(f), respectively. The boost and buck converter provide a non-inverting output voltage, whereas buck-boost converter provides an inverting output voltage. Recently, many DC-DC converters to attain high step-up/down conversion ratio using the front end structure of boost, buck and buck-boost converter are addressed [65], [69]. In the next section, unidirectional non-isolated DC-DC MPC categories, discussed with its sub-classes.

IV. UNIDIRECTIONAL NON-ISOLATED DC-DC MULTISTAGE POWER CONVERTER (MPC)

The conventional DC-DC converters, employed in various medium-voltage step-up applications. However, conventional converters are not a practical solution for high voltage step-up applications [89]–[91]. To satisfy the high voltage load demand and to make the system more reliable, efficient, small size, many solutions proposed in the last decades. DC-DC MPC topologies designed by utilizing numerous boosting stages along with conventional DC-DC converter [65]. The combinations of the conventional converter and numerous boosting stages form an extensive power converter configuration. Each converter topologies have its requirements, characteristics and features. It is quite difficult, confusing to survey and categorize the DC-DC MPC. In this work, numerous unidirectional DC-DC converters are reviewed and categorized to explain the global scenario of recently proposed DC-DC MPC in literature. This article assists in understanding the concept and structure of unidirectional MPC topologies, types of boosting stages with the advantages and disadvantage of MPC. The specific topologies describe in terms of their cost, reliability and applications. Based on the boosting stages and conversion ratio; all the non-isolated DC-DC multistage converters classified into the following three main categories:

- Low voltage step-up MPC (Derived Topologies/two-stage)
- Moderate voltage step-up MPC (Cascaded or Quadratic Boost converter topologies)
- High voltage step-up MPC (Hybridization with Switched Inductor (SI), Switched Capacitor (SC), transformer, coupled inductor etc.

A. LOW VOLTAGE STEP-UP MPC (DERIVED TOPOLOGIES)

Low voltage step-up MPC designed by hybridization of two conventional DC-DC power converters, hence called as derived topologies or two-stage converter. The classification of low step-up MPC shown in Fig. 6(a). Though based on the conversion ratio, many researchers claim that low step-up converter is a conventional DC-DC converter. However, these
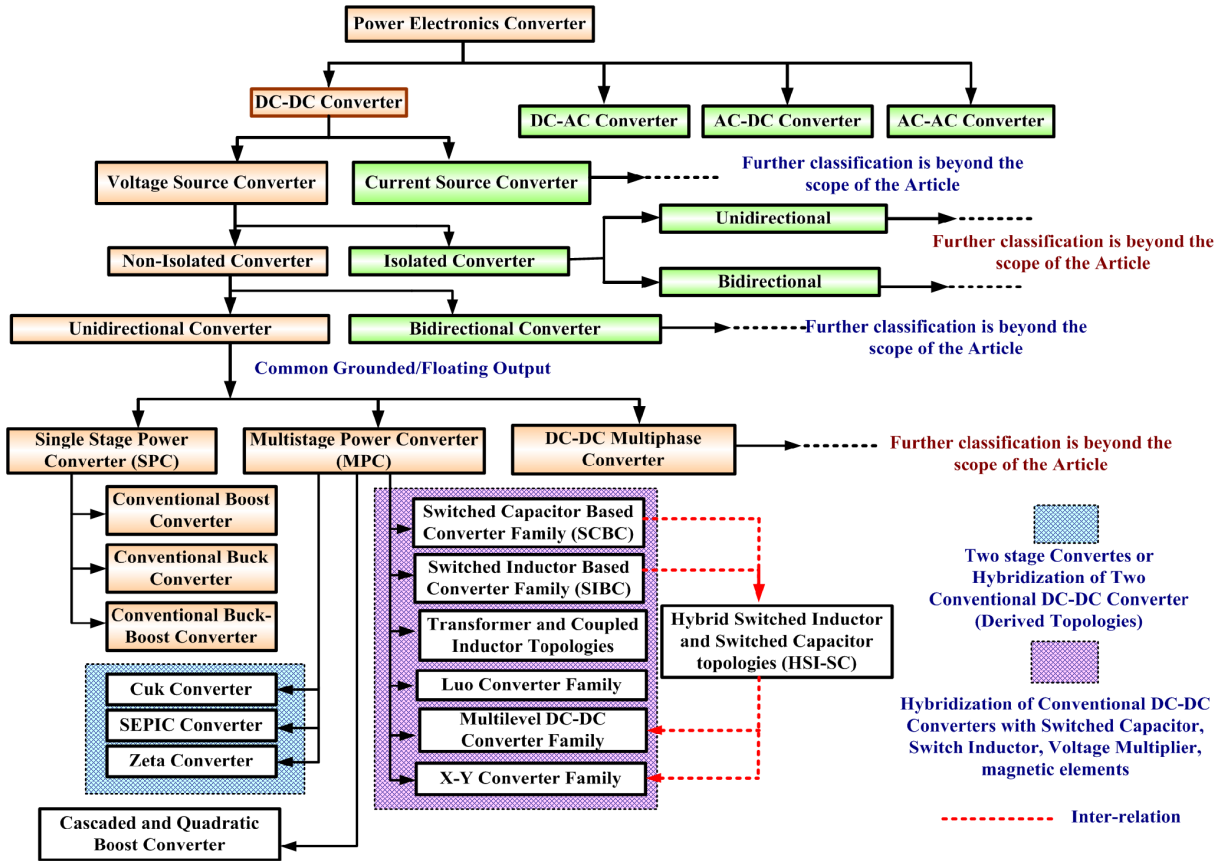
FIGURE 3. Classification of Power Electronics Converter with more focus on non-isolated unidirectional DC-DC Converter.
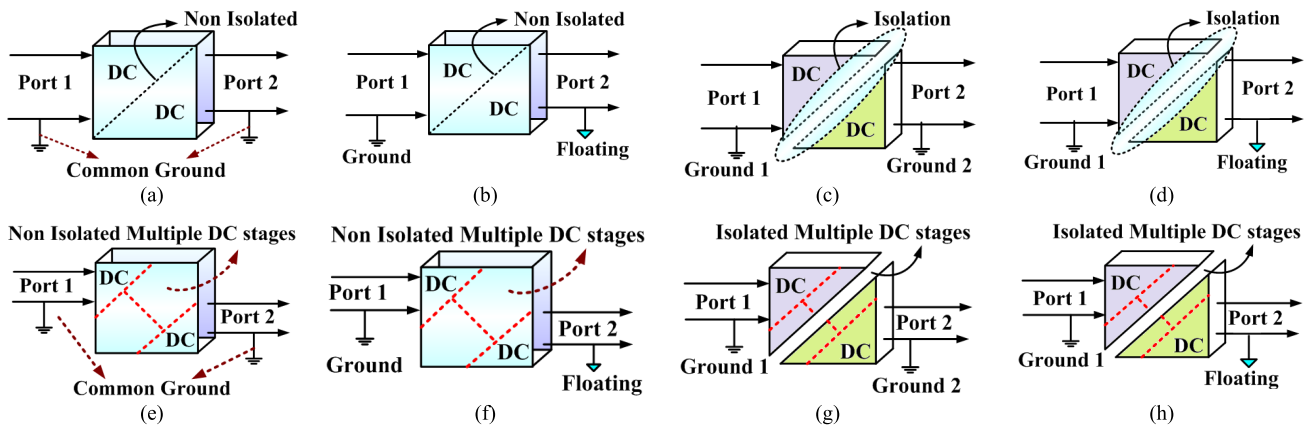

FIGURE 4. DC-DC unidirectional converter configurations (a) Non-isolated Common Ground Single-stage Converter (Non-isolated CGSC) (b) Non-isolated Floating Output Single-stage Converter (Non- isolated FOSC) (c) Isolated Grounded Single-stage Converter (Isolated GSC) (d) Isolated Floating Single-Stage Converter (Isolated FSC) (e) Non-isolated Common Ground Multistage Converter (Non-isolated CGMC) (f) Non-isolated Floating Output Multistage Converter (Non-isolated FOMC) (g) Isolated Grounded Multistage Converter (Isolated GMC) (h) Isolated Floating Multistage Converter (Isolated FMC).

converters designed by utilizing two converters to achieve excellent benefits and to avoid the drawback of conventional converters structure. The various combinations of conventional DC-DC converters to derive low voltage MPC shown in Fig. 6(b). Cuk converter is step-up/down inverting output

DC-DC MPC designed by hybridization of popular Boost and buck converter. In Cuk converter, front end structure is a conventional boost converter and load side structure is conventional buck converter [84]–[86]. The Single-Ended Primary Inductance Converter (SEPIC) is a step-up/down non-
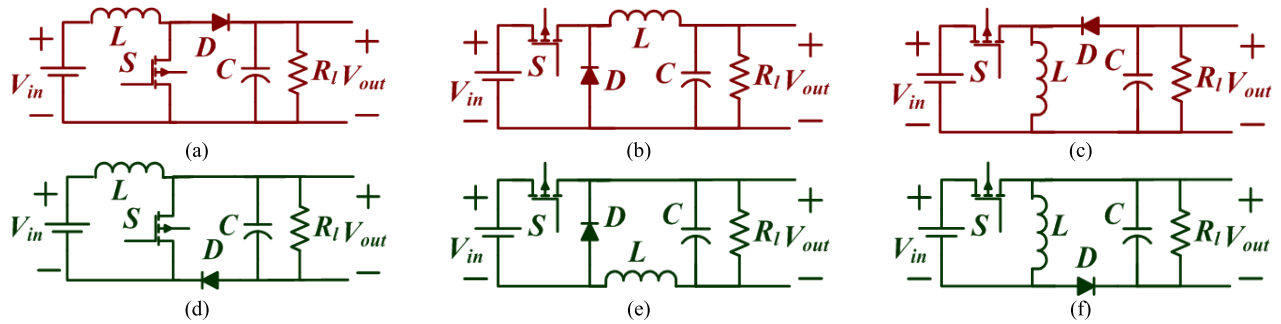
FIGURE 5. DC-DC unidirectional conventional common ground and floating power converter (a) Common Grounded Boost Converter (boost or step-up converter) (b) Common Grounded Buck Converter (buck or step-down converter) (c) Common Grounded Buck-Boost Converter (buck-boost or up-down converter) (d) Floating Boost Converter (floating boost or step-up converter) (e) Floating Buck Converter (floating buck or step-down converter) (f) Floating Buck-Boost Converter (floating buck-boost or up-down converter).
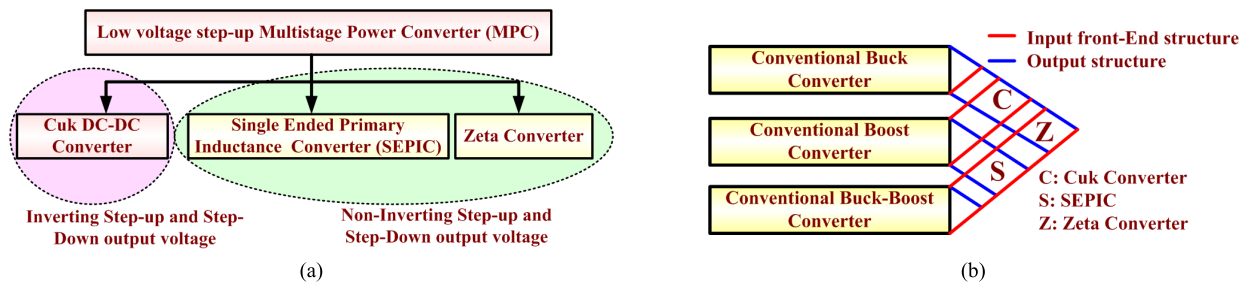

FIGURE 6. Classification and possible combinations (a) Classification of Low voltage DC-DC Multistage Power Converter (MPC) (b) Hybridization of conventional DC-DC converter to derive Low Voltage MPC (Cuk, SEPIC and ZETA derivation).

inverting output DC-DC MPC designed by hybridization of the standard boost converter and buck-boost converter [84]–[86]. In SEPIC, the front-end structure is the traditional boost converter, and the load side structure is a traditional buck-boost converter. The ZETA converter is a step-up/down non-inverting output DC-DC MPC designed by hybridization of the traditional buck-boost converter and buck converter. Inside ZETA converter, the front-end structure is the traditional buck-boost converter, and the load side structure is the traditional buck converter. Cuk, SEPIC, ZETA converters are single switch (Power MOSFET, IGBT etc.) controlled converter, and to design these converters; two inductors, two capacitors, along with single power diode are required [84]–[87]. The power circuit of Cuk, SEPIC and ZETA converter depicted in Fig. 7(a)-(c) respectively.

B. MODERATE VOLTAGE STEP-UP MPC (CASCADED OR QUADRATIC BOOST CONVERTER)

The classical DC-DC converters are not adequate for high or moderate voltage applications [88], [89]. Several standard DC-DC converters are connected in a cascaded manner to achieve a moderated voltage. The generalized structure of the N-stage cascaded converter shown in Fig. 8(a). The cascaded power converters provide an average voltage conversion ratio by increasing the number of switches [90]–[93]. The input supply directly fed to the first stage of the cascaded converter, and the voltage stepped up by increasing the duty cycle to maximize margin. The remaining stages

operated with a lower duty cycle, thus switching losses is reduced [69]. Due to several switches, sophisticated circuitry and increased complexity in control switches of each stage. The high voltage conversion ratio achieved but compromised in robustness due to several numbers of inductors, diodes, capacitors and active switches. In [94], cascaded Cuk converter approach is employed, but result in reduced efficiency and higher losses due to a large number of components. In [95], a multistage converter with a magnetic component-free proposed by using diodes and capacitor network to attain the maximum conversion ratio. The drawback, an additional number of diodes and capacitors. Also, the conversion ratio limited due to the restriction of the number of stages.

The limitation of the active power switch overcome by the Quadratic Boost Converter (QBC) [96]–[98]. The generalized structure of QBC shown in Fig. 8(b). QBC strategy employed for several stages using a single switch and utilizing the number of uncontrolled switches (diodes). The overall gain of the QBC is the product of the voltage gain of all stages, considerable downside still exists. The main drawback of the QBC is the voltage stress across the controlled switch; poor efficiency and complexity increased due to the fourth-order system. The voltage stress across the controlled switch is equal to the total output voltage. Hence, required higher rating switch, which increases the cost of the converter. For improved efficiency, several approaches are addressed in the literature [98]. In [99], 3-level Quadratic Boost Converter (3-level QBC) proposed for high step-up application by utilizing
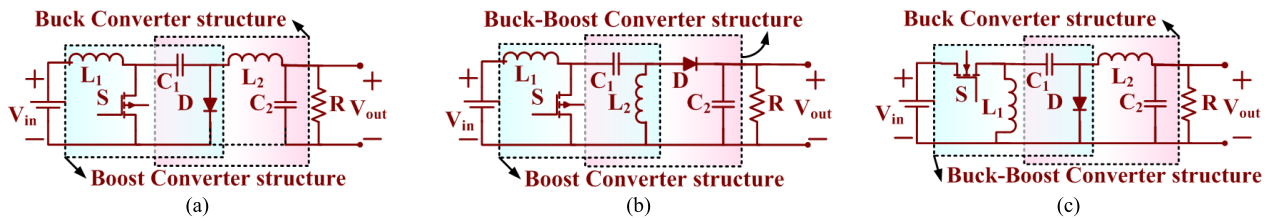
FIGURE 7. Power circuit of Low Step-Up DC-DC Multistage Power Converter (MPC) or derived two stage topologies (a) Cuk Converter (b) Single Ended Primary Inductance Converter (c) ZETA converter.
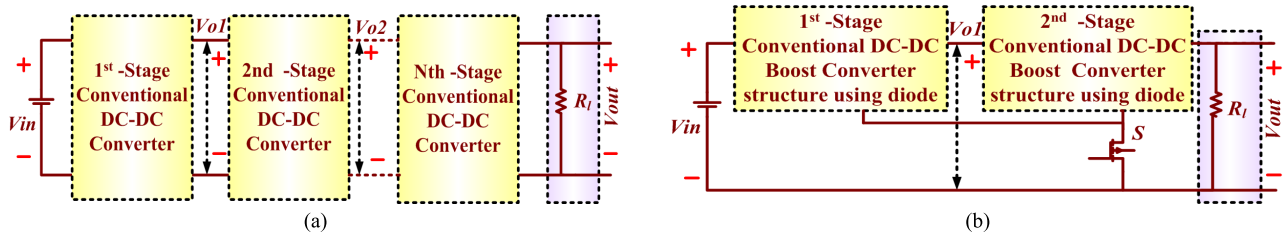

FIGURE 8. Moderate Voltage Converter (a) Generalized Structure of Cascaded Boost Converter (CBC) (b) Generalized Structure of Quadratic Boost Converter (QBC).

two switches at the output side. However, the utilization of two inductors is another drawback of the converter and restricted to the low or moderate voltage and power application. Switched Capacitor (SC), Switched Inductor (SI) or a combination of Switched Inductor and Switched-Capacitor (HSI-SC) employed in converters order to generate the high voltage (explained in the next section).

C. HIGH VOLTAGE STEP-UP MULTISTAGE POWER CONVERTER

High Voltage (HV) step-up MPC have high gain conversion ratio and their power circuits designed by hybridization of classical DC-DC power converters. These converters also designed by using Front End Structure (FES) or full converter along with numerous boosting stages like Switched Capacitors (SC) (designed with the help of diode-capacitor circuitry), Switched Inductor (SI), Voltage Lift Switched Inductor (VLSI) cell, modified Voltage Lift Switched Inductor cell (mVLSI), Voltage Multiplier (VM) etc. [65].

The numerous structures of Switched Capacitor (SC) cells using diodes, switches and capacitor shown in Fig. 9(a)-(o) [100]–[125]. Recently, the Switched Inductor (SI) and Hybrid combination of Switched Inductor and Switched-Capacitor (HSI-SC) proposed to lift the voltage with high conversion ratio [65], [88]–[91]. The VLSI and mVLSI are the famous structure of HSI-SC used for the DC-DC converter. For simplicity, this article HSI-SC configuration considered as a part of SI. The numerous structures of SI and HSI-SC showed in Fig. 10(a)-(s) using a diode, inductors, capacitors and controlled switch [98], [117]–[119], [126]–[139]. All the high step-up DC-DC MPCs classified into the following six subclasses:

- Switched Capacitor Based Converter (SCBC) series.

- Switched Inductor Based Converter (SIBC) series, /or a hybrid combination of SI and SC, i.e. HSI-SC.
- Transformer, Coupled Inductor Based Converter family.
- Luo converter series.
- Multilevel DC-DC converter series.
- X-Y converter series.

V. MULTISTAGE SWITCHED CAPACITOR BASED CONVERTER FAMILY (M-SCBC FAMILY)

Recently, the Switched Capacitors (SC) circuitries are proposed for various step-up applications to achieve a high gain conversion. Various SC circuitries showed in Fig. 9(a)-(o). Multistage Switched-Capacitor Based Converters (M-SCBC) are favored by simple structure, the modular approach and potential for monolithic integration. In SC, all the capacitors are charged in parallel and discharged in series to achieve a high gain conversion ratio [100]–[107]. The gain ratio depends on the number of capacitor and arrangement of capacitors in the converter. Apart from this, some SC circuits follow the charge pumping concept, i.e. transfer of energy from one capacitor to another capacitor, hence also called charge pump network [103], [108]–[114]. These SC or charge pump provides a viable solution to step-up the voltage with a high conversion ratio and for various applications. Numerous high step-up DC-DC MPC addressed in literature by using SC stages in conventional boost converter or derived converters (Cuk, SEPIC and ZETA) [100]–[125].

A. M-SCBC WITH BOOST AND BUCK-BOOST CONVERTER FES

Several M-SCBC topologies proposed with the boost and buck-boost front-end structure of the step-up applications. Popular M-SCBC topologies shown in Fig.11
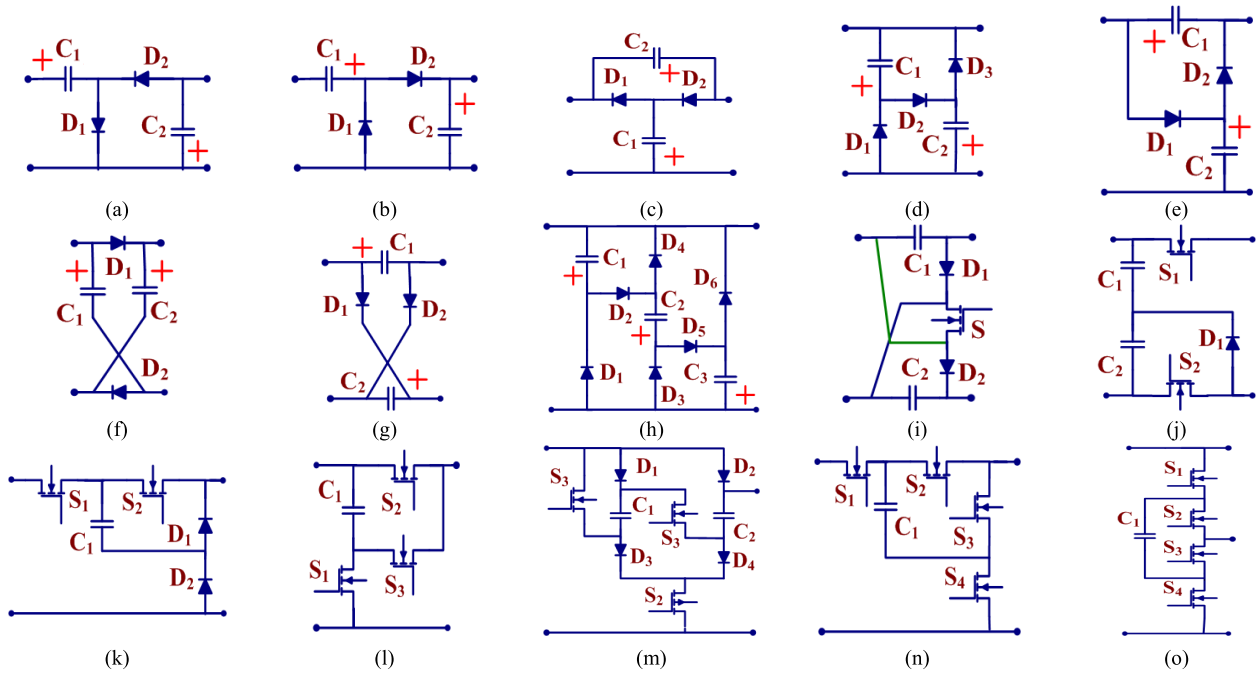
FIGURE 9. Recently proposed Switched Capacitor (SC) Structure (a)–(h) using uncontrolled switches and capacitor (i) SC using two diodes and one controlled switch (j) SC using one diodes and two controlled switch (k) SC using two diodes and two controlled switch (l) SC using three controlled switch (m) SC using four diodes three controlled switch (n)-(o) SC using four controlled switches.

FIGURE 10. Recently proposed Switched Inductor (SI) and Hybrid combination of Switched Inductor and Capacitor (HSI-SC) Structure (a)–(n) using uncontrolled switches (diodes) and inductor (o)-(s) HSI-SC structure using diodes, capacitor and controlled switch (MOSFET), Note: (a), (b) and (c) Structure of Switched Inductor and (d)-(s) Structure of HSI-SC.

FIGURE 11. Switched Capacitor based DC-DC Multistage Converter with boost and buck-boost front end structure (a) Three Switch High Voltage Boost Converter with FEBC structure (TS-HVBC) (b) Extension version of Three Switch High Voltage Boost Converter with FEBC structure (Extended TS-HVBC) (c) Inverting Switched Capacitor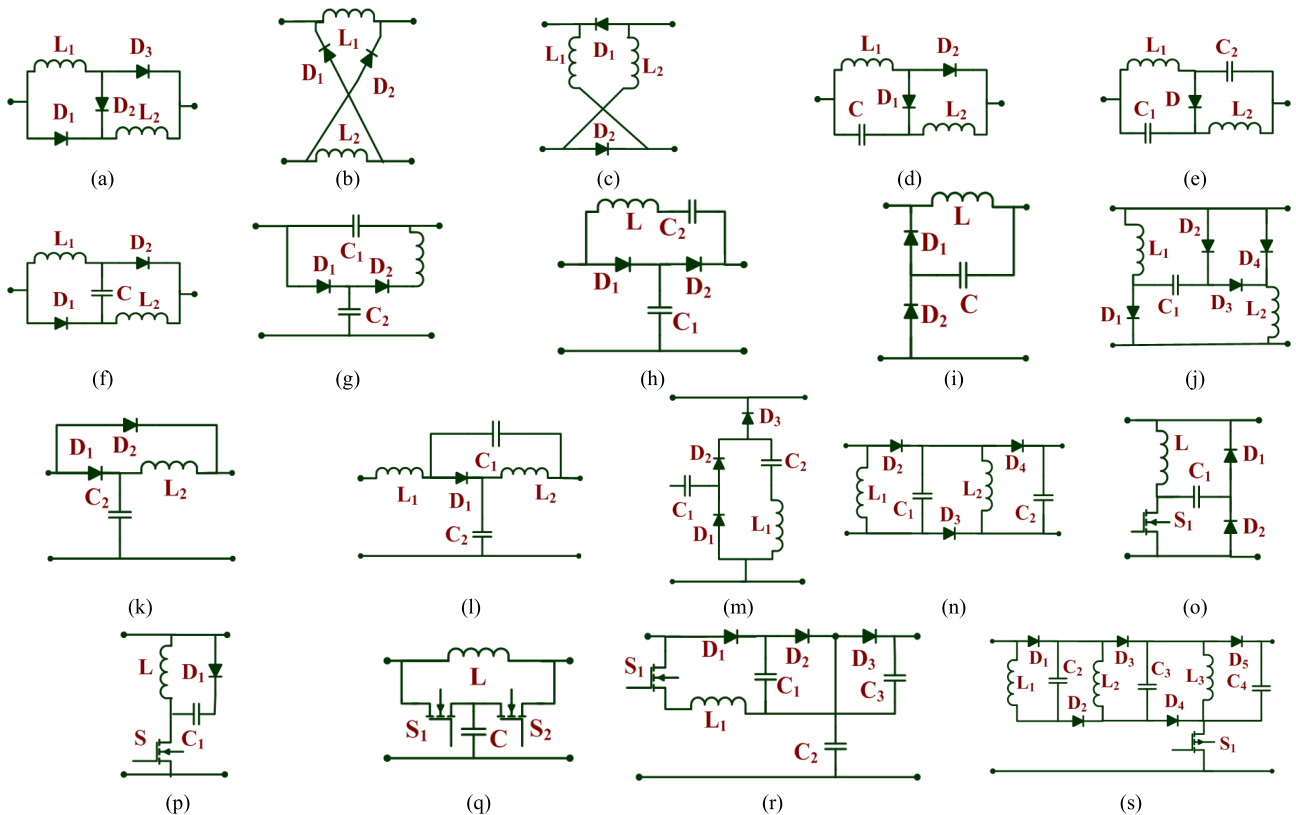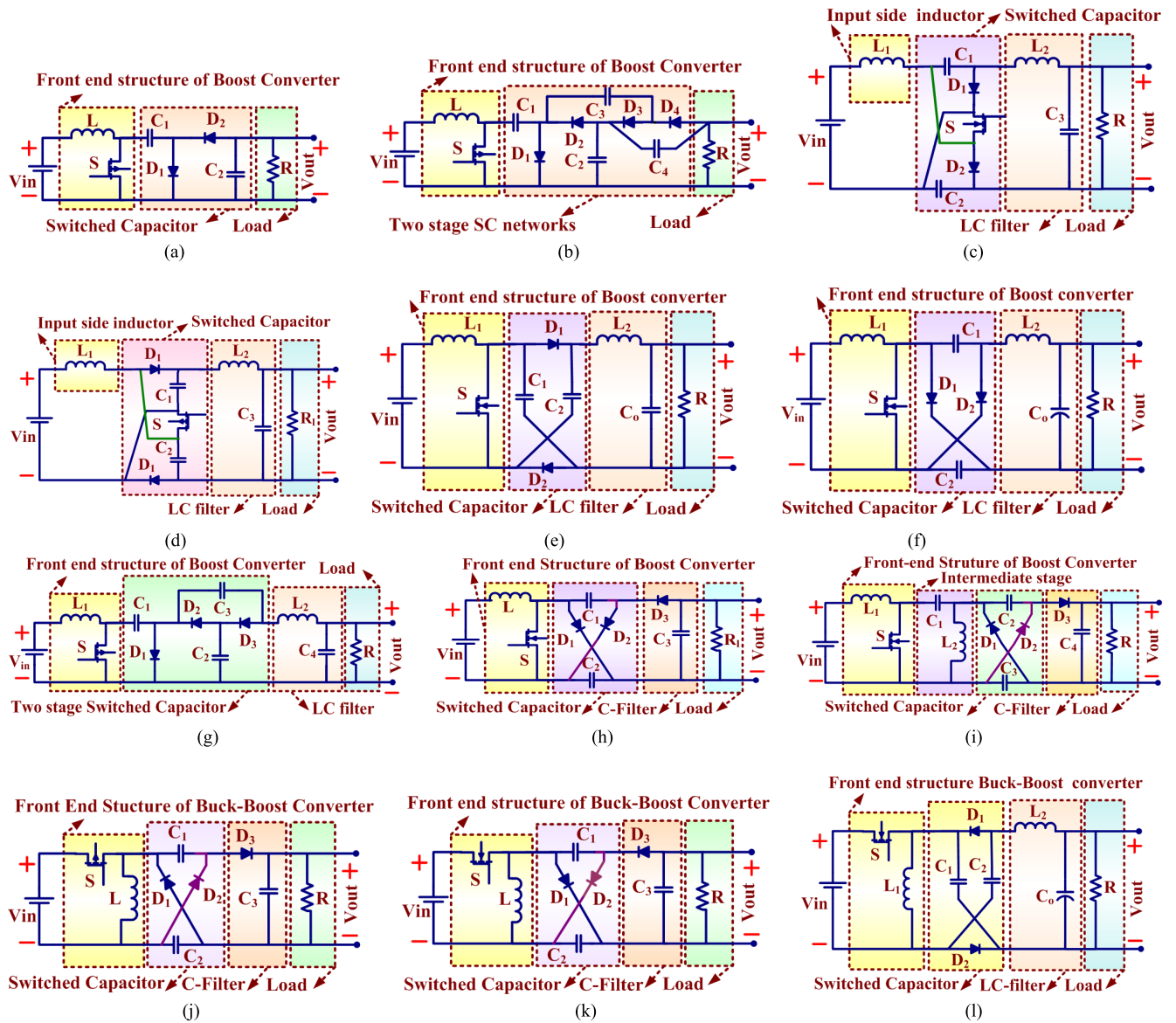 Converter with input side inductor (d) Non-Inverting Switched Capacitor Converter with Input side inductor (e) Non-Inverting Switched Capacitor Boost converter with FEBC structure and LC filter (f) Inverting Switched Capacitor Boost converter with FEBC and LC filter (g) Two stage Switched Capacitor Boost converter with FEBC and LC filter (h) Inverting Switched Capacitor Boost converter with FEBC and Unidirectional C- filter (HVDCC) (i) Non-Inverting Switched Capacitor Boost converter with FEBC structure and Unidirectional C-filter (HVDSC) (j) Non-Inverting Switched Capacitor Boost converter with FEB-BC structure and Unidirectional C-filter (HVDZC) (k) Inverting Switched Capacitor Boost converter with FEB-BC structure and Unidirectional C-filter (HVDIZC) (l) Inverting Switched Capacitor Boost converter with FEB-BC and Unidirectional LC-filter.

(a)-(l). In [107], and Three Switch High Voltage Boost Converter (TS-HVBC) elaborated. Three Switch High Voltage Boost Converter (TS-HVBC) designed by hybridization of Front End Boost Converter (FEBC) and SC. The power circuit of the TS-HVBC illustrated in Fig. 11(a). The power converter consists of two diodes, two capacitors and one inductor along with the single control switch—a two-stage converter with the inverting output and suitable for the medium or high boost applications. The converter is operating in the CCM when $k > D(1-D)^2$ and operate in DCM when $k < D(1-D)^2$. The conversion ratio of the TS-HVBC in CCM and DCM mode

is given in the equation (1) and (2) respectively.

$$\frac{V_{out}}{V_{in}} = \frac{-1}{1-D} = \frac{-T}{T-T_{on}} = \frac{-1}{1-f_S T_{on}} \qquad (1)$$

$$\frac{V_{out}}{V_{in}} = -\frac{1+\sqrt{1+\frac{4T_{on}^2}{T^2 k}}}{2}, \quad k = \frac{2L}{R_l Ts} \qquad (2)$$

where f_S is switching frequency, T is the total period, T_{on} is ON time of the switch, D is the duty cycle, and R_l is the load resistance. Theoretically, this converter has a power factor greater than 0.97 for conversion ratio higher than 1.5.

This converter provides a negative conversion ratio equivalent to inverting classical boost converter; the structure is easily modifiable and extendable by adding additional stages of SC and shown in Fig. 11(b). Two diodes and capacitors are required to add one stage of SC [107]. The voltage conversion ratio of the converter given as in the equation (3)

$$\frac{V_{out}}{V_{in}} = \frac{-2}{1-D} = \frac{-2T}{T-T_{on}} = \frac{-2}{1-f_s T_{on}} \quad (3)$$

In [108], the inverting SC converter with input side inductor discussed, and the power circuit shown in Fig. 11(c). The configuration is a three-stage step-up converter which consists of input inductor stage, switch capacitor stage, and LC filter. The converter provides a negative voltage conversion ratio. Two inductors, three capacitors, and two diodes along with the single control switch, are required to design this converter. The voltage conversion ratio of the converter given in equation (4).

$$\frac{V_{out}}{V_{in}} = \frac{-(1+D)}{1-D} = \frac{-(T+T_{on})}{T-T_{on}} = \frac{-(1+f_s T_{on})}{1-f_s T_{on}} \quad (4)$$

In [108], the non-inverting SC converter with input side inductor discussed, and the power circuit shown in Fig. 11(d). The configuration is three-stage step-up converters which consist of input inductor stage, switch capacitor stage, and LC filter. The converter provides a positive voltage conversion ratio. Two inductors, three capacitors, and two diodes along with single control switch, are required to design this converter—the voltage conversion ratio of the converter given in equation (5).

$$\frac{V_{out}}{V_{in}} = \frac{1+D}{1-D} = \frac{T+T_{on}}{T-T_{on}} = \frac{1+f_s T_{on}}{1-f_s T_{on}} \quad (5)$$

In [108]–[110], the non-inverting SC boost converter discussed with the low voltage stress across the switch. The power circuit discussed in [108] shown in Fig. 11(e). The converter designed by utilizing the SC network [102]. The configuration is a three-stage step-up converter which consists of FEBC structure, switch capacitor stage, and LC filter. The converter provides a positive voltage conversion ratio. Two inductors, three capacitors, and two diodes along with single control switch, are required to design this converter—the voltage conversion ratio of the converter given in equation (6).

$$\frac{V_{out}}{V_{in}} = \frac{1+D}{1-D} = \frac{T+T_{on}}{T-T_{on}} = \frac{1+f_s T_{on}}{1-f_s T_{on}} \quad (6)$$

In [108]–[110], the inverting SC boost converter discussed with low voltage stress of switch. The power circuit discussed in [108], [109] shown in Fig. 11(f). The converter designed by hybridization of SC in the classical boost converter [102]. The configuration is a three-stage step-up converter, consists of FEBC structure, switch capacitor stage, and LC filter. The converter provides a negative voltage conversion ratio. The converter required two inductor, three capacitors, and

two diodes along with a single control switch—the voltage conversion ratio of the converter given in equation (7).

$$\frac{V_{out}}{V_{in}} = \frac{-(1+D)}{1-D} = \frac{-(T+T_{on})}{T-T_{on}} = \frac{-(1+f_s T_{on})}{1-f_s T_{on}} \quad (7)$$

The two-stage switched-capacitor boost converter with reduced switch stress, and proposed for the high voltage conversion ratio [107]. The converter is also called as Three Switch High Voltage Cuk Converter (TS-HVCC) because the input characteristic of TS-HVCC is similar to the classical boost converter or Cuk converter. In comparison, the load side characteristic is similar to the Cuk converter. The power circuit of TS-HVCC shown in Fig. 11(g), having three stages; FEBC, SC, and LC filter. The converter provides a negative conversion ratio, which is higher than the Cuk converter and given in equation (8).

$$\frac{V_{out}}{V_{in}} = \frac{-(1+D)}{1-D} = \frac{-(T+T_{on})}{T-T_{on}} = \frac{-(1+f_s T_{on})}{1-f_s T_{on}} \quad (8)$$

In [113], a new DC-DC High Voltage Derived Cuk Converter (HVDC) discussed. The structure is inverting SCBC and has inductor at only the input terminal. The power circuit of the converter shown in Fig. 11(h). This circuit is a three-stage step-up converter which consists of FEBC, SC, and C-filter stages. Here, Cuk structure formed by combining the FEBC and SC stages. This converter provides a negative voltage conversion ratio and required single inductor, three capacitors, and three diodes along with single control switch to design the converter. This converter provides a higher conversion ratio compared to the conventional boost converter with low voltage stress on the switch at the same duty cycle—the voltage conversion ratio of the converter given in equation (9).

$$\frac{V_{out}}{V_{in}} = \frac{-2}{1-D} = \frac{-2T}{T-T_{on}} = \frac{-2}{1-f_s T_{on}} \quad (9)$$

In [111]–[113], a new DC-DC High Voltage Derived SEPIC converter (HVDSC) discussed. The structure is non-inverting SCBC and derived by employing SC in the SEPIC. The power circuit of the converter shown in Fig. 11(i). This configuration is a four-stage step-up converter which consists of FEBC, intermediate LC, SC and C-filter stages. The SEPIC structure formed by combining the FEBC and the intermediate LC stage. This converter provides a positive voltage conversion ratio. To design this converter, two inductors, four capacitors, and two diodes along with the single control switch, are required. This converter provides a high conversion ratio compared to a conventional boost converter with low voltage stress on the switch at the same duty cycle. The voltage conversion ratio of the converter given in equation (10). This configuration utilized to derive inverting voltage by changing the polarity of the capacitor, and the direction of the diodes.

$$\frac{V_{out}}{V_{in}} = \frac{2-D}{1-D} = \frac{2T-T_{on}}{T-T_{on}} = \frac{2-f_s T_{on}}{1-f_s T_{on}} \quad (10)$$

In [111]–[113], a new DC-DC High Voltage Derived ZETA converter (HVDZC) discussed. This converter is non-inverting SCBC and derived by using SC in the ZETA converter, and the second inductor replaced by a diode. The power circuit of the converter shown in Fig. 11(j). This configuration is a three-stage step-up converter which consists of Front-End Buck-Boost Converter (FEB-BC), SC and C-filter stages. The ZETA structure formed by combining the FEB-BC and SC stages. This converter provides a positive voltage conversion ratio ad required single inductor, three capacitors, and three diodes along with a single control switch. The control switch is floating and connected between the positive terminal of the input and inductor. This converter provides a high conversion ratio compared to the conventional boost converter with the low switch voltage stress. The voltage conversion ratio of the converter in the CCM and DCM given in the equation (11) and (12) respectively.

$$\frac{V_{out}}{V_{in}} = \frac{1+D}{1-D} = \frac{T+T_{on}}{T-T_{on}} = \frac{1+f_s T_{on}}{1-f_s T_{on}} \quad (11)$$

$$\frac{V_{out}}{V_{in}} = \frac{1+\sqrt{1+\frac{4T_{on}^2}{T^2 k}}}{2}, \quad k = \frac{2L}{RT_S} \quad (12)$$

In [111]–[113], a new DC-DC High Voltage Derived Inverting ZETA Converter (HVDIZC) discussed. This converter is inverting SCBC, and derived by using SC in the ZETA converter, and a diode replaces the second inductor. The power circuit of the converter shown in Fig. 11(k). This circuit is a three-stage step-up converter which consists of the FEB-BC, SC, and C-filter stages. The ZETA structure formed by combining the FEB-BC and SC stages. The converter required single inductor, three capacitors, and three diodes along with a single control switch. This converter provides a negative high conversion ratio compared to the conventional boost converter with low switch voltage stress. The voltage conversion ratio of the converter with CCM and DCM has given by the equation (13) and (14) respectively.

$$\frac{V_{out}}{V_{in}} = -\frac{2-D}{1-D} = -\frac{2T-T_{on}}{T-T_{on}} = -\frac{2-f_s T_{on}}{1-f_s T_{on}} \quad (13)$$

$$\frac{V_{out}}{V_{in}} = -1-\sqrt{1+\frac{T_{on}^2}{T^2 k}}, \quad k = \frac{2L}{RT_S} \quad (14)$$

In [109]–[113], ZETA DC-DC converter based on the diode assist capacitor derived. The power circuit discussed in [109] considered and shown in Fig. 11(l). This circuit is inverting SCBC, and derived by using SC in ZETA converter. The structure of the converter formed by combining FEB-BC and SC stages along with LC filter. This converter provides a negative voltage conversion ratio. Two inductors, three capacitors, and two diodes along with single control switch, are required to design this converter. The voltage conversion ratio of the converter is given in (15).

$$\frac{V_{out}}{V_{in}} = -\frac{2-D}{1-D} = -\frac{2T-T_{on}}{T-T_{on}} = -\frac{2-f_s T_{on}}{1-f_s T_{on}} \quad (15)$$

B. MULTISTAGE SWITCHED CAPACITOR CONVERTER (MSCC) WITHOUT FEBC AND FEB-BC

Numerous Multistage Switched-Capacitor Based Converters (MSCCs) addressed in the literature without the front-end of the Boost converter and the Buck-Boost converter structure (FEBC and FEB-BC). These converters are derived for the application of high step-up/down voltage and also suitable to satisfy the electrical load demand in the vehicle.

One interesting topology called Switched-Capacitor with Intermediate Boost Converter (SC-IBC) discussed in [114]. This topology provides a high step-up voltage conversion ratio and shown in Fig. 12(a). This topology derived by using a conventional boost converter as an intermediate stage. The switched capacitor directly connected to the input side of the converter. Three capacitors, five diodes and single inductor along with four control switches are needed to design SC-IBC. The voltage conversion ratio of the converter given in equation (16).

$$\frac{V_{out}}{V_{in}} = \frac{3-2D}{1-D} = \frac{3T-2T_{on}}{T-T_{on}} = \frac{3-2f_s T_{on}}{1-f_s T_{on}} \quad (16)$$

The switched capacitor based multistage step-down converter shown in Fig. 12(b)-(f) [115]–[125]. These converters do not provide a suitable solution for the power train of fuel cell applications. But these converters find an application to drive the low voltage luxurious loads in the vehicles.

C. MSCC WITH QUADRATIC BOOST FRONT-END STRUCTURE (FUTURE DIRECTION)

Based on the literature survey, in this section, four new converter topologies are proposed for the future direction of MSCC for high step-up applications. Quadratic Boost Converter (QBC) provides a suitable solution with SC to attain a high voltage conversion ratio. Following four new topologies are proposed:

- Quadratic Multistage Switched-Capacitor Converter with C-filter. (QMSCC with C filter) (shown in Fig. 13(a))
- Quadratic Multistage Switched-Capacitor Converter with LC-filter (QMSCC with LC filter) (shown in Fig. 13(b))
- Quadratic Multistage Switched-Capacitor Converter with intermediate stage and C-filter (QMSCC with intermediate stage and C filter) (shown in Fig. 13(c))
- Quadratic Multistage Switched Capacitor Converter with intermediate stage and LC-filter (QMSCC with intermediate stage and LC filter) (shown in Fig. 13(d)).

The voltage conversion ratio of QMSCC with C-filter given in equation (17). The voltage conversion ratio of QMSCC with LC-filter given in the equation (18). The voltage conversion ratio of QMSCC with intermediate stage and C-filter given in the equation (19). The voltage conversion ratio of QMSCC with intermediate stage and LC-filter given in the equation (20).

$$\frac{V_{out}}{V_{in}} = \frac{2}{(1-D)^2} = \frac{2T^2}{(T-T_{on})^2} = \frac{2}{(1-f_s T_{on})^2} \quad (17)$$
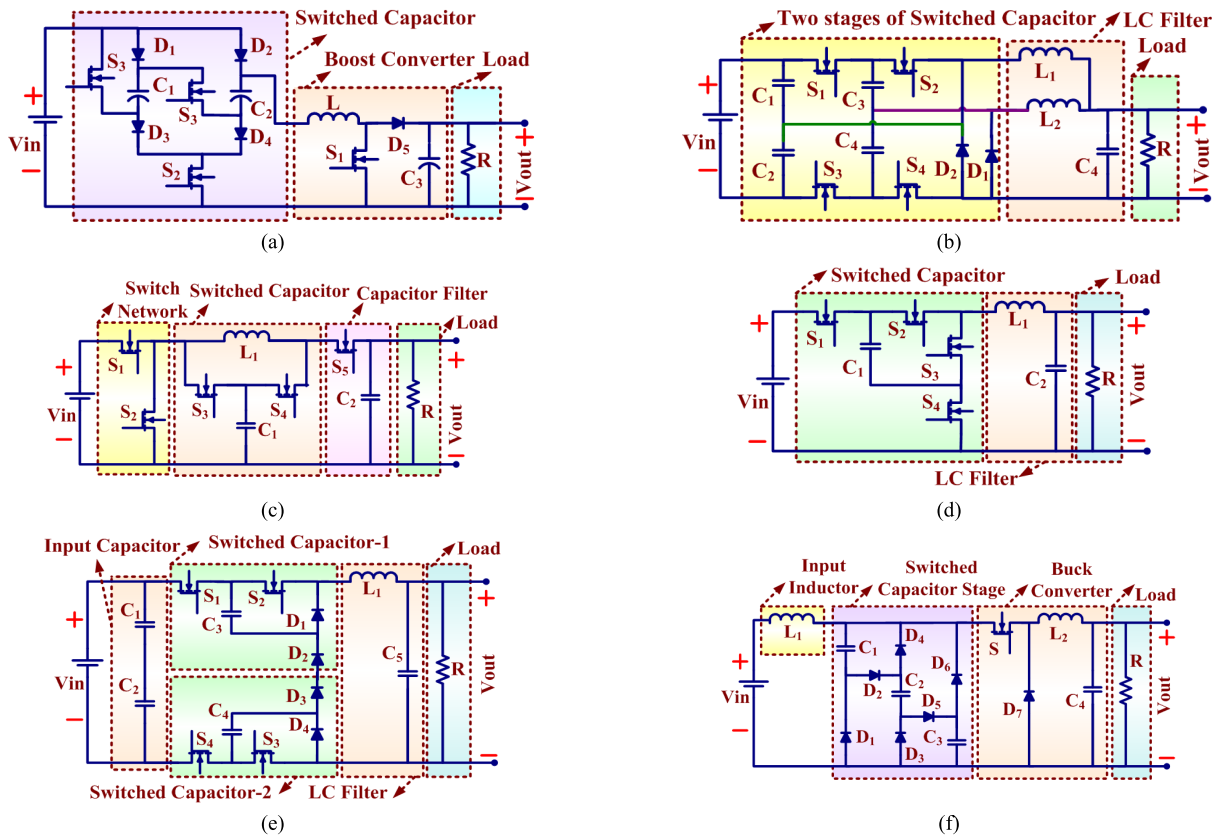
FIGURE 12. Multistage Switched Capacitor Converter without Boost Front-End Structure (a) Multistage Switched capacitor converter with boost converter intermediate stage (b) Modified switched capacitor interleaved buck converter (c) Switched capacitor quadratic buck converter (d) Four switch switched capacitor based multistage buck converter (e) Two switched capacitor based multistage buck converter (f) Switched capacitor buck multistage converter with buck converter intermediate stage.
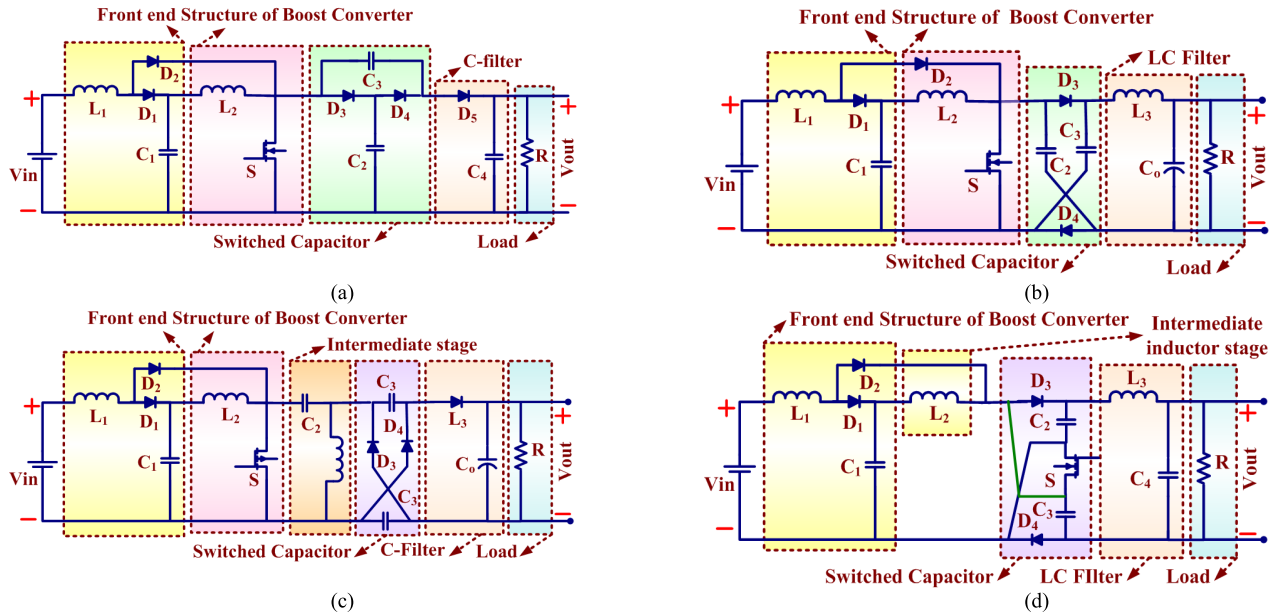
FIGURE 13. Multistage Switched Capacitor converter with Quadratic Boost Front-End Structure (a) Quadratic multistage switched capacitor converter with C-filter (b) Quadratic multistage switched capacitor converter with LC-filter (c) Quadratic multistage switched capacitor converter with intermediate stage and C-filter (d) Quadratic multistage switched capacitor converter with intermediate stage and LC-filter.

$$\frac{V_{out}}{V_{in}} = \frac{1+D}{(1-D)^2} = \frac{T^2(T+T_{on})}{(T-T_{on})^2} = \frac{1+f_sT_{on}}{(1-f_sT_{on})^2} \quad (18)$$

$$\frac{V_{out}}{V_{in}} = \frac{2-D}{(1-D)^2} = \frac{T^2(2T-T_{on})}{(T-T_{on})^2} = \frac{2-f_sT_{on}}{(1-f_sT_{on})^2} \quad (19)$$

$$\frac{V_{out}}{V_{in}} = \frac{1+D}{(1-D)^2} = \frac{T^2(T+T_{on})}{(T-T_{on})^2} = \frac{1+f_sT_{on}}{(1-f_sT_{on})^2} \quad (20)$$

The detail classification of multistage switched-capacitor based converter shown in Fig. 14 and the comparison of the SBSC and the other parameters discussed in the comparison section of this article.
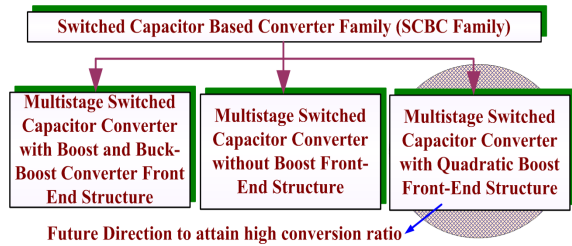
FIGURE 14. Classification of Multistage Switched Capacitor Based Converter Family (M-SBSC Family) based on recently addressed article.

VI. MULTISTAGE SWITCHED INDUCTOR BASED CONVERTER FAMILY (M-SIBC FAMILY)

Switched Inductor (SI) is another popular technique employed in DC-DC converter to increase the voltage with a large conversion ratio. In Switched Inductor (SI), inductors are discharged in series and charge in parallel [98], [117]–[119], [126]–[139]. Multistage Switched Inductor Based Converters (M-SIBC) provides a high voltage conversion ratio using less number of components. These converters structures are simple, and the inductance rating (value) of both inductors are the same. The same core utilized to integrate the inductors (to form switched inductor network) to reduce converter weight and size. A hybrid combination of Switched Inductor and Switched Capacitors (HSI-SC) is another admired solution to attain a high conversion ratio. Numerous M-SIBC topologies proposed for the large step-up and step-down conversion ratio. Power circuits of the M-SIBC shown in Fig. 15(a)-(l).

In [126], Switched Inductor (SI) concept discussed to attain a high voltage conversion ratio. The power circuit of the primary version Switched Inductor Boost Converter (SIBC) shown in Fig. 15(a). The basic SIBC designed by replacing inductor in the traditional boost conventional by the basic Switched Inductor (SI) circuitry. The basic SIBC required two similar inductors (equal in value), one capacitor, and four diodes along with the single control switch. The voltage conversion ratio of SIBC given in equation (21). The power circuit divided into three stages; SI network, Switching stage and C-filter stage.

$$\frac{V_{out}}{V_{in}} = \frac{1+D}{1-D} = \frac{T+T_{on}}{T-T_{on}} = \frac{1+f_sT_{on}}{1-f_sT_{on}} \quad (21)$$

In [98], Quadratic Boost Converter (QBC) proposed with low buffer capacitor stress and higher conversion ratio. This converter designed by using the hybrid combination of SI and SC (here called HSI-SC). The power circuit of the HSI-SC based QBC shown in Fig. 15(b). The circuit consists of three stages; HSI-SC stage, switching stage and C-filter stage. The circuit designed by using HSI-SC in the conventional Boost converter. This converter provides a high conversion ratio precisely equal to the conventional QBC. This converter is more suitable to attain the high voltage conversion ratio compared to the conventional QBC due to low voltage across the buffer capacitor. The voltage conversion ratio of the QBC, with low the buffer capacitor voltage is given in equation (22).

$$\frac{V_{out}}{V_{in}} = \frac{1}{(1-D)^2} = \frac{T^2}{(T-T_{on})^2} = \frac{1}{(1-f_sT_{on})^2} \quad (22)$$

In [127], the boost converter proposed with HSI-SC (here act as voltage multiplier). Along with this converter, HSI-SC arranged along with voltage multiplier and attached in the middle of the boost converter. The power circuit of the converter shown in Fig. 15(c). The inclusion of the inductor with SC allows the semiconductor control switch to operate with ZCS (Zero current switching) turn-on. The reverse recovery effect of the diodes also reduced. Thus, commutation losses reduced, and it is suitable to operate at high frequency. The converter structure is easily extendable to the N-stages of employing the additional number of multiplier stages. The intermediate HSI-SC stage is employed to boost the voltage with high value, and C-filter is used to reduce output ripples. The voltage conversion ratio of the converter with one stage and with N-stage of multiplier cell given in the equation (23) and (24) respectively.

$$\frac{V_{out}}{V_{in}} = \frac{2}{1-D} = \frac{2T}{T-T_{on}} = \frac{2}{1-f_sT_{on}} \quad (23)$$

$$\frac{V_{out}}{V_{in}} = \frac{N+1}{1-D} = \frac{(N+1)T}{T-T_{on}} = \frac{(N+1)}{1-f_sT_{on}} \quad (24)$$

In [128], High efficiency, high step-up soft switching boost converter proposed by using HSI-SC stage with an additional capacitor. This converter provides a high voltage conversion ratio compared to the conventional boost converter, and the power circuit of the high step-up soft-switching converter shown in Fig. 15(d). The power circuit divided into three main stages; FEBC, HSI-SC with additional capacitor and C-filter. This converter needs complex driver circuitry, and there is no need for additional separation because of both switches at operating at the same ground level. However, complex structure due to the utilization of fiver components addition, including inductor and switch is the main disadvantage of this converter—the voltage conversion ratio by equation (25).

$$\frac{V_{out}}{V_{in}} = \frac{1}{1-(D_1+D_2)} = \frac{1}{1-(f_sT_{on1}+f_sT_2)} \quad (25)$$

In [129], HSI-SC based ultra-step-up DC-DC converter proposed. The power circuit of the ultra-step-up DC-DC converter shown in Fig. 14(e). The proposed technique designed
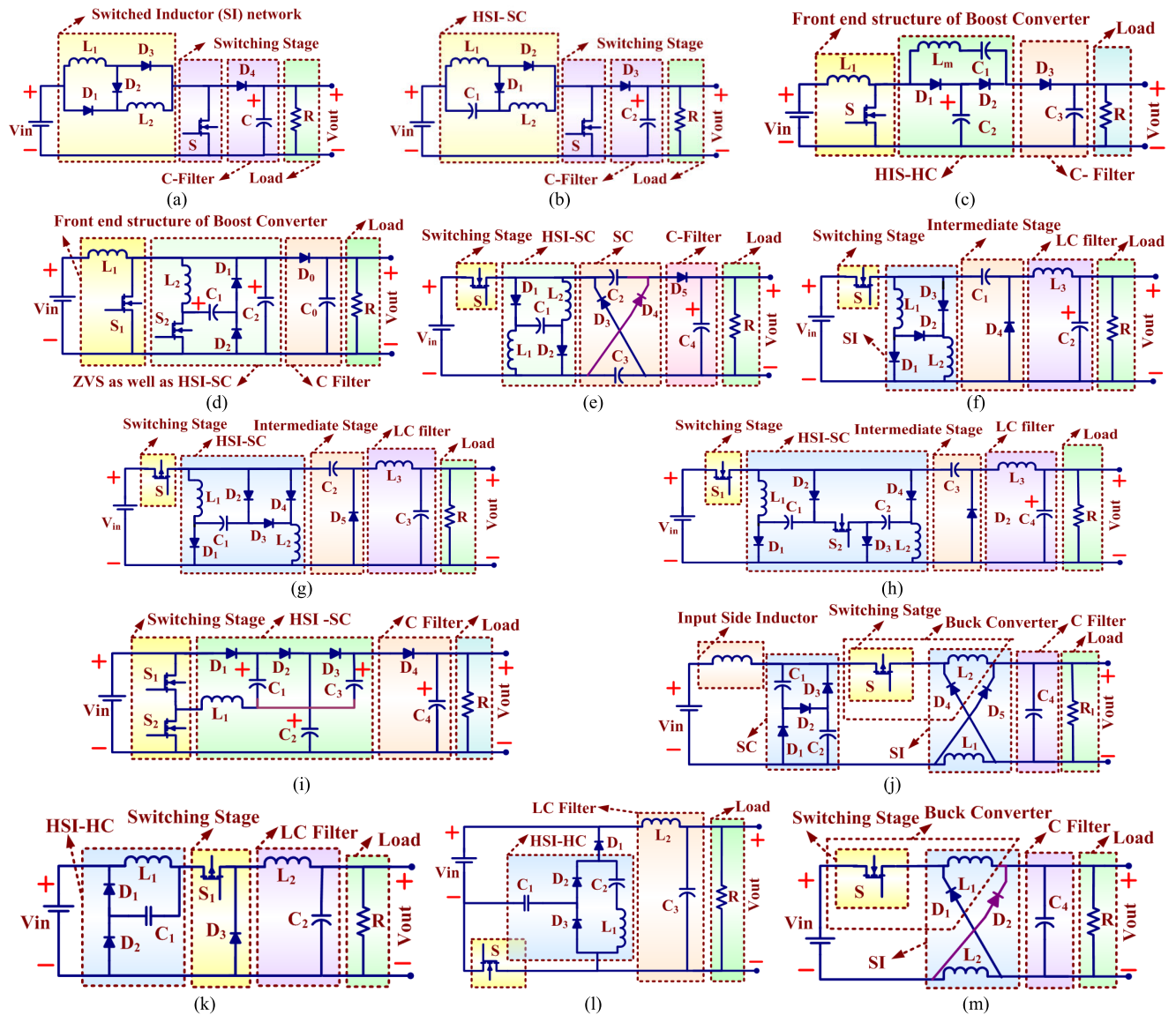
FIGURE 15. Multistage SI and HSI-SC Based Converter (a) Basic switch inductor boost converter (b) Quadratic boost converter with lower buffer capacitor voltage (c) Boost converter with integrated HSI-SC (d) High efficiency high step-up soft switching boost converter based on HSI-SC (e) HSI-SC based ultra-step-up dc-dc converter (f) Positive output hybrid converter with switched inductor (Luo Converter with SI) (g) Self-lift positive output hybrid converter with HSI-SC (h) Double self-lift positive output hybrid converter with HSI-SC (Luo Converter with HSI-SC) (i) Triple mode converter (j) HSI-SC buck converter (k) Quadratic buck converter based on front end HSI-SC structure (l) HSI-SC buck converter (m) Buck converter with basic switched inductor cell.

by utilizing the three stages; one is HSI-SC, and another is SC within conventional Buck-Boost converter and C-filter with opposite polarity. The proposed ultra-converter provides a high voltage conversion ratio with a moderate duty cycle. The stress across the switch is less, which enables the use of low rating semiconductor-controlled devices; hence the cost of the converter is reduced. The voltage stress across diodes is also less. Thus, the converter circuit designed by using Schottky diodes. The voltage conversion ratio provided in equation (26).

$$\frac{V_{out}}{V_{in}} = \frac{3+D}{1-D} = \frac{3T + T_{on}}{T - T_{on}} = \frac{3 + f_s T_{on}}{1 - f_s T_{on}} \quad (26)$$

In [130], positive output hybrid converters with Switched Inductor (Luo converter with SI), and self-lift positive output hybrid converter with HSI-SC, double self-lift positive output hybrid converter with HSI-SC (Luo converter with HSI-SC) presented to attain the higher conversion ratio, and the power circuit shown in Fig. 15(f)-(h), respectively. These converters derived by employing the SI and SC in the boost converter. These converters consist of four stages; switching stage, HSI-SC, intermediate C-filter stage and LC-filter. In other words, these converter topologies derived by employing SI, self-lift SI and double voltage lift SI in ZETA converter. The conversion ratio of the positive output hybrid converter with SI, self-lift positive output hybrid

converter with HSI-SC and double self-lift positive output hybrid converter with HSI-SC given in equation (27)-(29), respectively.

$$\frac{V_{out}}{V_{in}} = \frac{D + D^2}{1 - D} = \frac{f_s T_{on} + f_s^2 T_{on}^2}{1 - f_s T_{on}} \tag{27}$$

$$\frac{V_{out}}{V_{in}} = \frac{2D}{1 - D} = \frac{2f_s T_{on}}{1 - f_s T_{on}} \tag{28}$$

$$\frac{V_{out}}{V_{in}} = \frac{3D - D^2}{1 - D} = \frac{3f_s T_{on} - f_s^2 T_{on}^2}{1 - f_s T_{on}} \tag{29}$$

In [131], the N stage high step-up converter proposed to attain a high conversion ratio. The power circuit discussed in [131] shown in Fig. 15(i). The proposed converter is working with the concept of the SC, but categorized in HSI-SC because of an inductor or resonant tank utilized to assist ZCS. Due to the ZCS spike in currents reduced, which generally exists in the case of SC. The whole circuit is divided into three stages, switching stage, HSI-SC stage and C-filter stage.

In [109], [115], [117] buck converter is derived by utilizing HSI-SC. The power circuit of the converter discussed in [115] depicted in Fig. 15(j). Three inductors, three capacitors, five diodes along with single controlled switch, are required to design the power circuit of the converter. This converter provides a high step-down voltage conversion ratio with reasonable efficiency. The voltage conversion ratio of the converter provided is given by equation (30). This converter power circuit consists of four stages; input side inductor stage, SC, SI switching stages.

$$\frac{V_{out}}{V_{in}} = \frac{D}{(2 - D)^2} = \frac{T^2 T_{on}}{(2T - T_{on})^2} = \frac{f_s T_{on}}{(2 - f_s T_{on})^2} \tag{30}$$

In [115], Quadratic Buck Converter (QBC) based on the front end HSI-SC structure proposed. The power circuit of the converter shown in Fig. 15(k). In this converter, HSI-SC structure combined with conventional buck converters. This converter provides a large step-down ratio and conversion ratio provided in the equation (31).

$$\frac{V_{out}}{V_{in}} = D^2 = f_s^2 T_{on}^2 \tag{31}$$

In [127], HSI-SC buck converter proposed by employing a multiplier cell in a buck converter. The power circuit of the converter showed in Fig. 15(l). The arrangement of reactive components reduces the drawback of the reverse recovery current problem. In this circuit, HSI-SC is operating as a regenerative clamping circuit, therefore reducing the problem with the layout and the Electromagnetic Interference (EMI). In [115], [117]–[119], [132], [133], buck converter with Switched Inductor (SI) proposed. The inductor of the conventional buck converter is replaced by SI to obtain the circuit of the buck converter. The power circuit discussed in [115] showed in Fig. 15(m) and the voltage conversion ratio provided in the equation (32).

$$\frac{V_{out}}{V_{in}} = \frac{D}{2 - D} = \frac{f_s T_{on}}{2 - f_s T_{on}} \tag{32}$$

In [126], a transformer-less DC-DC converter proposed by utilizing two switches instead of three diodes in the switched inductor. Three new converters named as converter-I, converter-II and converter-III proposed by employing the switched inductor and lift technique in the boost converter. The power circuit of the converter-I and converter-II and converter-III showed in Fig. 16(a)-(c) and voltage conversion ratio provided in the equation (33)-(35) respectively.

$$\frac{V_{out}}{V_{in}} = \frac{1 + D}{1 - D} = \frac{T + T_{on}}{T - T_{on}} = \frac{1 + f_s T_{on}}{1 - f_s T_{on}} \tag{33}$$

$$\frac{V_{out}}{V_{in}} = \frac{2}{1 - D} = \frac{2T}{T - T_{on}} = \frac{2}{1 - f_s T_{on}} \tag{34}$$

$$\frac{V_{out}}{V_{in}} = \frac{3 + D}{1 - D} = \frac{3T + T_{on}}{T - T_{on}} = \frac{3 + f_s T_{on}}{1 - f_s T_{on}} \tag{35}$$

Apart from this, recently many DC-DC converters based on Switched Inductor (SI) and Switch Capacitor (SC) concept proposed with the coupled inductor, transformer and voltage multiplier to attain the large conversion ratio [139]–[173]. Some SI converters with coupled inductor and transformer, and with voltage multiplier discussed in the following sections.

VII. TRANSFORMER AND COUPLED INDUCTOR BASED DC-DC CONVERTER TOPOLOGIES

To achieve high voltage boost output, magnetic coupling utilized in both isolated and non-isolated converters. Transformer and coupled inductor-based DC-DC converters classified into two categories isolated and non-isolated. In DC-DC converter topologies, the built-in transformer is providing a viable solution to achieve a high voltage conversion ratio [65], [69]. In built-in transformer technique, one winding direct connected to load, and energy is transferred to another magnetic coupling to achieve the high voltage conversion ratio. The coupled inductor is another solution to increase the voltage conversion ratio [65]. To limit the falling rate of diode current and to minimize the reverse recovery problem, leakage inductance utilized. To achieve a high conversion ratio and to minimize the current ripple, coupled inductors are an alternative solution to skip transformer.

There are many applications where electrical isolation is not necessary and require. Therefore, for these types of applications, non-isolated converters are the best solution to achieve high voltage—both tapped and untapped inductive coupling used in the DC-DC converters. In [140]–[142], a complete review of tapping DC-DC converter and its types discussed.

In [143], coupled inductor-based converter flying structure with the common ground discussed for the step-up applications. The power circuit of the converter discussed in [143] shown in Fig. 17(a). By using a coupled inductor, it is easy to achieve a high conversion ratio; but due to leakage inductance, the converter efficiency decreased. Also, high voltage stress occurs across the switch; hence large rating switches are required—the converter derived by combining the front-
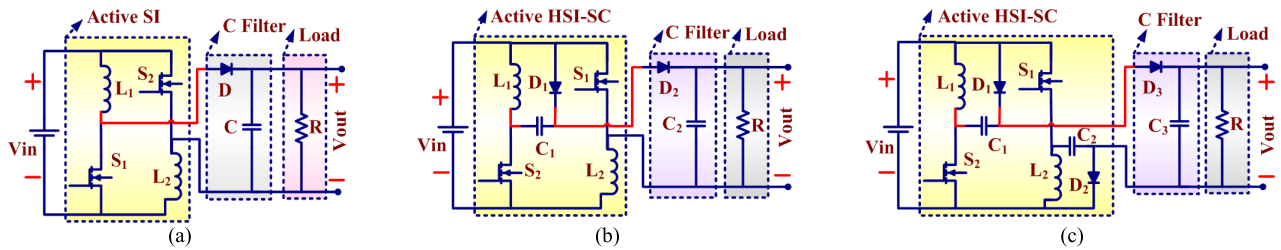
FIGURE 16. Step-Up DC-DC converter with two switches active switched inductor network (a) Converter-I (b) Converter-II (c) Converter-III.

end structure of the fly-back converter and C-filter by common grounding. Ideally, the boosting depends on the coupling factor, coupling ratio and duty cycle—the voltage conversion ratio provided in equation (36).

$$\frac{V_{out}}{V_{in}} = \frac{-D\left(1 + \frac{N_2}{N_1}\right)\left(\frac{K+1}{2}\right)}{1 - D} = \frac{-f_s T_{on}\left(1 + \frac{N_2}{N_1}\right)\left(\frac{K+1}{2}\right)}{1 - f_s T_{on}} \quad (36)$$

where N_2 and N_1 are Coupled inductor winding turns ratio, k is $L_m/(L_m + L_k)$, L_m and L_k coupled inductor magnetising and leakage inductance.

In [144], the coupled inductor is employed as a transformer to attain high voltage at the output terminal of the converter. The power circuit of the converter discussed in [128], [144] shown in Fig. 17(b). The high voltage achieved by adjusting the right turn's ratio and duty cycle. Coupled inductor network of this converter is similar to HSI-SC. The primary side winding is acting as a filter, and secondary side winding operates as a series voltage source. The power circuit of the converter divided into three stages; HSI-SC with the coupled inductor, switching stage and C-filter. It is possible to integrate both coupled inductors with the single magnetic core to reduce the size of the converter.

The coupled inductor based DC-DC high step-up converters are proposed with SC or charge Pump [128], [144]–[146]. The power circuit of the converter discussed in [128] shown in Fig. 17(c). The converter divided into three main stages; FEBC with the coupled inductor, HSI-SC, Intermediate inductance and C-filter stages. Here, the intermediate stage designed by using the coupled inductor. It is an active clamp circuit, and it helps to recycle the energy. High voltage readily achieved by adjusting the turn's ratio and the duty cycle. The converters have high voltage stress, and losses due to leakage induce energy.

The hybrid combination of the conventional boost converter and fly-back converter (Hybrid-Boost-Fly-back Converter) are discussed in [144], [147], [148]. The power circuit of the converter discussed in [144], [147] shown in Fig. 17(d). The converter divided into four stages; Front end structure of fly-back, switching stage and two C-filter. With this converter, transformer of fly-back converter and inductor of boost converter combined, and the outputs of both converters are

connected in series to extend the range of voltage conversion ratio with reduced switch stress.

In [148], the high step-up boost converter integrated with transformers which act as an auxiliary circuit. The power circuit of the converter discussed in [148] depicted in Fig. 17(e). The converter circuit derived by combining the auxiliary circuit on the top of the boost converter. The auxiliary circuit integrated with the transformer and capacitors to avoid broad input current ripple. Due to a simple structure, the doubler employed in the auxiliary circuit to step-up the voltage. The quasi-resonant mode of operation makes the current sinusoidal due to the resonant tank formed by transformer and capacitors. The converter divided into three stages; FEBC structure, resonant tank circuit and C-filter. This converter provides a viable solution to achieve high voltage by adjusting turns of a transformer.

In [149], Quadratic Boost Converter (QBC) is proposed with the coupled inductor to obtain a high voltage conversion ratio. The power circuit of the converter depicted in Fig. 17(f). The converter divided into four stages. First two stages are conventional boost converter which forms a QBC, the third stage is HSI-SC with the coupled inductor, and the fourth stage is the C-filter. This converter combines the function of QBC, coupled with inductor and HSI-SC.

Tapped Buck Converter (TBC) discussed, which provides a lossless clamping [115], [150]. The additional lossless clamp circuit is employed to recover the voltage spike of the switch. The power circuit of the converter discussed in [115], [150] depicted in Fig. 17(g). The converter divided into two stages; one is HSI-SC, and another is a buck converter. The standard coupling provided between inductor of HSI-SC and buck converter. The voltage conversion ratio of the TBC given in equation (37).

$$\frac{V_{out}}{V_{in}} = \frac{D}{D + N(1 - D)} = \frac{f_s T_{on}}{f_s T_{on} + N(1 - f_s T_{on})} \quad (37)$$

where N is winding ratio.

In [151], a new high step-up converter with multiplier stage proposed in which two capacitors are charged in parallel and discharged in series with energy stored in the inductor. Also, using clamp circuit leakage energy of the coupled inductor is recycled. The power circuit of the converter discussed in [151] shown in Fig. 17(h). The converter divided into
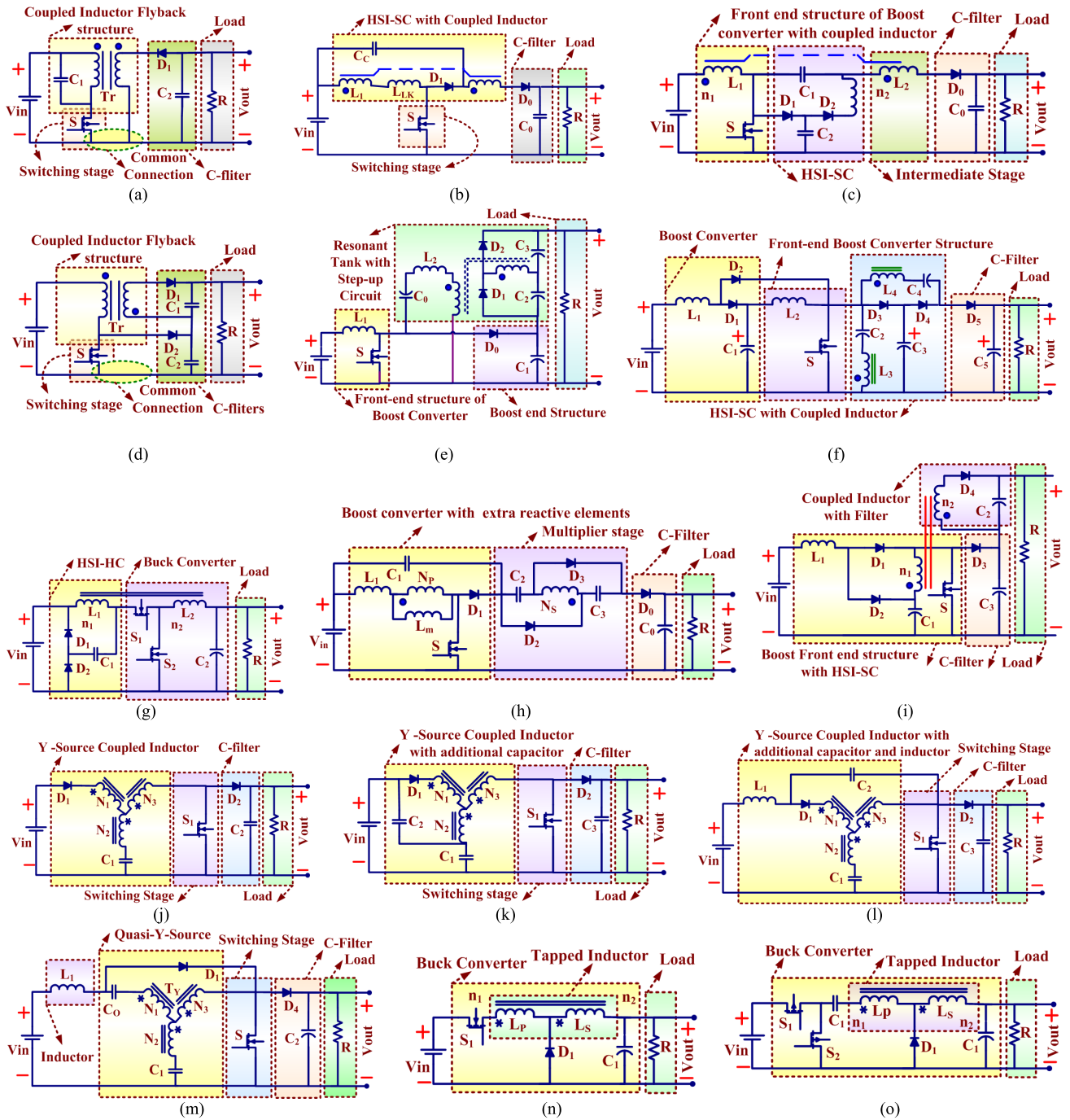
FIGURE 17. Transformer and Coupled Inductor Based Converter (a) Coupled inductor based fly- back structure (b) High step-up boost converter with coupled inductor (c) Coupled inductor based dc-dc high step-up converter with charge pump (d) Hybrid-boost- fly-back-converter (e) High step-up boost converter integrated with a transformers (f) Quadratic Boost Converter (QBC) with couple inductor (g) Tapped buck converter (h) High step-up converter with multiplier stage (in) Quadratic Boost Converter with coupled inductor at second stage (j) Y-source DC-DC converter with discontinuous current. (k) Y-source DC-DC converter with continuous current with additional capacitor. (l) Y-source DC-DC converter with continuous current with additional capacitor and inductor (m) Quasi-Y-source converter (n) Buck converter with tapped coupled inductor (o) Tapped buck converter.

three stages; one is a boost converter with additional reactive elements, second is the multiplier stage designed by the coupled inductor, and the third stage is the C-filter. Moreover, the low resistance power control switch is adopted to reduce the losses.

In [152], Quadratic Boost Converter (QBC) proposed to attain a high voltage conversion ratio. The power circuit of the converter discussed in [152] shown in Fig. 17(i). The converter divided into three stages; first is front end structure with HSI-SC, the second stage is the boost converter with

the coupled inductor, and the third stage is the C-filter. The converter provides a high voltage at the output with less voltage across the switch. Moreover, the conversion ratio of the converter quickly increased by adjusting the coupling factor.

In [153]–[156], DC-DC Z source and Y-source based converter proposed for high conversion ratio. The power circuit of the converter discussed in [154] shown in Fig. 17(j). The converter divided into three stages; Y-source impedance network, switching stage and C-filter. It comes into all the advantages of the original Y-source converter. Moreover, the converter provides a high voltage conversion ratio even with lesser duty cycle. The drawback of the converters is discontinuous and pulsating current which is not suitable for most of the practical application.

In [154]–[156], to overcome the drawback of discontinuous current, a new DC-DC Y-source converter is proposed with simple modification by adding a capacitor to smoothen the current. The power circuit of the converter discussed in [155] shown in Fig. 17(k). The converter divided into three stages; Y-source network with an additional capacitor in parallel, switching stage and C-filter. The modified network provides a continuous current, but only when capacitors set on the perfect and appropriate value. The converter faces the problem of high inrush current due to input parasitic reactance.

In [153]–[156], a new DC-DC Y-source converter is proposed with additional inductor and capacitor at the input side to smoothen the current. The power circuit of the converter shown in Fig. 17(l) and divided into three main stages; the first stage is Y-Source network with additional inductor and capacitor, the second stage is the switching stage, and the third stage is C-filter. Unfortunately, this converter has high voltage stress across the devices.

In [153]–[156], DC-DC converter proposed with another technique by employing quasi-Y-source network to smoothen the current by adding one additional capacitor and inductor. The power circuit of the Quasi–Y-Source boost converter shown in Fig. 17(m). The converter divided into three stages; the first stage is Quasi-Y-Source, the second stage is the switching stage, and the third stage is C-filter. This converter has a high conversion ratio and continuous input current. To prevent the core from saturation, two capacitors placed in such a way that they block the dc-current flowing through the coupled inductor.

Buck converter proposed with the tapped coupled inductor [150], [157]–[159]. The voltage conversion ratio adjusted by changing the tapping of the inductors. This technique also reduces the switching losses and conduction losses, but high voltage spike occurs across the switches due to leakage inductance of coupled inductors. The power circuit of the converter discussed in [150], [158] shown in Fig. 17(n). The converter combines the features of the buck converter and the tapped coupled inductor.

In [159], [160], a new tapped buck converter proposed; the high step-down ratio achieved compared to the conventional buck converter. This converter designed by employing the active clamp circuit for voltage spike problem. A clamped capacitor connected in series with the tapped coupled inductor winding. The power circuit of the converter discussed in [160] shown in Fig. 17(o). This converter combines the features of tap inductor, active clamp circuit and buck converter.

In [161], Interleaved Boost Converter (IBC) proposed with the coupled inductor and Switched Capacitor (SC). The power circuit of the converter discussed in [161] depicted in Fig. 18(a). The switched capacitor used to increase the voltage conversion ratio and to reduce the stress of the switch. Switching losses reduced due to Zero Voltage Transition (ZVT) throughout the switching cycles. The converter divided into three stages; the first stage is interleaved boost converter with coupled inductor; the second stage is the switched capacitor, and the third stage is the C-filter.

In [162], Interleaved Boost Converter (IBC) proposed with a voltage multiplier cell. The high conversion ratio achieved by adjusting the coupled ratio of the inductor and duty cycle. To design the converter, low rating switch and small inductor are suitable due to current sharing capability at the input side. The power circuit of the converter discussed in [162] depicted in Fig. 18(b). The converter divided into three stages. The first stage is the interleaved converter with the coupled inductor, the second stage coupled inductor stage or voltage multiplier, and the third stage is C-filter. The voltage multiplier circuit designed by utilizing two secondary of the coupled inductor, one diode and one capacitor. The converter performance increased due to the Zero Current Technique (ZCT), which reduces switching losses and EMI.

In [163], a new interleaved boost converter proposed with a built-in transformer. The power circuit of the converter discussed in [163] shown in Fig. 18(c). The full-bridge rectifier circuit is employed with the interleaved structure to design the circuit. Leakage of the transformer limits the recovery current of the bridge—high efficiency confirmed by the soft-switching technique. The converter divided into three stages. The first stage interleaved boost converter; the second stage coupled inductor as an intermediate stage, and the third stage is the rectifier with filter.

In [164], to achieve a high voltage conversion ratio and ZCS, a new interleaved winding coupled inductor boost converter proposed. The voltage conversion ratio easily changed by changing the turns of the coupled inductor. The practical clamp circuit utilized to limit the voltage stress of a switch. The ZCS achieved due to leakage inductance of coupled inductor; hence switching losses are reduced. The power circuit of the converter discussed in [164] shown in Fig. 18(d). The converter divided into three stages. The first stage is the interleaved converter with the coupled inductor, the second stage coupled inductor network, and the third stage is the C-filter.

The Interleaved Boost Converter (IBC) proposed with a built-in transformer voltage doubler cell to step-up the voltage [165]. Three windings, two diodes and two capacitors used to design built-in transformer voltage doubler cell. The
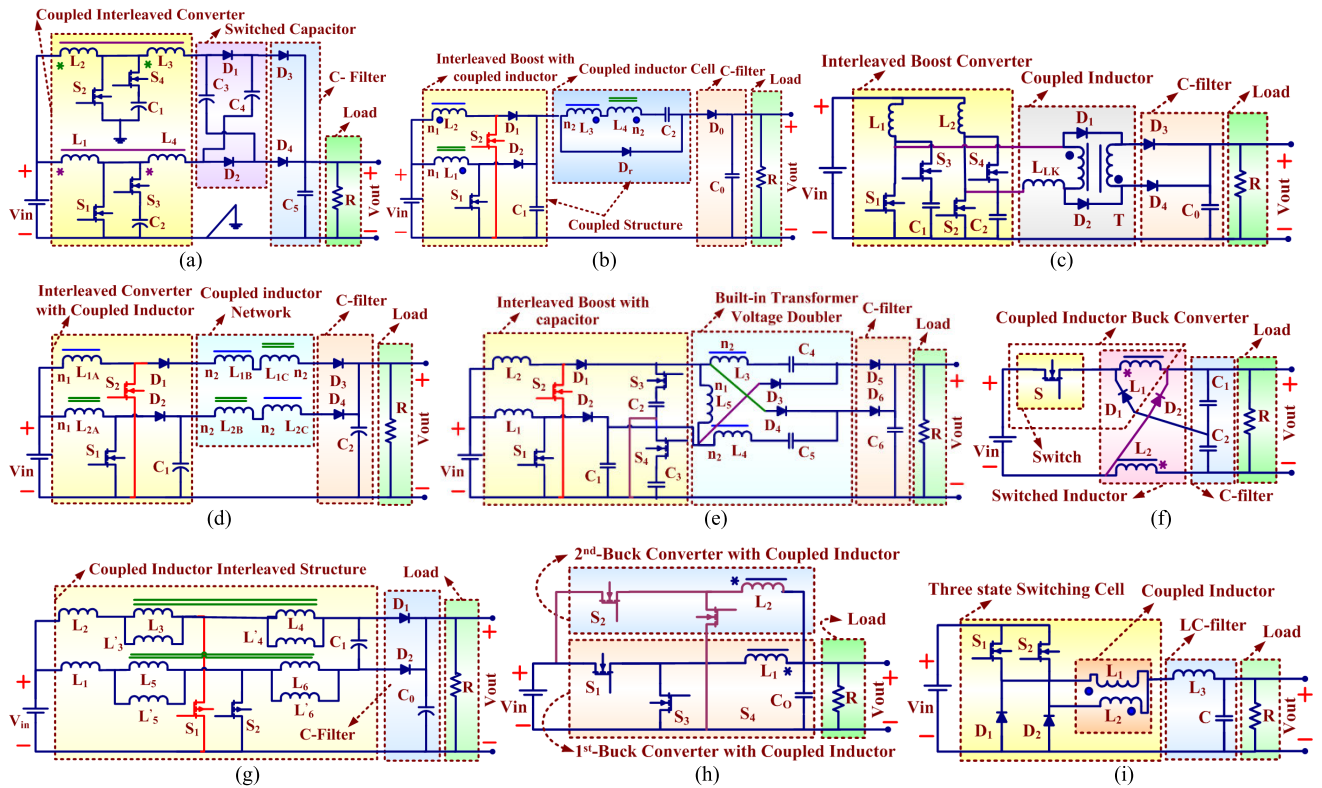
FIGURE 18. Transformer and coupled inductor based Interleaved converter (a) Interleaved converter with coupled inductor and switched capacitor (b) Interleaved converter with multiplier cell (c) Interleaved converter with built-in transformer (d) Interleaved winding coupled inductor Boost converter (e) Interleaved boost converter with built-in transformer voltage doubler cell (f) Switched coupled inductor based buck converter (g) Interleaved Boost converter with coupled inductor. (h) Interleaved buck converter is proposed with coupled inductor (i) Buck Converter with three states switching.

capacitors are charged in parallel and discharged in series to double the voltage. The power circuit of the converter discussed in [165] shown in Fig. 18(e). The converter divided into three stages; the first stage is interleaved boost converter with an additional capacitor, the second stage is the built-in transformer voltage doubler, and the third stage is the C-filter. The active clamp technique is used in the converter to recycle the leakage energy.

In [166], switched coupled inductor based buck converter proposed. The power circuit of the converter shown in Fig. 18(f). The filter of the conventional buck converter replaced by the coupled inductor and diodes. The power circuit of the converter divided into three stages; the first stage is the switching device which used to control the output voltage; the second stage coupled Switched Inductor (SI), and the third is the capacitive filter. Leakage energy recovered without using clamp circuitry.

In [167], Interleaved Boost Converter (IBC) proposed with the coupled inductor. The power circuit of the converter discussed in [167] shown in Fig. 18(g). The intermediate capacitor snubber is employed to reduce switching losses of the converter and to improve the efficiency. In [168]–[171], the interleaved buck converter proposed with the coupled inductor. The power circuit of the converter discussed in [169] shown in Fig. 18(h). The converter provides the less output

current ripple, and the inductor current ripple is depending on the coupling of inductors. In [172], the multilevel buck converter proposed by using several active switches for high voltage step-up application. In [151], [173] buck converter is proposed by the three state switching cells to reduce the current peak of the active switch—the three-state switching cell designed by using the two coupled inductors, two diodes and two switches. The power circuit of the converter discussed in [151], [173] shown in Fig. 18(i). Converter divided into two stages; the first stage is the three-state switching cells, and another stage is LC filter. Three-stage switching cells are employed to reduce ripple and current peak.

VIII. LUO CONVERTERS
In the last decades, a Luo DC-DC converter is one of the famous converter families in power electronics, which provides a suitable solution to achieve a high conversion ratio. Voltage lift technique is employed to overcome the effect of the parasitic element in the power circuit of the Luo converter [174]–[178]. The Luo converter power circuits are simple and easily extendable, and it also provides a high voltage with reasonable efficiency and high density.

Many Luo DC-DC converter topologies addressed in the literature based on the Switched Inductor (SI), Switched Capacitor (SC), self-lift, re-lift, triple-lift, quadruple-lift etc.

All the lift stages derived by utilizing the Switched Inductor (SI) and Switched Capacitor (SC) concept with the conventional DC-DC converter [174], [175].

In [174]–[176], Positive output re-lifts Luo converter presented with two controlled power switches. This converter provides a high positive conversion ratio by employing a re-lift structure. The power circuit of the positive re-lift Luo converter shown in Fig. 19(a). The converter divides into three main stages; FEB-BC, re-lift, and LC-filter stages. The re-lift circuit derived by combining the structure of switched capacitor and HSI-SC. This converter provides two times voltage conversion ratio compared to traditional boost converters. The voltage conversion ratio of the converter given in equation (38).

$$\frac{V_{out}}{V_{in}} = \frac{2}{1-D} = \frac{2T}{T-T_{on}} = \frac{2}{1-f_s T_{on}} \qquad (38)$$

In [174]–[176], positive output, triple-lift Luo converter presented with two controlled power switches. This converter provides a high positive conversion ratio by employing a triple-lift structure. The power circuit of the positive triple-lift Luo converter shown in Fig. 19(b). The converter circuit is divide's into three main stages; FEB-BC, triple-lift, and LC-filter stages. The triple-lift circuit derived by combining the structure of switched capacitor and double-stage HSI-SC. This converter provides three times higher voltage conversion ratio compared to the traditional boost converter. The voltage conversion ratio of the converter given in equation (39).

$$\frac{V_{out}}{V_{in}} = \frac{3}{1-D} = \frac{3T}{T-T_{on}} = \frac{3}{1-f_s T_{on}} \qquad (39)$$

In [174]–[176], positive output quadruple-lift Luo converter is presented with two controlled power switches. This converter provides a high positive conversion ratio by employing the quadruple-lift structure. The power circuit of the positive quadruple-lift Luo converter shown in Fig. 19(c). The converter divides into three main stages; FEB-BC, quadruple-lift, and LC-filter stages. The quadruple-lift circuit derived by combining the structure of switched capacitor and Triple-stage HSI-SC. This converter provides four times voltage conversion ratio compared to the traditional boost converter. The voltage conversion ratio of the converter given in equation (40).

$$\frac{V_{out}}{V_{in}} = \frac{4}{1-D} = \frac{4T}{T-T_{on}} = \frac{4}{1-f_s T_{on}} \qquad (40)$$

In [174]–[176], the simplified re-lift structure is the design of the re-lift positive output Luo converter and used a single switch. The power circuit of the simplified re-lift Luo converter is shown by Fig. 19(d). The converter divided into two main stages; simplified re-lift structure and LC-filter stages. The simplified re-lift structure is designed by employing two HSI-SC with a self-lift structure or switched capacitor. This converter provides two times voltage conversion ratio compared to traditional boost converters. The voltage conversion

ratio of the converter given in equation (41).

$$\frac{V_{out}}{V_{in}} = \frac{2}{1-D} = \frac{2T}{T-T_{on}} = \frac{2}{1-f_s T_{on}} \qquad (41)$$

In [174]–[176], to use a single switch, the simplified triple-lift structure is used to design triple-lift positive output Luo converter. The power circuit of the simplified triple-lift Luo converter shown in 19(e). The converter divided into two main stages; simplified triple-lift and LC-filter stages. The simplified triple-lift structure is designed by employing three HSI-SC and simplified self-lift structure or switched capacitor. This converter provides a three times voltage conversion ratio compared to traditional boost converters. The conversion ratio of simplified positive output, triple-lift Luo converter is given in the equation (42).

$$\frac{V_{out}}{V_{in}} = \frac{3}{1-D} = \frac{3T}{T-T_{on}} = \frac{3}{1-f_s T_{on}} \qquad (42)$$

In [174]–[176], the simplified quadruple-lift structure used to design quadruple-lift positive output Luo converter to reduce switch count. The power circuit of the simplified quadruple-lift Luo converter shown in Fig. 19(f). The converter divided into two main stages; simplified quadruple-lift and LC-filter stages. The simplified quadruple-lift structure is designed by employing the four HSI-SC and the simplified self-lift structure or switched capacitor. This converter provides a four times voltage conversion ratio compared to the traditional boost converter. The conversion ratio of the converter given in equation (43).

$$\frac{V_{out}}{V_{in}} = \frac{4}{1-D} = \frac{4T}{T-T_{on}} = \frac{4}{1-f_s T_{on}} \qquad (43)$$

In [174], [177], the negative output Luo converter is proposed for the high negative voltage conversion ratio by combining the concept of negative simplified lift-techniques. The power circuit of the negative re-lifts Luo converter shown in Fig. 20(a). The converter divided into two stages; negative re-lift and LC filter stages. The negative re-lift structure derived by combining the circuit of two HSI-SC stages with the negative simplified self-lift technique. The power circuit of the negative triple-lift Luo converter shown in Fig. 20(b). The converter divided into two stages; negative, triple-lift structure and LC filter. The negative triple-lift structure derived by combining the circuit of three HSI-SC stages with negative simplified self-lift technique. The power circuit of the negative output quadruple-lift Luo converter shown in Fig. 20(c). The converter divided into two main stages; negative quadruple-lift structure, and LC filter. The negative quadruple-lift structure derived by combining the circuit of four buck-boost converters with negative simplified self-lift technique. The conversion ratio of negative output re-lifts, triple-lift and the quadruple lift Luo converter provided in equation (44)-(46), respectively.

$$\frac{V_{out}}{V_{in}} = \frac{-2}{1-D} = \frac{-2T}{T-T_{on}} = \frac{-2}{1-f_s T_{on}} \qquad (44)$$
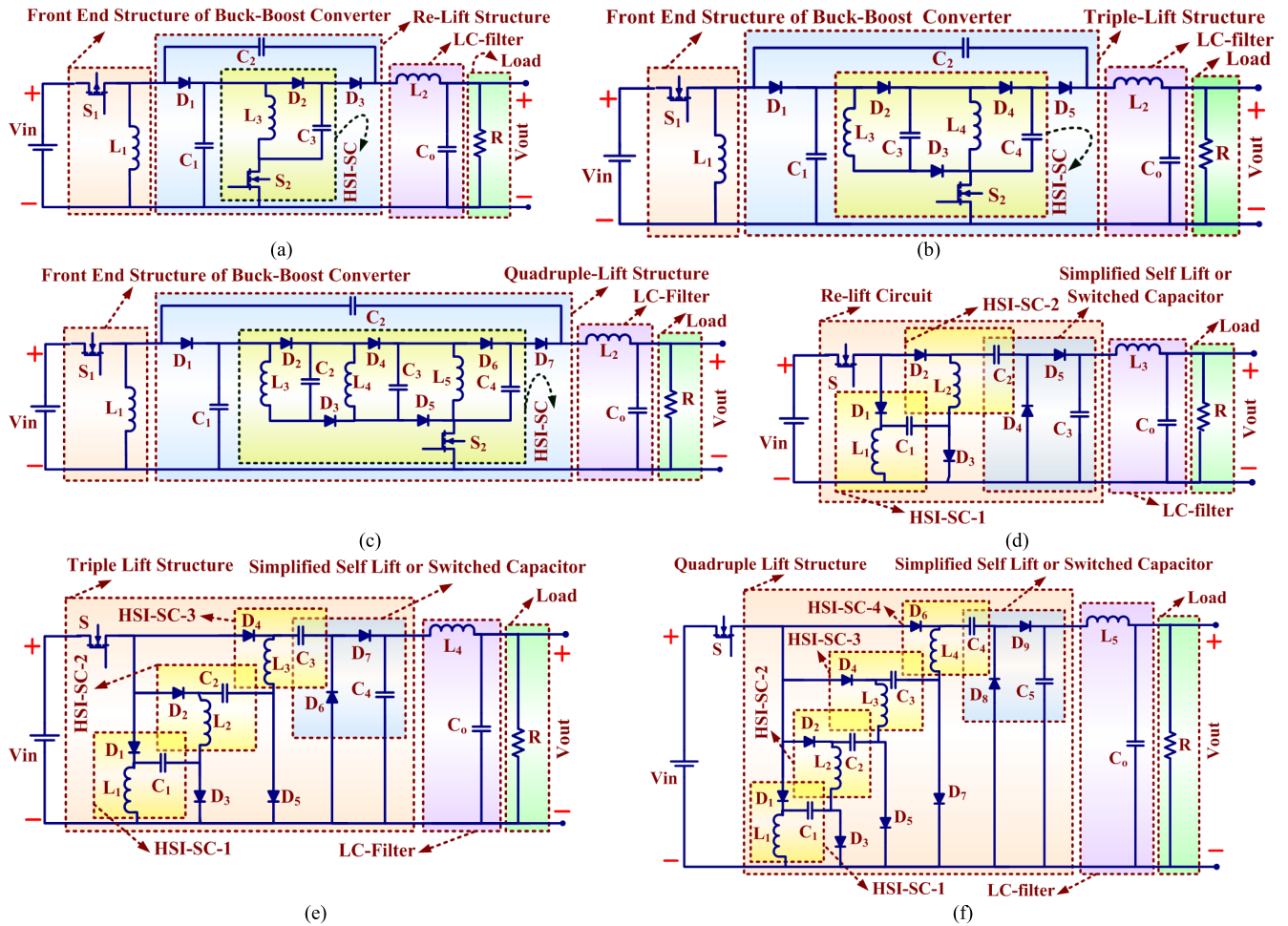
FIGURE 19. Positive Output Luo Converter (a) Re-lift Luo converter (b) Triple-lift Luo converter (c) Quadruple-lift Luo converter (d) Single switch Re-lift Luo converter (e) Single switch Triple-lift Luo converter (f) Single switch Quadruple-lift Luo converter.

$$\frac{V_{out}}{V_{in}} = \frac{-3}{1-D} = \frac{-3T}{T-T_{on}} = \frac{-3}{1-f_s T_{on}} \tag{45}$$

$$\frac{V_{out}}{V_{in}} = \frac{-4}{1-D} = \frac{-4T}{T-T_{on}} = \frac{-4}{1-f_s T_{on}} \tag{46}$$

IX. DC-DC MULTILEVEL/MULTIPLIER CONVERTER

To achieve high voltage conversion ratios, recently many topologies addressed by combining the feature of N-level voltage-multiplier or diode-capacitor networks with conventional DC-DC converters. The advantages of multilevel converters are: i) Less voltage stress across power device ii) High conversion ratio using moderate duty cycle iii) Easy to add several levels without touching the primary circuit iv) Modular structure v) Provides a viable solution to integrate with multilevel inverters vi) Few numbers of switches [179]–[181].

In [179]–[181], DC-DC step-up converter derived by combining the circuit of N-stage voltage multiplier (VMC) with the conventional buck-boost or boost converter for high step-up application. The power circuit of the boost converter with voltage multiplier shown in Fig. 21(a). Each stage consists

of two diodes and two capacitors. The output stages can easily add to increase the output voltage of the converter. The voltage stress across the switch is also less. This converter provides a non-inverting high voltage output and the voltage conversion ratio of the converter given in the equation (47), where N is the number of diode capacitor stages connected at the output of the converter. The power circuit of the converter divided into three sections (note: here section word is used to avoid confusion between numbers of multiplier stages and power converter stages); first section FEBC stage, the second section is diode-capacitor N-stages, and the last section is the C-filter. The conversion ratio of the converter depends on the number of stages and the duty cycle.

$$\frac{V_{out}}{V_{in}} = \frac{N-1}{1-D} = \frac{T(N-1)}{T-T_{on}} = \frac{N-1}{1-f_s T_{on}} \tag{47}$$

In [179]–[181], Cockcroft Walton Voltage Multiplier Cell (CW-VMC) based DC-DC converter topology proposed. The power circuit of the converter shown in Fig. 21(b). The converter divided into three sections; the first section is the single common source with four switches boost converter
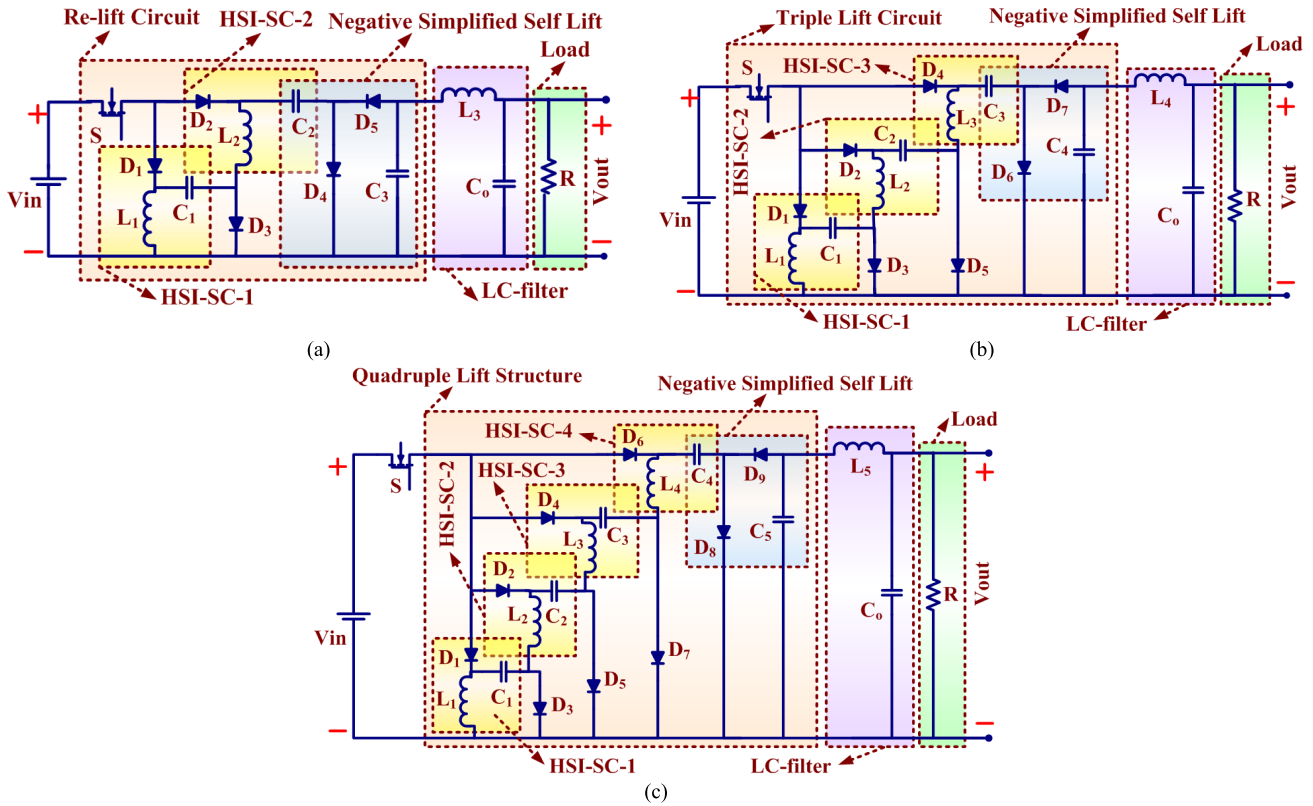
FIGURE 20. Negative Output Luo Converter (a) Re-lift Luo converter (b) Triple-lift Luo converter (c) Quadruple-lift Luo converter.

front end structure; the second section is N-stage voltage multiplier (VMC), and the third section is the C-filter. The converter derived by combining the features of voltage multiplier and four-switch boost converter. This converter provides a high voltage conversion ratio with a moderate duty cycle and without utilizing transformer and coupled inductor. The conversion ratio of the converter depends on the number of stages and the duty cycle—the voltage conversion ratio given in equation (48).

$$\frac{V_{out}}{V_{in}} = \frac{N}{1-D} = \frac{NT}{T-T_{on}} = \frac{N}{1-f_sT_{on}} \quad (48)$$

In [95], [182], two-switch voltage multiplier (VMC) is proposed and discussed without utilizing the magnetic components. The power circuit of the converter shown in Fig. 21(c). The filter capacitor is not required, since the series structure of the capacitor at the output side of the multiplier. The output voltage is dependent on the number of capacitors at the output. Two switches alternatively operated to boost the voltage.

In [183], the hybrid DC-DC converter is proposed based on the three-state switching cell, voltage multiplier and transformer. The power circuit of the converter shown in Fig. 21(d). Half of the output current is flowing through both switches. Hence low rating switches are suitable to design the converter. However, more output stage added to increase more the number of levels. High switching frequency is suit-

able to reduce the size, volume and current/voltage ripple of the converter.

In [184]–[190], new DC-DC converters proposed by combining the feature of conventional DC-DC converters and derived converter (Cuk and SEPIC) with Cockcroft Walton Voltage Multiplier (CW-VMC). The main feature of these converters is: i) High voltage conversion ratio achieved without using a transformer and coupled inductor at moderate duty cycle ii) Low voltage stress iii) Single switch topologies iv) Extendable structure (easy to extend the number of levels) without modifying the circuit of the conventional converter v) Self-balance structure. Two diodes and two capacitors are required to increase one stage of the converter. The power circuit of the Nx Multilevel Boost Converter (Nx MBC), Multilevel Buck-Boost Converter (MBBC) Multilevel Cuk Converter, Multilevel SEPIC Converter is shown in Fig. 21(e)-(h), respectively. The Nx Multilevel Boost Converter (MBC) gives N-times higher conversion ratio compared to a conventional boost converter [184], [185]. The voltage conversion ratio of MBC provided in equation (49). The conversion ratio of MBBC and multilevel Cuk converter is the same and provided in equation (50).

$$\frac{V_{out}}{V_{in}} = \frac{N}{1-D} = \frac{TN}{T-T_{on}} = \frac{N}{1-f_sT_{on}} \quad (49)$$

$$\frac{V_{out}}{V_{in}} = -(\frac{1+(N-1)D}{1-D}) = -(\frac{1+(N-1)f_sT_{on}}{1-f_sT_{on}}) \quad (50)$$
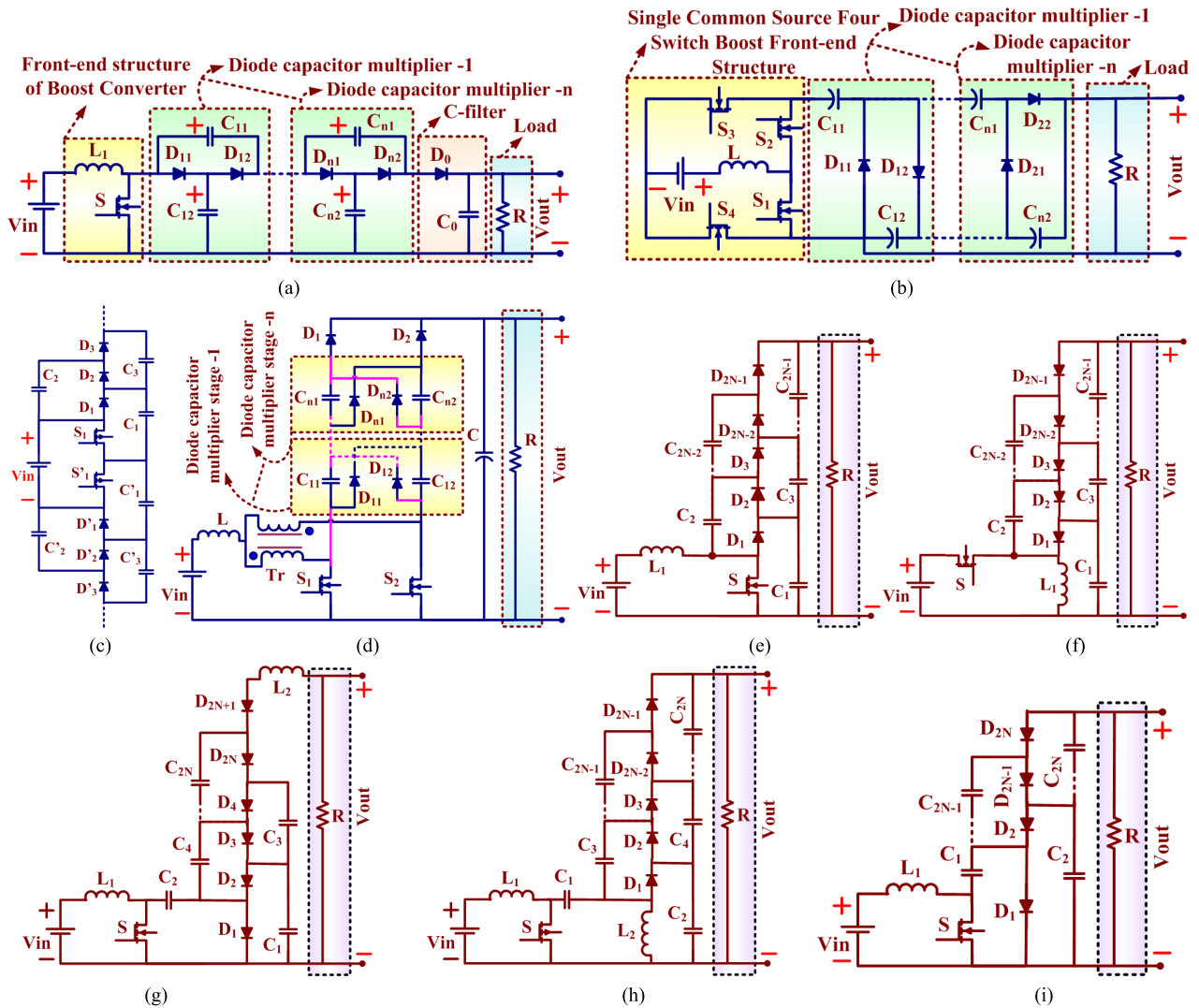
FIGURE 21. Multilevel converters based on diode-capacitor multiplier network or Cockcroft Walton (CW) multiplier (a) DC-DC step-up converter with n-stage Voltage Multiplier Cell (VMC) (b) Cockcroft Walton Voltage Multiplier Cell (CW-VMC) based DC–DC converter topology (c) Two-switch voltage multiplier (VMC) without utilizing the magnetic components (d) Hybrid DC-DC converter based on the three state switching cell (e) Nx Multilevel Boost Converter (Nx MBC) (f) Nx Multilevel Buck-Boost Converter (Nx MBBC) (g) Nx Multilevel Cuk Converter (h) Nx Multilevel SEPIC Converter (i) Inverting Nx Multilevel Boost Converter (Inverting Nx MBC).

The conversion ratio of Multilevel SEPIC converter is provided by the equation (51).

$$\frac{V_{out}}{V_{in}} = \frac{1 + (N-1)D}{1-D} = \frac{1 + (N-1)f_s T_{on}}{1 - f_s T_{on}} \quad (51)$$

To achieve the inverting voltage, a new inverting Nx MBC proposed in [191]. The power circuit of the converter shown in Fig. 21(i). This converter combines the feature of the conventional boost converter and negative Voltage Multiplier Cell (negative VMC). This converter provides an inverting N-times higher conversion ratio compared to a conventional boost converter with low switch stress across the switch—the voltage conversion ratio provided in equation (52).

$$\frac{V_{out}}{V_{in}} = \frac{-N}{1-D} = \frac{-TN}{T - T_{on}} = \frac{-N}{1 - f_s T_{on}} \quad (52)$$

In [192], SI concept is employed in DC-DC Multilevel Boost Converter (MBC) to achieve a high conversion ratio with the reduced number of levels and a single switch. The power circuit of the Switched Inductor Multilevel Boost Converter (SI-MBC) shown in Fig. 22(a).

The SI-MBC combines the features of a Switch Inductor (SI) and Voltage Multiplier Cell (VMC) with a conventional boost converter. For increasing the conversion ratio, the number of levels increased by adding more stage of multiplier without modifying the switched inductor structure. This converter gives a high conversion ratio compared to MBC. The conversion ratio of the SI-MBC given in equation (53).

$$\frac{V_{out}}{V_{in}} = \frac{N(1+D)}{1-D} = \frac{N(T + T_{on})}{T - T_{on}} = \frac{N(1 + f_s T_{on})}{1 - f_s T_{on}} \quad (53)$$
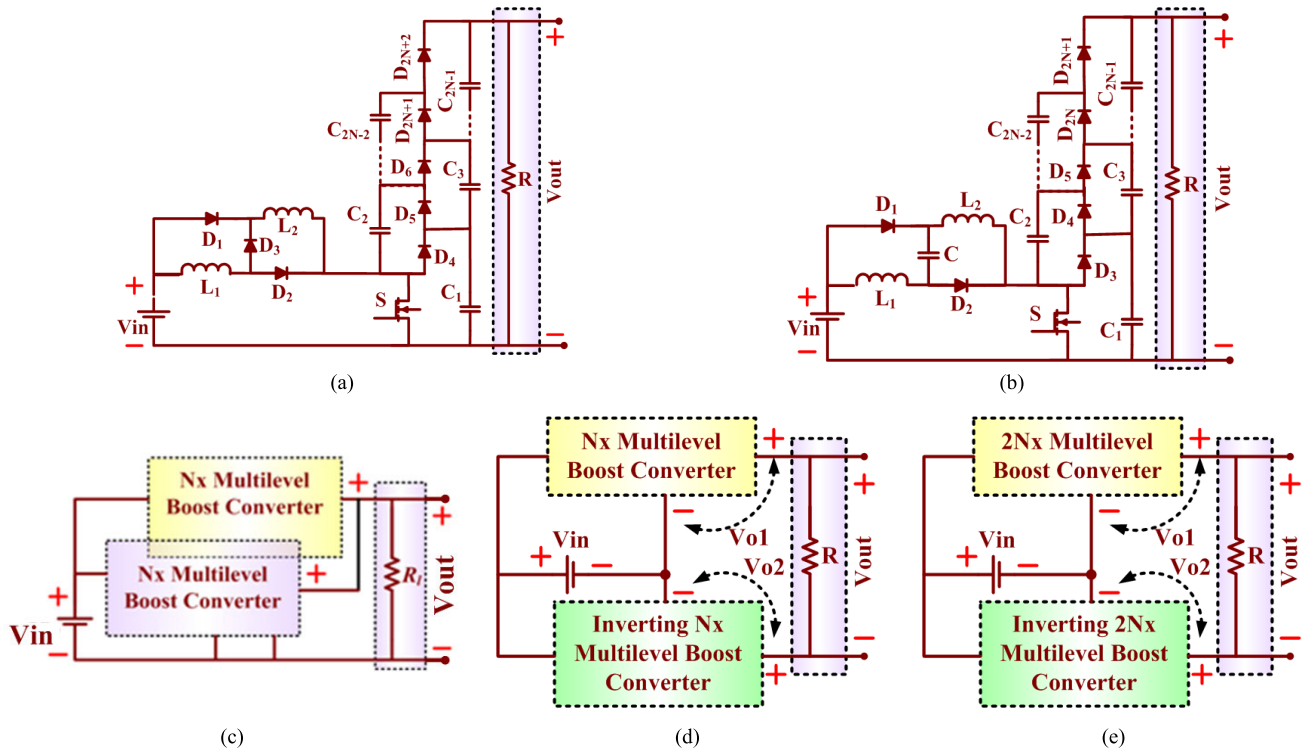
FIGURE 22. Advanced multilevel converter based on diode-capacitor multiplier network or Cockcroft Walton (CW) Multiplier (a) Switched Inductor Multilevel Boost Converter (SI-MBC) (b) Inverting Nx Multilevel Boost Converter (Inverting 2Nx MBC) (c) Nx Interleaved Multilevel Boost Converter (Nx IMBC) (d) 2Nx Interleaved Multilevel Boost Converter (2Nx IMBC) (e) 4Nx Interleaved Multilevel Boost Converter (4Nx IMBC).
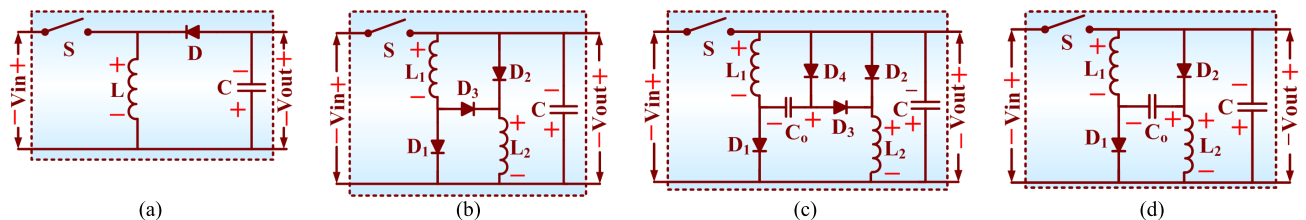
FIGURE 23. Stages of X-Y Converter Family (a) L-converter or BBC (b) 2L-Converter or SI BBC (c) 2LC-Converter or VLSI BBC (d) 2LC$_m$-converter $_m$VLSI BBC.

In [193], inverting 2Nx converter is proposed to achieve a high negative voltage conversion ratio. This converter combines the feature of the Voltage-Lift Switched-Inductor (VLSI, category of HSI-SC), voltage multiplier with the conventional boost converter. The power circuit of the inverting 2Nx Multilevel Boost Converter (Inverting 2Nx MBC) shown in Fig. 22(b). For increasing the conversion ratio, the number of levels increased by adding a more significant number of stages of multiplier without modifying the HSI-SC cell. This converter provides a higher conversion ratio compared to the Nx MBC. The voltage conversion ratio of the converter provided in equation (54).

$$\frac{V_{out}}{V_{in}} = \frac{-2N}{1-D} = \frac{-2NT}{T-T_{on}} = \frac{-2N}{1-f_sT_{on}} \quad (54)$$

In [194], Nx Interleaved Multilevel Boost Converter (Nx IMBC) proposed to reduce the input current ripple with a high
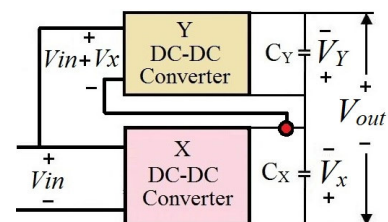
FIGURE 24. Universal structure of X-Y Converter.

conversion ratio. This converter provides a better dynamic behaviour as compared to the conventional boost converter and Multilevel Boost Converter (MBC); however, it required a large number of capacitor and diodes. The power circuit of the Nx-IMBC shown in Fig. 22(c). This converter derived by combining the two MBC in an interleaving way. The conversion ratio of the Nx-IMBC is equal to Nx-MBC. The advantage of the converter is high voltage gain with reduced
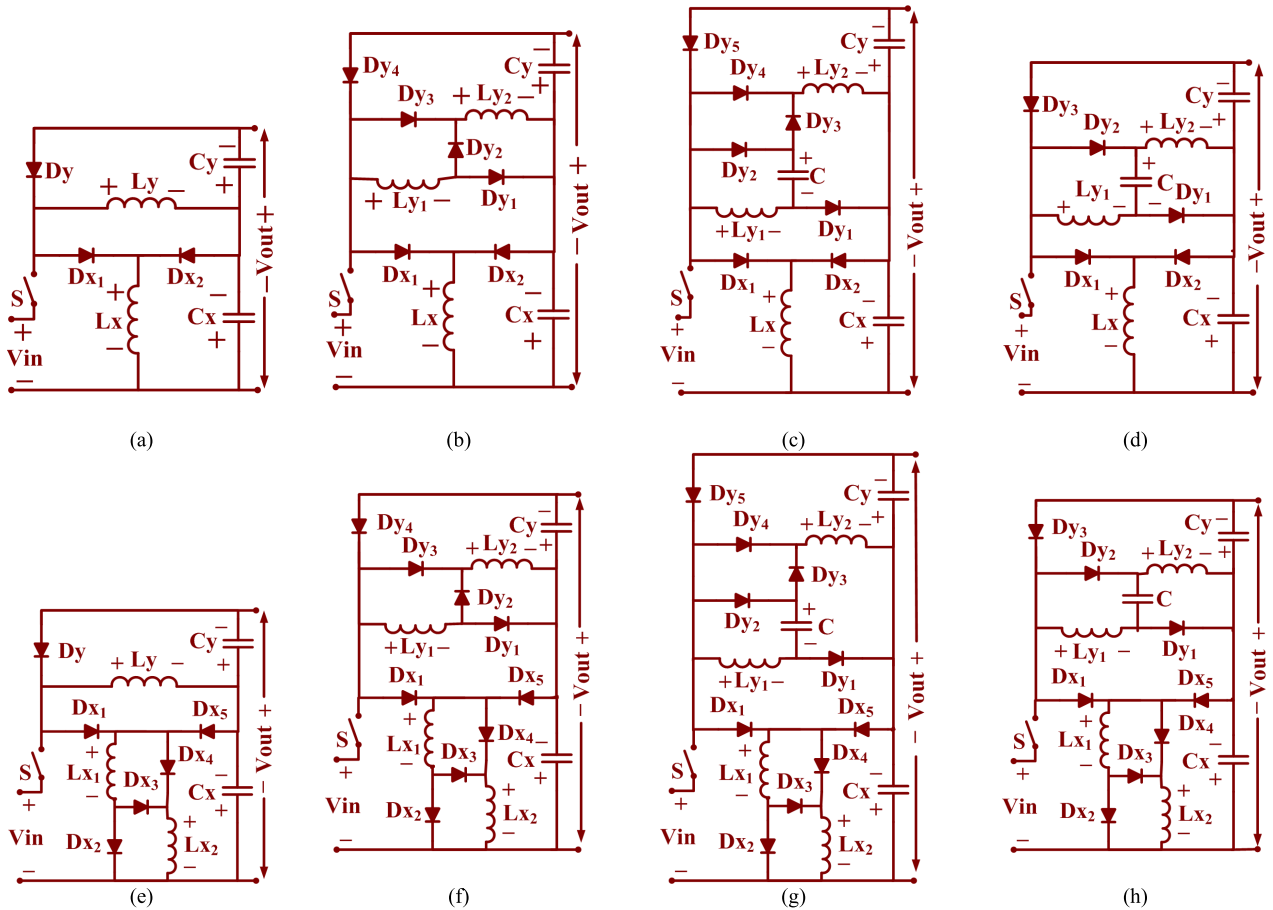
FIGURE 25. Power Circuit of X-Y converter topologies (a) L-L power converter (b) L-2L power converter (c) L-2LC power converter (d) L-2LCm power converter (e) 2L-L power converter (f) 2L-2L power converter (g) 2L-2LC power converter (h) 2L-2LC$_m$ power converter.

input ripple. However, this converter requires a large number of switches.

In [195], a new 2Nx Interleaved Multilevel Boost Converter (2Nx IMBC) proposed to increase the voltage conversion ratio of the interleaved converter. This converter provides two times conversion ratio compared to Nx-IMBC. The power circuit of the 2Nx-IMBC shown in Fig. 22(d).

In [196], a new 4Nx Interleaved Multilevel Boost Converter (4Nx-IMBC) proposed to increase the voltage conversion ratio of the interleaved converter. This converter provides four times conversion ratio compared to Nx-IMBC. The power circuit of the 4Nx-IMBC shown in Fig. 22(e). 4Nx-IMBC converter combines the feature of HSI-SC, the Voltage Multiplier (VMC) and interleaved converter.

In general, DC-DC MBC is the best solution to achieve a high voltage conversion ratio without utilizing transformer and coupled inductor at a moderate duty cycle. These converters are an extension of the conventional boost converter without increasing the number of inductors. A fewer number of switches used and to design a multilevel converter.

X. X-Y CONVERTER FAMILY

X-Y converter family (a new breed of the buck-boost converter) is proposed for high voltage step-up applications to overcome the drawback of DC-DC multilevel converters, cascaded converters and isolated converters [197]–[200]. The proposed X-Y power converter family can offer a higher output voltage by using the minimum number of semiconductor devices and reactive components. These converters are best suitable for application which requires DC-DC conversion with high conversion ratio; such as the vehicular power train, automotive application, renewable energy application, fuel cell application and DC-link applications.

Sixteen configurations proposed for the X-Y family. These converters are two-stage converter topologies and derived by combining the features of the Switch Inductor (SI or 2L), voltage-lift-switch-inductor (VLSI or 2LC) and modified voltage-lift-switch-inductor ($_m$VLSI or 2LC$_m$). Four new converter topologies derived from designing the stages of the X-Y converter family by using the structure of buck-boost converter, SI or 2L, VLSI or 2LC and $_m$VLSI or 2LC$_m$.

The special conspicuous features of the X-Y converter family [197]–[203] are:

- Single control switches
- Provide negative output voltage
- Non-isolated topologies
- High voltage conversion ratio without high duty cycle.
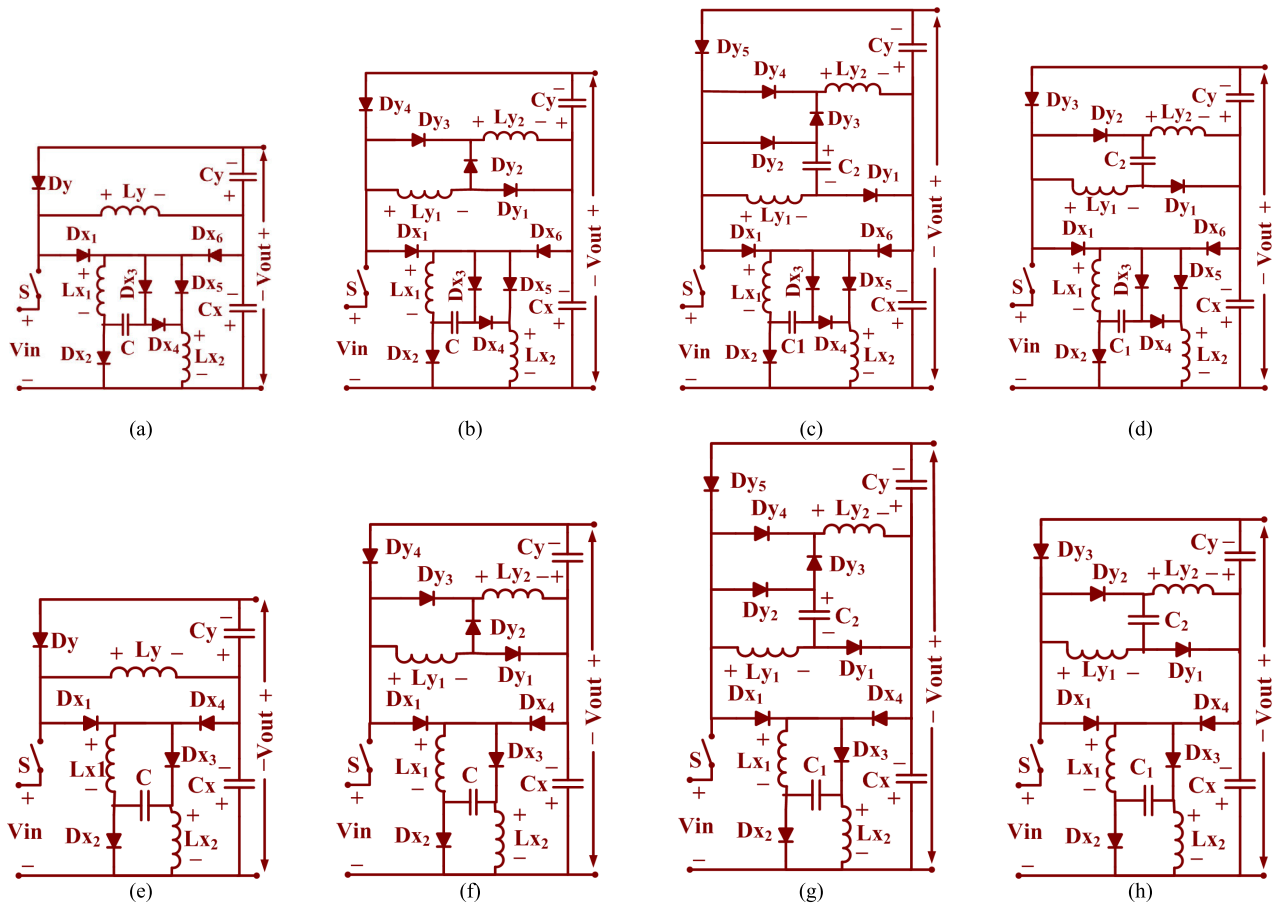- Modular structure.

FIGURE 26. Power circuit of XY converter topologies (a) 2LC-L power converter, (b) 2LC-2L power converter, (c) 2LC-2LC power converter, (d) 2LC-2LCm power converter, (e) 2LCm-L power converter, (f) 2LCm-2L power converter, (g) 2LCm-2LC power converter, h) 2LCm-2LCm power converter.

Fig. 23(a) shows the power circuit of conventional Buck-Boost Converter (BBC or L converter). Fig. 23(b) shows the power circuit of Switched Inductor Buck-Boost Converter (SI-BBC) or 2L converter. The 2L converter is a step-up converter and derived by combining the features of the Switched Inductor (SI or 2L) and conventional BBC. Fig. 23(c) shows the power circuit of Voltage–Lift-Switched-Inductor Buck-Boost Converter (VLSI BBC) or 2LC converter. 2LC converter is a step-up converter and derived by combining the features of the Voltage-Lift-Switched Inductor (VLSI or 2LC) and conventional BBC. Fig. 22(d) shows the power circuit of a modified Voltage-Lift-Switched-Inductor Buck-Boost Converter (modified VLSI BBC) or 2LCm converter. 2LCm converter is a step-up converter and derived by combining the features of modified Voltage-Lift-Switched-Inductor (modified VLSI or 2LCm) and conventional BBC.

Fig. 24 shows the universal structure of the X-Y converter family [197]–[203]. Two separate converter stages named as an X-converter and Y-converter is used to design topologies of X-Y family. The X-converter is directly fed by input power supply and the input of the Y-converter is algebraic addition of the output voltage of the X-converter and input supply. The inverting output voltage appears at the output terminal,

which is equal to the inverting sum of the output voltage of X and Y converter. The output voltage of the X-Y converter is calculated by using equation (55).

$$V_{out} = -\left(V_x + V_y\right) \qquad (55)$$

In the X-Y converter family, a total of sixteen topologies formed by numerous appropriate grouping of the new BBCs (stages of X-Y converter) and the power circuits shown in Fig. 25(a)-(h) and Fig. 26(a)-(h) [197].

In [198], a new member of the X-Y family, named as novel L-Y converters proposed to attain the higher conversion ratio. Novel L-Y topologies formed by combining the features of Voltage Doubler (VD) with an L-Y converter group or family (topologies of X-Y converter). L-Y, 2L-Y, 2LC-Y and 2LCm-Y converters are four groups of X-Y converter family [201]–[203]. L-Y category of X-Y family consists of the L-L converter, L-2L converter, L-2LC converter and L-2LCm converter. In L-Y converter category; X converter is a conventional Buck-Boost converter (BBC or L Converter). Two separate converter stages named as L-Converter and Y-Converter used to derive new topologies of X-Y family. The input power supply directly feeds the L-converter, and the input of the Y-converter is the algebraic addition of the output voltage of
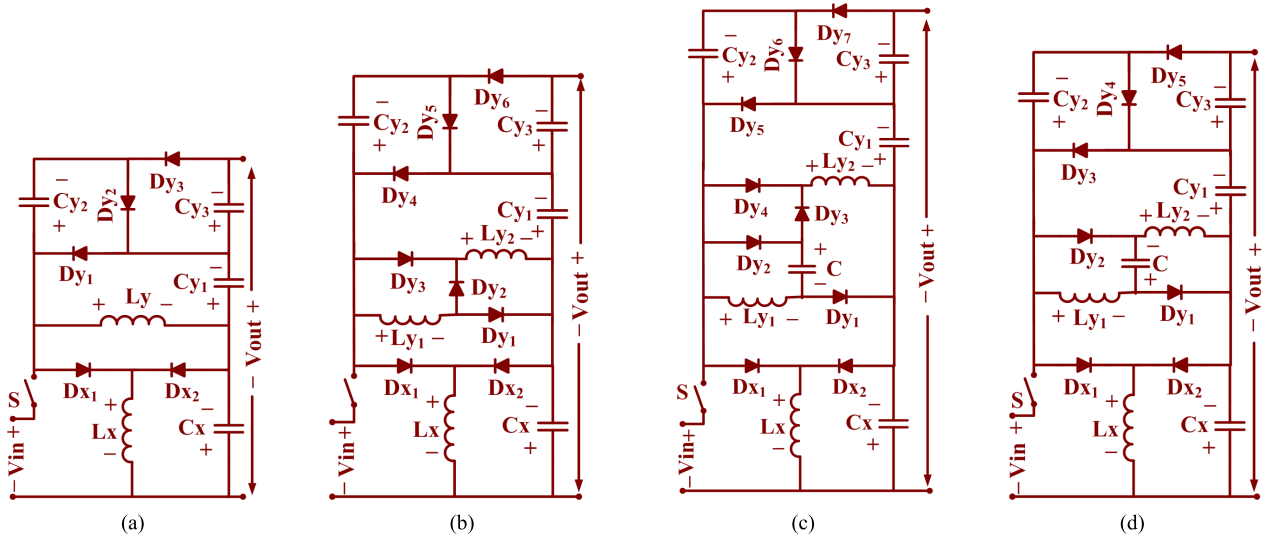
FIGURE 27. Power circuit of L-Y converter topologies (a) L-LVD power converter, (b) L-2LVD power converter, (c) L-2LCVD power converter, (d) L-2LCmVD power converter.

the L converter and input supply. The inverting output voltage appears at the output terminal, which is equal to the inverting sum of the output voltage of L and Y converter. The output voltage of L-Y converter calculated by using equation (56).

$$V_{out} = -(V_L + V_y) \qquad (56)$$

The power circuit of the novel L-Y converter topologies (L-LVD, L-2LVD, L-2LCVD and L-2LC$_m$VD converter) are shown in Fig. 27(a)-(d) [197]. These new L-Y converter member (L-LVD, L-2LVD, L-2LCVD and L-2LC$_m$VD converter) provides a higher voltage conversion ratio compared to existing the L-Y converter topologies L-L, L-2L, L-2LC and L-2LC$_m$ converter). The detail description of suitable combinations of the X-converter and the Y-converter to derive X-Y family and novel L-Y converter topologies shown in Fig. 28.

A separate new combination showed which combines the feature of the old L-Y converter and the Voltage Doubler (VD). Recently X-Y converters are also combined with voltage doubler [201]–[203], voltage multiplier [204]–[208] to achieve higher output voltage. In [209], a new member called XL members derived in X-Y family. The converters derived by using SI, 2LC, 2LCm network in X converters. In [209]–[211], single input double output DC-DC converters derived for vehicular loads. This converter provides a solution to achieve two output voltages by using a single input and a single switch.

XI. COMPARISON AND APPLICATION OF MULTISTAGE FAMILIES

To select appropriate and suitable boost converter (to drive the truncation motor via an inverter) or buck converter (to drive the low voltage luxurious loads) for fuel vehicular power train. From the above-aforementioned families, it is essential to compare converter as mentioned above in terms of voltage conversion ratio, number of inductors, number of capacitors,
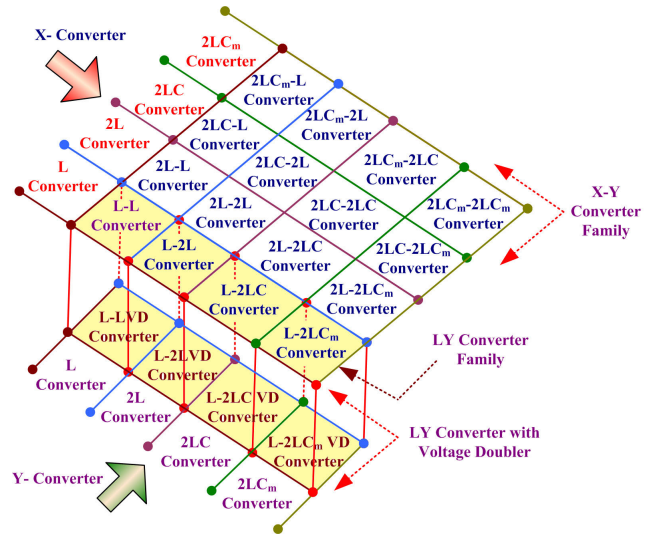
FIGURE 28. Various Combinations of X-converter and Y-converter to derive X-Y converter family and L-Y new members with voltage doubler.

number of diodes, number of switches, voltage stress across switch the switches, number of stages and number of transformers. In table 1-6, all the converters as mentioned above of the M-SCBC family, the M-SIBC family, transformer and coupled inductor based MPC, the Luo converter, the DC-DC multilevel power converters, the X-Y converter family compared respectively.

The vehicles are typically classified based on the Gross Vehicle Weight Rating (GVWR) or Gross Trailer Weight Rating (GTWR) and power required to drive the power train. There are three major categories of vehicles; light-duty vehicles; medium-duty vehicles, and high duty vehicles. The typical schematic layout of the power train of light-duty shown in Fig. 29(a). Fuel cell output voltage is very low, thus need to step-up using a suitable unidirectional boost

TABLE 1. Comparison of switched-capacitor based converter family.

Fig. No.	Switch Voltage Stress	NL	NC	NS	ND	NT	Converter input Current	Number of stages and Description of stages
11(a) [107]	$V_{in}/(1-D)$	1	2	1	2	-	Continuous	Two-stage Converter (FEBC+SC)
11(b) [107]	$V_{in}/(1-D)$	1	4	1	4	-	Continuous	Two-stage Converter (FEBC+ two-stage SC)
11(c) [108]	$V_{in}/(1-D)$	2	3	1	2	-	Continuous	Three-stage Converter (Input Inductor + SC+LC-filter)
11(d) [108]	$V_{in}/(1-D)$	2	3	1	2	-	Continuous	Three-stage Converter (Input Inductor + SC+LC-filter)
11(e) [109]-[110]	$V_{in}/(1-D)$	2	3	1	2	-	Continuous	Three stage Converter (FEBC + SC+LC-filter)
11(f) [109]-[110]	$V_{in}/(1-D)$	2	3	1	2	-	Continuous	Three stage Converter (FEBC + SC+LC-filter)
11(g) [107]	$V_{in}/(1-D)$	2	4	1	3	-	Continuous	Three-stage Converter (FEBC + two-stage SC+LC-filter)
11(h) [113]	$V_{in}/(1-D)$	1	3	1	3	-	Continuous	Three-stage Converter (FEBC + SC+C-filter)
11(i) [111]-[113]	$V_{in}/(1-D)$	2	4	1	3	-	Continuous	Four stage Converter (FEBC + Intermediate LC + SC+C-filter)
11(j) [111]-[113]	$V_{in}/(1-D)$	1	3	1	3	-	Discontinuous	Three-stage Converter (FEB-BC + SC+C-filter)
11(k) [111]-[113]	$V_{in}/(1-D)$	1	3	1	3	-	Discontinuous	Three-stage Converter (FEB-BC + SC+C-filter)
11(l) [111]-[113]	$V_{in}/(1-D)$	2	3	1	2	-	Discontinuous	Three-stage Converter (FEB-BC + SC+LC-filter)
12(a) [114]	Max. V_{out}	1	3	4	5	-	Continuous	Two-stage Converter (SC + Boost Converter)
13(a) (New)	$V_{in}/(1-D)^2$	2	4	1	5	-	Continuous	Four stage Converter (FEBC+FEBC+ SC+C-filter)
13(b) (New)	$V_{in}/(1-D)^2$	3	4	1	4	-	Continuous	Four stage Converter (FEBC+FEBC+ SC+LC-filter)
13(c) (New)	$V_{in}/(1-D)^2$	3	5	1	5	-	Continuous	Five stage Converter (FEBC+FEBC+ Intermediate LC+SC+C-filter)
13(d) (New)	$V_{in}/(1-D)^2$	3	4	1	4	-	Continuous	Four stage Converter (FEBC+ Intermediate L +SC+LC-filter)

NL, NC, NS, ND, NT: Number of Inductor, Capacitor, Switch, Diode and Transformer

TABLE 2. Comparison of switched inductor based converter family.

Fig. No.	Voltage Stress	NL	NC	NS	ND	NT	Converter input Current	Number of stages and Description of stages
15(a) [126]	V_{out}	2	1	1	4	-	Continuous	Three-stage Converter(SI+ Switch +C-filter)
15(b) [98]	V_{out}	2	2	1	3	-	Continuous	Three-stage Converter(HSI-SC+ Switch +C-filter)
15(c) [127]	$V_{in}/(1-D)$	2	3	1	3	-	Continuous	Three stage Converter(FEBC + HSI-SC +C-filter)
15(d) [128]	Max $V_{in}/(1-D)$	2	3	2	3	-	Continuous	Three stage Converter(FEBC + HSI-SC +C-filter)
15(e) [129]	$V_{in}(1+D)/(1-D)$	2	4	1	5	-	Discontinuous	Four stage Converter(Switch+ HSI-SC + SC+C-filter)
15(f) [130]	$V_{in}(1+D)/(1-D)$	3	2	1	4	-	Discontinuous	Four stage Converter(Switch+ SI + Intermediate C+LC-filter)
15(g) [130]	$2V_{in}/1-D$	3	3	1	5	-	Discontinuous	Four stage Converter(Switch+ HSI-SC + Intermediate C +LC-filter)
15(h) [130]	$V_{in}(3-k)/(1-D)$	3	4	2	5	-	Discontinuous	Four stage Converter(Switch+ HSI-SC + Intermediate C +LC-filter)
16(a) [126]	$(V_{out}+V_{in})/2$	2	1	2	1	-	Continuous	Two-stage Converter (Active switched network +C-filter)
16(b) [126]	$V_{out}/2$	2	2	2	2	-	Continuous	Two stage Converter (Active switched network with additional one capacitor +C-filter)
16(c) [126]	$(V_{out}-V_{in})/2$	2	2	2	3	-	Continuous	Two stages (Active switched network with two capacitors +C-filter)

HSI-SC is with Coupled Inductor, NL, NC, NS, ND, NT: Number of Inductor, Capacitor, Switch, Diode and Transformer

TABLE 3. Comparison of transformer and coupled inductor based converter family.

Fig. No.	NL	NC	NS	ND	NT /CI	Converter input Current	Number of stages and Description of stages
17(a) [143]	-	2	1	1	2	Continuous	Three stage Converter (CIFS+ Switch +C-filter)
17(b) [145]	1	2	1	2	2	Continuous	Three stage Converter (HSI-SC+ Switch +C-filter)
17(c) [144]-[146]	1	3	1	2	3	Continuous	Four stages, (FEBC with Coupled Inductor + HSI-SC+ Intermediate stage +C-filter)
17(d) [147]	-	2	1	2	2	Continuous	Three stage Converter (CIFS+ Switch +C-filter)
17(e) [148]	2	4	1	3	2	Continuous	Three stage Converter (FEBC+ Resonant Tank + C-filter)
17(f) [149]	2	5	1	5	2	Continuous	Four stage Converter (Boost Converter+ FEBC+ HSI-SC +C-filter)
17(g) [150]	-	2	1	2	2	Continuous	Two stage Converter (HSI-SC + Buck Converter with coupled Inductor)
17(h) [151]	1	4	1	4	2	Continuous	Three stages, (Boost converter with reactive element + Multiplier stage +C-filter)
17(i) [152]	1	3	1	4	2	Continuous	Three stage Converter (HSI-SC + Coupled Inductor +C-filter)
17(j) [153]-[156]	-	2	1	2	3	Continuous	Three stage Converter(Y-Source + Switching stage +C-filter)
17(k) [155]	-	3	1	2	3	Continuous	Three stage Converter (Y-Source with capacitor + Switching stage +C-filter)
17(l) [153]-[156]	1	3	1	2	3	Continuous	Three stage Converter (Y-Source with capacitor and inductor + Switching stage +C-filter)
17(m) [153]-[166]	1	3	1	2	3	Continuous	Four stage Converter(Inductor + Y-source+ Switching stage +C-filter)
17(n) [157], [158]	-	1	1	1	2	Discontinuous	Two stage Converter(Switching stage + Tapped Inductor)
17(o) [160]	-	2	2	1	2	Discontinuous	Two stage Converter(Switching stage + Tapped Inductor)

CIFS: Coupled Inductor Fly-back Structure, Note HSI-SC is with Coupled Inductor
NL, NC, NS, ND, NT/CI: Number of Inductor, Capacitor, Switch, Diode and Transformer/Coupled inductor

TABLE 4. Comparison of LUO converter family.

Fig. No.	NL	NC	NS	ND	NT	Converter input Current	Number of stages and Description of stages
19(a) [174]-[176]	3	4	2	3	-	Discontinuous	Three stage Converter (FEB-BC+ Re lift Structure+ LC-filter)
19(b) [174]-[176]	4	5	2	5	-	Discontinuous	Three stage Converter (FEB-BC+ Triple lift Structure+ LC-filter)
19(c) [174]-[176]	5	6	2	7	-	Discontinuous	Three stage Converter (FEB-BC+ Quadruple lift Structure+ LC-filter)
19(d) [174]-[176]	3	4	1	5	-	Discontinuous	Two stage Converter (Simplified Re lift Structure+ LC-filter)
19(e) [174]-[176]	4	5	1	7	-	Discontinuous	Two stage Converter (Simplified Triple lift Structure+ LC-filter)
19(f) [174]-[176]	5	6	1	9	-	Discontinuous	Two stage Converter (Simplified Quadruple lift Structure+ LC-filter)
20(a) [174], [177]	3	4	1	5	-	Discontinuous	Two stage Converter (Simplified Re lift Structure+ LC-filter)
20(b) [174], [177]	4	5	1	7	-	Discontinuous	Two stage Converter (Simplified Triple lift Structure+ LC-filter)
20(c) [174], [177]	5	6	1	9	-	Discontinuous	Two stage Converter (Simplified Quadruple lift Structure+ LC-filter)

NL, NC, NS, ND, NT: Number of Inductor, Capacitor, Switch, Diode and Transformer

TABLE 5. Comparison of DC-DC multilevel converter family.

Fig. No.	Voltage Stress	NL	NC	NS	ND	NT	Converter input Current	Number of stages and Description of stages
21(a) [179]-[181]	$V_{in}/(1-D)$	1	2N+1	1	2N+1	-	Continuous	N+1 stage (FEBC +N stage multiplier)
21(b) [179]-[181]	$V_{in}/(1-D)$	1	2N	4	2N	-	Continuous	N+1 stage (FEBC +N stage multiplier)
21(c) [182]	V_{in}	1	2N-2	2	2N-2	-	Continuous	N stage(N stage multiplier)
21(d) [183]	V_{out}/N	1	2N	2	2N+2	2	Continuous	N+2 stage Converter (Interleaved FEBC + N stage multiplier +C-filter)
21(e) [184]-[190]	V_{out}/N	1	2N-1	1	2N-1	-	Continuous	N+1 stage (FEBC +N stage multiplier)
21(f) [184]-[190]	$V_{in}/(1-D)$	1	2N-1	1	2N-1	-	Discontinuous	N+1 stage(FEBC +N stage multiplier)
21(g) [184]-[190]	$V_{in}/(1-D)$	1	2N-1	1	2N+1	-	Continuous	N+2 stage(Cuk front End+N stage multiplier +LC-filter)
21(h) [184]-[190]	$V_{in}/(1-D)$	2	2N	1	2N-1	-	Continuous	N+1 stage(SEPIC front End+ N stage multiplier)
21(i) [191]	$V_{in}/(1-D)$	1	2N	1	2N	-	Continuous	N+1 stage(FEBC +N stage multiplier)
22(a) [192]	$V_{in}(1+D)/(1-D)$	2	2N-1	1	2N+2	-	Continuous	N+1 stage(FEBC with switched Inductor+ N stage multiplier)
22(b) [193]	$2V_{in}/(1-D)$	2	2N	1	2N+1	-	Continuous	N+1 stage(FEBC with VLSI+N stage multiplier)

NL, NC, NS, ND, NT: Number of Inductor, Capacitor, Switch, Diode and Transformer

TABLE 6. Comparison of X-Y converter family.

Fig. No.	Voltage Conversion ratio	NL	NC	NS	ND	Converter input Current	Number of stages and Description of stages
25(a) [197]	$(D^2-2D)/(1-D)^2$	2	2	1	3	Discontinuous	Two-stage Converter (L +L Converter)
25(b) [197]	$(D^2-3D)/(1-D)^2$	3	2	1	6	Discontinuous	Two-stage Converter (L +2L Converter)
25(c) [197]	$(D^2-2D-1)/(1-D)^2$	3	3	1	7	Discontinuous	Two-stage Converter (L +2LC Converter)
25(d) [197]	$(D^2-2D-1)/(1-D)^2$	3	3	1	5	Discontinuous	Two-stage Converter (L+2LC$_m$ Converter)
25(e) [197]	$(D^2-3D)/(1-D)^2$	3	2	1	6	Discontinuous	Two-stage Converter (2L +L Converter)
25(f) [197]	$-4D/(1-D)^2$	4	2	1	9	Discontinuous	Two stage Converter (2L +2L Converter)
25(g) [197]	$(D^2-4D-1)/(1-D)^2$	4	3	1	10	Discontinuous	Two-stage Converter (2L +2LC Converter)
25(h) [197]	$(D^2-4D-1)/(1-D)^2$	4	3	1	8	Discontinuous	Two-stage Converter (2L+2LC$_m$ Converter)
26(a) [197]	$(D^2-2D-1)/(1-D)^2$	3	3	1	7	Discontinuous	Two-stage Converter (2LC +L Converter)
26(b) [197]	$(D^2-4D-1)/(1-D)^2$	4	3	1	10	Discontinuous	Two-stage Converter (2LC +2L Converter)
26(c) [197]	$(D^2-2D-3)/(1-D)^2$	4	4	1	11	Discontinuous	Two-stage Converter (2LC +2LC Converter)
26(d) [197]	$(D^2-2D-3)/(1-D)^2$	4	4	1	9	Discontinuous	Two-stage Converter (2LC+2LC$_m$ Converter)
26(e) [197]	$(D^2-2D-1)/(1-D)^2$	3	3	1	5	Discontinuous	Two-stage Converter (2LC$_m$ +L Converter)
26(f) [197]	$(D^2-4D-1)/(1-D)^2$	4	3	1	8	Discontinuous	Two-stage Converter (2LC$_m$ +2L Converter)
26(g) [197]	$(D^2-2D-3)/(1-D)^2$	4	4	1	9	Discontinuous	Two-stage Converter (2LC$_m$ +2LC Converter)
26(h) [197]	$(D^2-2D-3)/(1-D)^2$	4	4	1	7	Discontinuous	Two-stage Converter (2LC$_m$+2LC$_m$ Converter)
27(a) [198], [201]-[203]	Refer [262]	2	4	1	5	Discontinuous	Two-stage Converter (L +LVD Converter)
27(b) [198], [201]-[203]	Refer [262]	3	4	1	8	Discontinuous	Two-stage Converter (L +2LVD Converter)
27(c) [198], [201]-[203]	Refer [262]	3	5	1	9	Discontinuous	Two-stage Converter (L +2LCVD Converter)
27(d) [198], [201]-[203]	Refer [262]	3	5	1	7	Discontinuous	Two-stage Converter (L +2LC$_m$VD Converter)

NL, NC, NS, ND, NT: Number of Inductor, Capacitor, Switch, Diode and Transformer

converter to attain the required voltage at the terminal of inverter to drive the traction motor—the speed and torque of the motor drive controlled through power converters (DC-DC and DC-AC). The battery used to provide supplies for inverter in the absence of fuel cell energy and a warm-up time of fuel cell. The typical schematic layout of the power train of high duty shown in Fig. 29(b). High duty vehicles required a DC-DC converter with a high conversion ratio and

TABLE 7. Reliability, cost, efficiency, advantage, disadvantages and application of multistage families.

| Unidirectional DC-DC Multistage Family	Reliability	cost	Efficiency	Advantages	Disadvantages	Applications
Switched Capacitor Based Converter Family (M-SCBC)	High	Average	Very High	Small Size, Low weight, modular	Poor Voltage regulation, High startup Current, Large number of capacitors	Power train of low duty vehicle and Luxurious low power, High voltage loads
Switched Inductor Based Converter Family (M-SIBC)	Very High	High	High	Very high Conversion ratio, merge with many Converter	large number of Inductor, weighted, poor performance for high power	Power train of low duty vehicle and Luxurious low power, High voltage loads
Transformer and Coupled Inductor Based Converter Family	Average	Very High	High	high power, soft switching, Tunable turns ratio, High Conversion ratio	Bulky, More losses due to magnetic coupling, Complex	Power train of high duty vehicles and Luxurious high power, high voltage load
Luo converter Family	High	High	Average	Very high Conversion ratio, Average in size	Large number of Inductor, capacitor and diodes. Complex in control, high losses	Power train of low as well as high duty vehicle and Luxurious low power, High voltage loads
Multilevel converter	Average	High	Very high	Self-Balanced, Modular, extendable structure, low number of switches	Large number of capacitor and diodes	Power train of high duty vehicles, luxurious high/low power, high voltage power luxurious load
X-Y converter Family	High	Average	High	Single switch, High conversion ratio, Extendable Structure	Large number of diodes, Discontinuous input current	Power train of low and high duty vehicles and luxurious high voltage power luxurious load
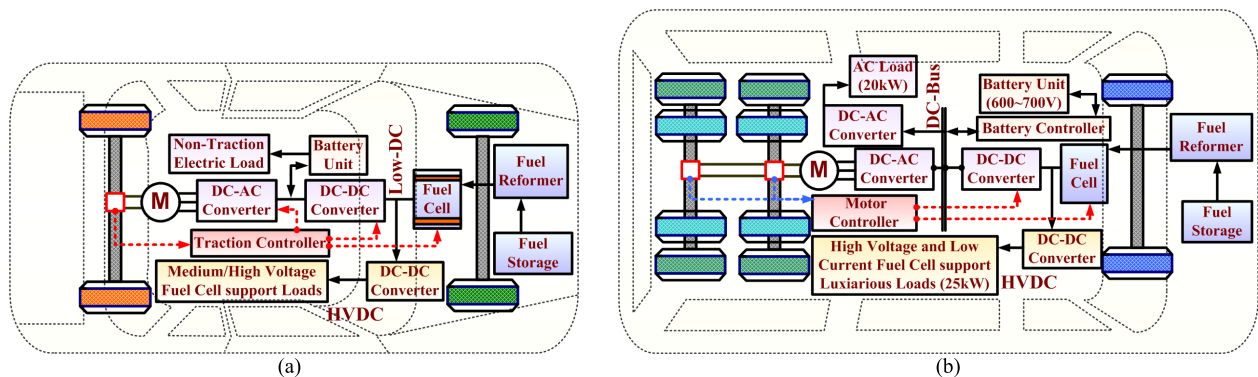
FIGURE 29. Typical schematic layout of power train (a) low duty vehicle (b) high duty vehicle.

high power to drive the vehicles. Apart from this, fuel cell voltage also used to drive advanced, luxurious features of the vehicle. Thus, numerous loads fed by utilizing appropriate DC-DC and DC-AC converter. The major challenge in designing the fuel cell VPT is a selection of proper DC-DC and DC-AC converter to convert the voltage/current of the fuel cell to the required voltage/current level, selection of best fuel cell and power management. Nowadays, numerous DC-DC converter options are available in the literature, and it is essential to select the most efficient and cost-effective DC-DC converter. Table-7, aforementioned DC-DC converters family reliability, efficiency, cost, advantages, disadvantages and application discussed in detail.

XII. FUTURE DIRECTION OF DC-DC CONVERTER FOR VEHICULAR APPLICATIONS

Advancement in electric and electronic systems of the Vehicular Power Train (VPT) is compulsory to improve the

navigation system, mobile integration, satellite system, comfort, suitability, convenience, entertainment facilities, protection and safety, ecological issue and communication system etc. [212], [213]. Most of the electronics applications work on the DC power supply. Thus, it is compulsory to improve the power converters stages to satisfy the need and requirement of the future generation. It is needed to design a good DC-DC converter to supply the loads as well as to drive the train.

There are more opportunities to improve DC-DC converters stages in terms of cost, efficiency, number of components, modularity, and controllability by using recent multistage technologies. There is scope for the hybrid DC-DC and multi-ports converter topologies for the high voltage conversion ratio and multiple outputs to drive multiple loads as well as vehicular train at a time using the same converter. High conversion ratio and multi-ports DC-DC converters can be achieved by combining the topologies as mentioned above.

XIII. CONCLUSION

The performance of the numerous unidirectional multi-stage DC-DC converter families has been comprehensively reviewed and articulated to improve the Tank-To-Wheel (TTW) efficiency to lower cost, eco-friendly, zero-emission and high-power Fuel Cell Vehicles (FCVs). For selecting the best fuel cell for FCVs, classification is presented based on the working temperature and power capability. Also based on the type and characteristics, DC-DC converters broadly classified as SCBC, SIBC, Transformer and Coupled Inductor Based Converter, Luo converter, Multilevel converter and X-Y converter family. Each multistage converter family has its advantages and disadvantages.

Based on the review of numerous multistage converters, concluded that the existing topologies, again and again, combine with switched inductor and several boosting techniques to improve the performance for various applications. HSI-SC, multilevel and X-Y converters are the better choice for the Fuel Cell VPT in term of cost and efficiency. Details of the individual converter with the comparative study presented to select the best converter to drive power train and to supply a luxurious load of FCVs.

Moreover, the role, challenges and future scenario of the DC-DC converter for a vehicular power train discussed in detail. Advantages, disadvantages, and application of each multistage family discussed more specific to the power train of the small vehicle (Cars, Motorcycle etc.), as well as larger vehicles (Bus, trucks etc.).

ACKNOWLEDGMENT

REFERENCES

[1] F. Querini, S. Dagostino, S. Morel, and P. Rousseaux, "Greenhouse gas emissions of electric vehicles associated with wind and photovoltaic electricity," *Energy Procedia*, vol. 20, pp. 391–401, Jan. 2012.

[2] J. Y. Yong, V. K. Ramachandaramurthy, K. M. Tan, and N. Mithulananthan, "A review on the state-of-the-art technologies of electric vehicle, its impacts and prospects," *Renew. Sustain. Energy Rev.*, vol. 49, pp. 365–385, Sep. 2015.

[3] T. Ida, K. Murakami, and M. Tanaka, "A stated preference analysis of smart meters, photovoltaic generation, and electric vehicles in Japan: Implications for penetration and GHG reduction," *Energy Res. Social Sci.*, vol. 2, pp. 75–89, Jun. 2014.

[4] U. S. Energy Information Administration (EIA), "International Energy Outlook," U.S. Dept. Energy, Office Energy Anal., Washington, DC, USA, Tech. Rep. DOE/EIA-0484(2013), 2013.

[5] S. S. Williamson, A. K. Rathore, and F. Musavi, "Industrial electronics for electric transportation: Current State-of-the-Art and future challenges," *IEEE Trans. Ind. Electron.*, vol. 62, no. 5, pp. 3021–3032, May 2015.

[6] H. Shareef, M. M. Islam, and A. Mohamed, "A review of the stage-of-the-art charging technologies, placement methodologies, and impacts of electric vehicles," *Renew. Sustain. Energy Rev.*, vol. 64, pp. 403–420, Oct. 2016.

[7] X. Xu, H. Wang, N. Zhang, Z. Liu, and X. Wang, "Review of the fault mechanism and diagnostic techniques for the range extender hybrid electric vehicle," *IEEE Access*, vol. 5, pp. 14234–14244, 2017.

[8] F. Un-Noor, S. Padmanaban, L. Mihet-Popa, M. Mollah, and E. Hossain, "A comprehensive study of key electric vehicle (EV) components, technologies, challenges, impacts, and future direction of development," *Energies*, vol. 10, no. 8, p. 1217, Aug. 2017.

[9] C. Liu, K. T. Chau, D. Wu, and S. Gao, "Opportunities and challenges of vehicle-to-home, vehicle-to-vehicle, and vehicle-to-Grid technologies," *Proc. IEEE*, vol. 101, no. 11, pp. 2409–2427, Nov. 2013.

[10] Z. Q. Zhu and D. Howe, "Electrical machines and drives for electric, hybrid, and fuel cell vehicles," *Proc. IEEE*, vol. 95, no. 4, pp. 746–765, Apr. 2007.

[11] S. G. Chalk and J. F. Miller, "Key challenges and recent progress in batteries, fuel cells, and hydrogen storage for clean energy systems," *J. Power Sour.*, vol. 159, no. 1, pp. 73–80, Sep. 2006.

[12] *Energy Technology Perspectives 2012-Pathways to a Clean Energy System*, International Energy Agency, Paris, France, 2012.

[13] D. B. Richardson, "Electric vehicles and the electric grid: A review of modeling approaches, impacts, and renewable energy integration," *Renew. Sustain. Energy Rev.*, vol. 19, pp. 247–254, Mar. 2013.

[14] J. P. Ribau, C. M. Silva, and J. M. C. Sousa, "Efficiency, cost and life cycle CO2 optimization of fuel cell hybrid and plug-in hybrid urban buses," *Appl. Energy*, vol. 129, pp. 320–335, Sep. 2014.

[15] *Global EV Outlook-Beyond one million Electric Cars*, International Energy Agency, Paris, France, 2016.

[16] *International Energy Outlook Transportation Sector Energy Consumption*, U.S. Energy Information Administration, Washington, DC, USA, 2016.

[17] S. G. Wirasingha and A. Emadi, "Pihef: Plug-in hybrid electric factor," *IEEE Trans. Veh. Technol.*, vol. 60, no. 3, pp. 1279–1284, Mar. 2011.

[18] E. A. Grunditz and T. Thiringer, "Performance analysis of current BEVs based on a comprehensive review of specifications," *IEEE Trans. Transp. Electrific.*, vol. 2, no. 3, pp. 270–289, Sep. 2016.

[19] C. C. Chan, "The state of the art of electric, hybrid, and fuel cell vehicles," *Proc. IEEE*, vol. 95, no. 4, pp. 704–718, Apr. 2007.

[20] O. M. F. Camacho, P. B. Norgard, N. Rao, and L. Mihet-Popa, "Electrical vehicle batteries testing in a distribution network using sustainable energy," *IEEE Trans. Smart Grid*, vol. 5, no. 2, pp. 1033–1042, Mar. 2014.

[21] EG&G Technical Services, Science Application Intl. Corporation, *The Fuel Cell Handbook*, 6th ed., U.S. Department of Energy, Morgantown, WV, USA, 2002.

[22] P. Goli and W. Shireen, "PV powered smart charging station for PHEVs," *Renew. Energy*, vol. 66, pp. 280–287, Jun. 2014.

[23] P. Degauque, I. Stievano, S. Pignari, V. Degardin, F. Canavero, F. Grassi, and F. Canete, "Power-line communication: Channel characterization and modeling for transportation systems," *IEEE Veh. Technol. Mag.*, vol. 10, no. 2, pp. 28–37, Jun. 2015.

[24] M. Yilmaz and P. T. Krein, "Review of battery charger topologies, charging power levels, and infrastructure for plug-in electric and hybrid vehicles," *IEEE Trans. Power Electron.*, vol. 28, no. 5, pp. 2151–2169, May 2013.

[25] R. Rose, *Questions and Answers about Hydrogen and Fuel Cells*, Report Style; U.S. Department of Energy: Washington, DC, USA, 2005.

[26] C. E. Thomas, "Fuel cell and battery electric vehicles compared," *Int. J. Hydrogen Energy*, vol. 34, no. 15, pp. 6005–6020, Aug. 2009.

[27] K. Rajashekara, "Present status and future trends in electric vehicle propulsion technologies," *IEEE J. Emerg. Sel. Topics Power Electron.*, vol. 1, no. 1, pp. 3–10, Mar. 2013.

[28] S. Samuelsen, "Why the automotive future will be dominated by fuel cells," *IEEE Spectr.*, to be published. [Online]. Available: https://spectrum.ieee.org/green-tech/fuel-cells/why-the-automotive-future-will-be-dominated-by-fuel-cells

[29] M. Nasri, I. Bürger, S. Michael, and H. E. Friedrich, "Waste heat recovery for fuel cell electric vehicle with thermochemical energy storage," in *Proc. 11th Int. Conf. Ecol. Vehicles Renew. Energies (EVER)*, Monte Carlo Monaco, Apr. 2016, pp. 1–6.

[30] U. R. Prasanna, P. Xuewei, A. K. Rathore, and K. Rajashekara, "Propulsion system architecture and power conditioning topologies for fuel cell vehicles," *IEEE Trans. Ind. Appl.*, vol. 51, no. 1, pp. 640–650, Jan. 2015.

[31] A. Tashakori Abkenar, A. Nazari, S. D. G. Jayasinghe, A. Kapoor, and M. Negnevitsky, "Fuel cell power management using genetic expression programming in all-electric ships," *IEEE Trans. Energy Convers.*, vol. 32, no. 2, pp. 779–787, Jun. 2017.

[32] M. Venturi, C. Mohrdieck, and J. Friedrich, "Mercedes-benz B-Class fuel cell: The world largest hydrogen vehicle fuel cell fleet experience," in *Proc. World Electr. Vehicle Symp. Exhib. (EVS27)*, Barcelona, Spain, Nov. 2013, pp. 1–11.

[33] M. Marchesoni and C. Vacca, "New DC–DC converter for energy storage system interfacing in fuel cell hybrid electric vehicles," *IEEE Trans. Power Electron.*, vol. 22, no. 1, pp. 301–308, Jan. 2007.

[34] X. He, T. Maxwell, and M. E. Parten, "Development of a hybrid electric vehicle with a hydrogen-fueled IC engine," *IEEE Trans. Veh. Technol.*, vol. 55, no. 6, pp. 1693–1703, Nov. 2006.

[35] M. Helsper and N. Ruger, "Requirements of hybrid and electric buses–a huge challenge for power electronics," in *Proc. 16th Eur. Conf. Power Electron. Appl.*, Lappeennranta, Finland, Aug. 2014, pp. 1837–1844.

[36] C. C. Chan, "The state of the art of electric and hybrid vehicles," *Proc. IEEE*, vol. 90, no. 2, pp. 247–275, Feb. 2002.

[37] O. C. Onar, J. Kobayashi, and A. Khaligh, "A fully directional universal power electronic interface for EV, HEV, and PHEV applications," *IEEE Trans. Power Electron.*, vol. 28, no. 12, pp. 5489–5498, Dec. 2013.

[38] X. Pan, X. Zhou, Z. Peng, A. Ghoshal, and A. K. Rathore, "Novel hybrid modulation based bidirectional electrolytic capacitor-less three-phase inverter for fuel cell vehicles," in *Proc. IEEE 3rd Int. Future Energy Electron. Conf. ECCE Asia (IFEEC-ECCE Asia)*, Kaohsiung, Taiwan, Jun. 2017, pp. 906–910.

[39] C. Jose and S. Meikandasivam, *A Review on the Trends and Developments in Hybrid Electric Vehicles* (Lecture Notes in Mechanical Engineering), Singapore: Springer, 2016, pp. 211–229.

[40] M. C. Kisacikoglu, B. Ozpineci, and L. M. Tolbert, "EV/PHEV bidirectional charger assessment for V2G reactive power operation," *IEEE Trans. Power Electron.*, vol. 28, no. 12, pp. 5717–5727, Dec. 2013.

[41] F. R. Salmasi, "Control strategies for hybrid electric vehicles: Evolution, classification, comparison, and future trends," *IEEE Trans. Veh. Technol.*, vol. 56, no. 5, pp. 2393–2404, Sep. 2007.

[42] X. Wang, J. Tao, and R. Zhang, "Fuzzy energy management control for battery/ultra-capacitor hybrid electric vehicles," in *Proc. Chin. Control Decis. Conf. (CCDC)*, Yinchuan, China, May 2016, pp. 6207–6211.

[43] S. S. Williamson, A. Emadi, and K. Rajashekara, "Comprehensive efficiency modeling of electric traction motor drives for hybrid electric vehicle propulsion applications," *IEEE Trans. Veh. Technol.*, vol. 56, no. 4, pp. 1561–1572, Jul. 2007.

[44] I. Aharon and A. Kuperman, "Topological overview of powertrains for battery-powered vehicles with range extenders," *IEEE Trans. Power Electron.*, vol. 26, no. 3, pp. 868–876, Mar. 2011.

[45] A. Khaligh and S. Dusmez, "Comprehensive topological analysis of conductive and inductive charging solutions for plug-in electric vehicles," *IEEE Trans. Veh. Technol.*, vol. 61, no. 8, pp. 3475–3489, Oct. 2012.

[46] J. Shen and A. Khaligh, "A supervisory energy management control strategy in a battery/ultracapacitor hybrid energy storage system," *IEEE Trans. Transp. Electrific.*, vol. 1, no. 3, pp. 223–231, Oct. 2015.

[47] H. S. Das, C. W. Tan, and A. H. M. Yatim, "Fuel cell hybrid electric vehicles: A review on power conditioning units and topologies," *Renew. Sustain. Energy Rev.*, vol. 76, pp. 268–291, Sep. 2017.

[48] S. Andreasen, L. Ashworth, I. Menjonremon, and S. Kar, "Directly connected series coupled HTPEM fuel cell stacks to a li-ion battery DC bus for a fuel cell electrical vehicle," *Int. J. Hydrogen Energy*, vol. 33, no. 23, pp. 7137–7145, Dec. 2008.

[49] S. J. Andreasen, J. L. Jespersen, E. Schaltz, and S. K. Kær, "Characterisation and modelling of a high temperature PEM fuel cell stack using electrochemical impedance spectroscopy," *Fuel Cells*, vol. 9, no. 4, pp. 463–473, Aug. 2009.

[50] S. J. Andreasen, J. R. Vang, and S. K. Kær, "High temperature PEM fuel cell performance characterisation with CO and CO$_2$ using electrochemical impedance spectroscopy," *Int. J. Hydrogen Energy*, vol. 36, no. 16, pp. 9815–9830, Aug. 2011.

[51] G. Avgouropoulos, J. Papavasiliou, M. K. Daletou, J. K. Kallitsis, T. Ioannides, and S. Neophytides, "Reforming methanol to electricity in a high temperature PEM fuel cell," *Appl. Catal. B, Environ.*, vol. 90, nos. 3–4, pp. 628–632, Aug. 2009.

[52] Electric Vehicles Initiative (EVI), *Global EV Outlook: Understanding the Electric Vehicle Landscape to 2020*," International Energy Agency (IEA), Paris, France, Apr. 2013.

[53] G. Tian, S. Wasterlain, D. Candusso, F. Harel, D. Hissel, and X. François, "Identification of failed cells inside PEMFC stacks in two cases: Anode/cathode crossover and anode/cooling compartment leak," *Int. J. Hydrogen Energy*, vol. 35, no. 7, pp. 2772–2776, Apr. 2010.

[54] *Fuel Cell Technologies Program*, U.S. Department of Energy (DOE), Washington, DC, USA, 2011.

[55] C. Graves, S. D. Ebbesen, M. Mogensen, and K. S. Lackner, "Sustainable hydrocarbon fuels by recycling CO$_2$ and H$_2$O with renewable or nuclear energy," *Renew. Sustain. Energy Rev.*, vol. 15, no. 1, pp. 1–23, Jan. 2011.

[56] W. Schmittinger and A. Vahidi, "A review of the main parameters influencing long-term performance and durability of PEM fuel cells," *J. Power Sources*, vol. 180, no. 1, pp. 1–14, May 2008.

[57] B. Felix, I. Minoru, and S. Thomas, *Polymer Electrolyte Fuel Cell Durability*. New York, NY, USA: Springer-Verlag, 2009.

[58] A. Afif, N. Radenahmad, Q. Cheok, S. Shams, J. H. Kim, and A. K. Azad, "Ammonia-fed fuel cells: A comprehensive review," *Renew. Sustain. Energy Rev.*, vol. 60, pp. 822–835, Jul. 2016.

[59] A. Emadi, S. S. Williamson, and A. Khaligh, "Power electronics intensive solutions for advanced electric, hybrid electric, and fuel cell vehicular power systems," *IEEE Trans. Power Electron.*, vol. 21, no. 3, pp. 567–577, May 2006.

[60] N. H. Jafri and S. Gupta, "An overview of fuel cells application in transportation," in *Proc. IEEE Transp. Electrific. Conf. Expo, Asia–Pacific (ITEC Asia–Pacific)*, Busan, South Korea, Jun. 2016, pp. 129–133.

[61] M. Ehsani, Y. Gao, S. Gay, and A. Emadi, *Modern Electric, Hybrid Electric, and Fuel Cell Vehicles-Fundamentals, Theory, and Design*, 2nd ed. Boca Raton, FL, USA: CRC Press, Sep. 2009.

[62] V. Das, S. Padmanaban, K. Venkitusamy, R. Selvamuthukumaran, F. Blaabjerg, and P. Siano, "Recent advances and challenges of fuel cell based power system architectures and control–A review," *Renew. Sustain. Energy Rev.*, vol. 73, pp. 10–18, Jun. 2017.

[63] P. Thounthong, S. Rael, and B. Davat, "Utilizing fuel cell and supercapacitors for automotive hybrid electrical system," in *Proc. 20th Annu. IEEE Appl. Power Electron. Conf. Expo. (APEC)*, Austin, TX, USA, Mar. 2005, pp. 90–96.

[64] S. S. Williamson and A. Emadi, "Comparative assessment of hybrid electric and fuel cell vehicles based on comprehensive Well-to-Wheels efficiency analysis," *IEEE Trans. Veh. Technol.*, vol. 54, no. 3, pp. 856–862, May 2005.

[65] M. Forouzesh, Y. Siwakoti, S. Gorji, F. Blaabjerg, and B. Lehman, "Step-up DC–DC converters: A comprehensive review of voltage-boosting techniques, topologies, and applications," *IEEE Trans. Power Electron.*, vol. 32, no. 12, pp. 9143–9178, Dec. 2017.

[66] A. Ajami, H. Ardi, and A. Farakhor, "A novel high step-up DC/DC converter based on integrating coupled inductor and switched-capacitor techniques for renewable energy applications," *IEEE Trans. Power Electron.*, vol. 30, no. 8, pp. 4255–4263, Aug. 2015.

[67] S. Padmanaban, M. S. Bhaskar, P. K. Maroti, F. Blaabjerg, and V. Fedák, "An original transformer and switched-capacitor (T & SC)-based extension for DC-DC boost converter for high-voltage/low-current renewable energy applications: Hardware implementation of a new T & SC boost converter," *Energies*, vol. 11, no. 4, p. 783, Apr. 2018.

[68] P. K. Maroti, P. Sanjeevikumar, M. S. Bhaskar, F. Blaabjerg, V. Ramachandaramurthy, P. Siano, and V. Fedák, "Multistage switched inductor boost converter for renewable energy application," in *Proc. IEEE Conf. Energy Convers. (CENCON)*, Kuala Lumpur, Malaysia, Oct. 2017, pp. 311–316.

[69] F. L. Tofoli, W. Josias de Paula, D. S. de Oliveira Júnior, and D. C. de Pereira, "Survey on non-isolated high-voltage step-up DC–DC topologies based on the boost converter," *IET Power Electron.*, vol. 8, no. 10, pp. 2044–2057, Oct. 2015.

[70] M. S. Bhaskar, S. Padmanaban, F. Blaabjerg, and P. W. Wheeler, "An improved multistage switched inductor boost converter (Improved M-SIBC) for renewable energy applications: A key to enhance conversion ratio," in *Proc. IEEE 19th Workshop Control Modeling Power Electron. (COMPEL)*, Padua, Italy, Jun. 2018, pp. 1–6.

[71] B. Sri Revathi and M. Prabhakar, "Non isolated high gain DC-DC converter topologies for PV applications–A comprehensive review," *Renew. Sustain. Energy Rev.*, vol. 66, pp. 920–933, Dec. 2016.

[72] L. Luckose, H. L. Hess, and B. K. Johnson, "Power conditioning system for fuel cells for integration to ships," in *Proc. IEEE Vehicle Power Propuls. Conf.*, Dearborn, MI, USA, Sep. 2009, pp. 973–979.

[73] X. Haiping, K. Li, and W. Xuhui, "Fuel cell power system and high power DC-DC converter," *IEEE Trans. Power Electron.*, vol. 19, no. 5, pp. 1250–1255, Sep. 2004.

[74] W. Rong-Jong and D. Rou-Yong, "High step-up converter with coupled-inductor," *IEEE Trans. Power Electron.*, vol. 20, no. 5, pp. 1025–1035, Sep. 2005.

[75] X. Hu, N. Murgovski, L. M. Johannesson, and B. Egardt, "Optimal dimensioning and power management of a fuel Cell/Battery hybrid bus via convex programming," *IEEE/ASME Trans. Mechatronics*, vol. 20, no. 1, pp. 457–468, Feb. 2015.

[76] A. Cardenas, K. Agbossou, and N. Henao, "Development of power interface with FPGA-based adaptive control for PEM-FC system," *IEEE Trans. Energy Convers.*, vol. 30, no. 1, pp. 296–306, Mar. 2015.

[77] D. W. Dees, "Overview of electrochemical power sources for electric and hybrid/electric vehicles," in *Proc. IEEE Int. Electric Mach. Drives Conf. (IEMDC)*, Seattle, WA, USA, May 1999, pp. 258–259.

[78] M. Catenacci, E. Verdolini, V. Bosetti, and G. Fiorese, "Going electric: Expert survey on the future of battery technologies for electric vehicles," *Energy Policy*, vol. 61, pp. 403–413, Oct. 2013.

[79] M. R. Mohamed, S. M. Sharkh, and F. C. Walsh, "Redox flow batteries for hybrid electric vehicles: Progress and challenges," in *Proc. IEEE Vehicle Power Propuls. Conf.*, vol. 9. Dearborn, MI, USA, Sep. 2009, pp. 551–557.

[80] Z. Darabi and M. Ferdowsi, "Aggregated impact of plug-in hybrid electric vehicles on electricity demand profile," *IEEE Trans. Sustain. Energy*, vol. 2, no. 4, pp. 501–508, Oct. 2011.

[81] A. Emadi, K. Rajashekara, S. Williamson, and S. Lukic, "Topological overview of hybrid electric and fuel cell vehicular power system architectures and configurations," *IEEE Trans. Veh. Technol.*, vol. 54, no. 3, pp. 763–770, May 2005.

[82] R. Erickson and D. Maksimovib, *Fundamentals of Power Electronics*, 2nd ed. New York, NY, USA: Springer, 2001.

[83] M. H. Rashid, *Power Electronics Handbook-Devices, Circuits and Applications*, 3rd ed. Amsterdam, The Netherlands: Elsevier, 2011.

[84] B. Bryant and M. K. Kazimierczuk, "Derivation of the cuk PWM DC-DC converter circuit topology," in *Proc. Int. Symp. Circuits Syst. (ISCAS)*, vol. 3. Bangkok, Thailand, May 2003, pp. 292–295.

[85] B. Bryant and M. K. Kazimierezuk, "Derivation of the buck-boost PWM DC-DC converter circuit topology," in *Proc. IEEE Int. Symp. Circuits Syst.*, vol. 2. Phoneix-Scottsdale, AZ, USA, May 2002, pp. 841–844.

[86] M. S. B. Ranjana, P. K. Maroti, and D. K. Prabhakar, "Novel topological derivations for DC-DC converters," *Int. J. Comput. Eng. Manage.*, vol. 16, no. 6, pp. 49–53, Nov. 2013.

[87] T. G. Wilson, "The evolution of power electronics," *IEEE Trans. Power Electron.*, vol. 15, no. 3, pp. 439–446, May 2000.

[88] B. Axelrod, Y. Berkovich, and A. Ioinovici, "Hybrid switched-capacitor-Cuk/Zeta/Sepic converters in step-up mode," *Proc. IEEE Int. Symp. Circuits Syst.*, vol. 5. Kobe, Japan, May 2005, pp. 1310–1313.

[89] A. Iqbal, M. S. Bhaskar, M. Meraj, S. Padmanaban, and S. Rahman, "Closed-loop control and boundary for CCM and DCM of nonisolated inverting N× multilevel boost converter for high-voltage step-up applications," *IEEE Trans. Ind. Electron.*, vol. 67, no. 4, pp. 2863–2874, Apr. 2020.

[90] A. Bratcu, I. Munteanu, S. Bacha, D. Picault, and B. Raison, "Cascaded DC–DC converter photovoltaic systems: Power optimization issues," *IEEE Trans. Ind. Electron.*, vol. 58, no. 2, pp. 403–411, Feb. 2011.

[91] P. Kiran Maroti, M. Sagar Bhaskar Ranjana, and B. Sri Revathi, "A high gain DC-DC converter using voltage multiplier," in *Proc. Int. Conf. Adv. Electr. Eng. (ICAEE)*, Vellore, India, Jan. 2014, pp. 1–4.

[92] G. R. Walker and P. C. Sernia, "Cascaded DC-DC converter connection of photovoltaic modules," *IEEE Trans. Power Electron.*, vol. 19, no. 4, pp. 1130–1139, Jul. 2004.

[93] M. Ortiz-Lopez, J. Leyva-Ramos, E. Carbajal-Gutierrez, and J. Morales-Saldaña, "Modelling and analysis of switch-mode cascade converters with a single active switch," *IET Power Electron.*, vol. 1, no. 4, pp. 478–487, Dec. 2008.

[94] R. D. Middlebrook, "Transformerless DC-to-DC converters with large conversion ratios," *IEEE Trans. Power Electron.*, vol. 3, no. 4, pp. 484–488, Oct. 1988.

[95] S. B. Mahajan, P. sanjeevikumar, F. Blaabjerg, "A multistage DC-DC step-up self-balanced and magnetic component-free converter for photovoltaic applications: Hardware implementation" *Energies*, vol. 10, no. 5, p. 719, May 2017.

[96] P. Yang, J. Xu, G. Zhou, and S. Zhang, "A new quadratic boost converter with high voltage step-up ratio and reduced voltage stress," in *Proc. 7th Int. Power Electron. Motion Control Conf.*, Jun. 2012, pp. 1164–1168.

[97] D. S. Wijeratne and G. Moschopoulos, "Quadratic power conversion for power electronics: Principles and circuits," *IEEE Trans. Circuits Syst. I, Reg. Papers*, vol. 59, no. 2, pp. 426–438, Feb. 2012.

[98] Y.-M. Ye and K. W. Eric Cheng, "Quadratic boost converter with low buffer capacitor stress," *IET Power Electron.*, vol. 7, no. 5, pp. 1162–1170, May 2014.

[99] Y. R. de Novaes, A. Rufer, and I. Barbi, "A new quadratic, three-level, DC/DC converter suitable for fuel cell applications," in *Proc. Power Convers. Conf. (Nagoya)*, vol. 7. Nagoya, Japan, Apr. 2007, pp. 601–607.

[100] S. Li, Y. Zheng, B. Wu, and K. Smedley, "A family of resonant two-switch boosting switched-capacitor converter with ZVS operation and a wide line regulation range," *IEEE Trans. Power Electron.*, vol. 33, no. 1, pp. 448–459, Jan. 2018.

[101] M. Forouzesh, Y. P. Siwakoti, S. A. Gorji, F. Blaabjerg, and B. Lehman, "A survey on voltage boosting techniques for step-up DC-DC converters," in *Proc. IEEE Energy Convers. Congr. Exposit. (ECCE)*, Milwaukee, WI, USA, Sep. 2016, pp. 1–6.

[102] B. Axelrod, Y. Berkovich, and A. Ioinovici, "Switched-capacitor (SC)/switched inductor (SL) structures for getting hybrid step-down Cuk/Sepic/Zeta converters," in *Proc. IEEE Int. Symp. Circuits Syst.*, Kos Island, Greece, May 2006, pp. 5063–5066.

[103] G. Palumbo and D. Pappalardo, "Charge pump circuits: An overview on design strategies and topologies," *IEEE Circuits Syst. Mag.*, vol. 10, no. 1, pp. 31–45, Mar. 2010.

[104] M. D. Seeman and S. R. Sanders, "Analysis and optimization of switched-capacitor DC–DC converters," *IEEE Trans. Power Electron.*, vol. 23, no. 2, pp. 841–851, Mar. 2008.

[105] M. Seeman, "A design methodology for switched-capacitor DC-DC converters," Elect. Eng. Comput. Sci., Univ. California, Berkeley, CA, USA, Tech. Rep. UCB/EECS-2009-78, May 2009.

[106] F. Lin Luo and H. Ye, "Investigation of switched-capacitorized DC/DC converters," in *Proc. IEEE 6th Int. Power Electron. Motion Control Conf.*, Wuhan, China, May 2009, pp. 1074–1079.

[107] D. Zhou, A. Pietkiewicz, and S. Cuk, "A three-switch high-voltage converter," *IEEE Trans. Power Electron.*, vol. 14, no. 1, pp. 177–183, Jan. 1999.

[108] D. Navamani, K. Vijayakumar, R. Jegatheeesanm, and A. Lavanya, "High step-up DC-DC converter by switched inductor and voltage multiplier cell for automotive applications," *J. Elect. Eng. Technol.*, vol. 11, pp. 1921–1935, Apr. 2016.

[109] B. Axelrod, Y. Berkovich, and A. Ioinovici, "Switched-capacitor/switched-inductor structures for getting transformerless hybrid DC–DC PWM converters," *IEEE Trans. Circuits Syst. I, Reg. Papers*, vol. 55, no. 2, pp. 687–696, Mar. 2008.

[110] A. Ioinovici, "Switched-capacitor power electronics circuits," *IEEE Circuits Syst. Mag.*, vol. 1, no. 3, pp. 37–42, Jan. 2001.

[111] Y. Berkovich and B. Axelrod, "Switched-coupled inductor cell for DC–DC converters with very large conversion ratio," *IET Power Electron.*, vol. 4, no. 3, pp. 309–315, Mar. 2011.

[112] Y. Wang, H. Yin, S. Han, A. Alsabbagh, and C. Ma, "A novel switched capacitor circuit for battery cell balancing speed improvement," in *Proc. IEEE 26th Int. Symp. Ind. Electron. (ISIE)*, Edinburg, U.K., Jun. 2017, pp. 1977–1982.

[113] E. H. Ismail, M. A. Al-Saffar, A. J. Sabzali, and A. A. Fardoun, "A family of single-switch PWM converters with high step-up conversion ratio," *IEEE Trans. Circuits Syst. I, Reg. Papers*, vol. 55, no. 4, pp. 1159–1171, May 2008.

[114] J. C. Rosas-Caro, J. M. Ramirez, F. Z. Peng, and A. Valderrabano, "A DC-DC multilevel boost converter," *IET Power Electron.*, vol. 3, no. 1, pp. 129–137, Jan. 2010.

[115] A. Farooq, Z. Malik, Z. Sun, and G. Chen, "A review of non-isolated high step-down DC-DC converters," *Int. J. Smart Home*, vol. 9, no. 8, pp. 133–150, Aug. 2015.

[116] W. Liou, M. Yeh, and Y. Kuo, "A high efficiency dual-mode buck converter IC for portable applications," *IEEE Trans. Power Electron.*, vol. 23, no. 2, pp. 667–677, Mar. 2008.

[117] I.-O. Lee, S.-Y. Cho, and G.-W. Moon, "Interleaved buck converter having low switching losses and improved step-down conversion ratio," *IEEE Trans. Power Electron.*, vol. 27, no. 8, pp. 3664–3675, Aug. 2012.

[118] E. Carbajal-Gutierrez, J. Morales-Saldana, and J. Leyva-Ramos, "Modeling of a single-switch quadratic buck converter," *IEEE Trans. Aerosp. Electron. Syst.*, vol. 41, no. 4, pp. 1450–1456, Oct. 2005.

[119] A. Ayachit and M. K. Kazimierczuk, "Steady-state analysis of PWM quadratic buck converter in CCM," in *Proc. IEEE 56th Int. Midwest Symp. Circuits Syst. (MWSCAS)*, Columbus, OH, USA, Aug. 2013, pp. 49–52.

[120] J. A. Morales-Saldana, J. Leyva-Ramos, E. E. Carbajal-Gutierrez, and M. G. Ortiz-Lopez, "Average current-mode control scheme for a quadratic buck converter with a single switch," *IEEE Trans. Power Electron.*, vol. 23, no. 1, pp. 485–490, Jan. 2008.

[121] F. L. de Sa, C. V. B. Eiterer, D. Ruiz-Caballero, and S. A. Mussa, "Double quadratic buck converter," in *Proc. Brazilian Power Electron. Conf.*, Gramado, Brazil, Oct. 2013, pp. 36–43.

[122] S. Birca-Galateanu, "Triple step-down DC-DC converters," in *Proc. 27th Annu. IEEE Power Electron. Spec. Conf.*, Baveno, Italy, Jun. 1996, pp. 408–413.

[123] S. Xiong, S.-C. Tan, and S.-C. Wong, "Analysis and design of a High-Voltage-Gain hybrid switched-capacitor buck converter," *IEEE Trans. Circuits Syst. I, Reg. Papers*, vol. 59, no. 5, pp. 1132–1141, May 2012.

[124] Y. Jiao and F. Luo, "N-switched-capacitor buck converter: Topologies and analysis," *IET Power Electron.*, vol. 4, no. 3, pp. 332–341, Mar. 2011.

[125] N. Muntean, O. Cornea, O. Pelan, and C. Lascu, "Comparative evaluation of buck and hybrid buck DC-DC converters for automotive applications," in *Proc. 15th Int. Power Electron. Motion Control Conf. (EPE/PEMC)*, Novi Sad, Serbia, Sep. 2012, pp. 1–6.

[126] L. Yang, T. Liang, and J. Chen, "Transformerless DC–DC converters with high step-up voltage gain," *IEEE Trans. Ind. Electron.*, vol. 56, no. 8, pp. 3144–3152, Aug. 2009.

[127] M. Prudente, L. Pfitscher, G. Emmendoerfer, E. Romaneli, and R. Gules, "Voltage multiplier cells applied to non-isolated DC–DC converters," *IEEE Trans. Power Electron.*, vol. 23, no. 2, pp. 871–887, Mar. 2008.

[128] A. Tomaszuk and A. Krupa, "High efficiency high step-up DC/DC converters-a review," *Bull. Polish Acad. Sci., Tech. Sci.*, vol. 59, no. 4, pp. 475–483, Jan. 2011.

[129] A. A. Fardoun and E. H. Ismail, "Ultra step-up DC–DC converter with reduced switch stress," *IEEE Trans. Ind. Appl.*, vol. 46, no. 5, pp. 2025–2034, Sep. 2010.

[130] Y. Jiao, F. Luo, and M. Zhu, "Voltage-lift-type switched-inductor cells for enhancing DC–DC boost ability: Principles and integrations in Luo converter," *IET Power Electron.*, vol. 4, no. 1, pp. 131–142, Jan. 2011.

[131] K. K. Law, K. W. E. Cheng, and Y. P. B. Yeung, "Design and analysis of switched-capacitor-based step-up resonant converters," *IEEE Trans. Circuits Syst. I, Reg. Papers*, vol. 52, no. 5, pp. 943–948, May 2005.

[132] S. Xiong, S.-C. Wong, and S.-C. Tan, "A series of exponential step-down switched-capacitor converters and their applications in two-stage converters," in *Proc. IEEE Int. Symp. Circuits Syst. (ISCAS)*, Beijing, China, May 2013, pp. 701–704.

[133] M. S. B. Ranjana, R. M. Kulkarni, K. Anita, and C. Pooja, "Non isolated switched inductor SEPIC converter topologies for photovoltaic boost applications," in *Proc. Int. Conf. Circuit, Power Comput. Technol. (ICCPCT)*, Nagarcoil, India, Mar. 2016, pp. 1–6.

[134] Y. Zhang, C. Zhang, J. Liu, and Y. Cheng, "Comparison of conventional DC-DC converter and a family of diode-assisted DC-DC converter," in *Proc. 7th Int. Power Electron. Motion Control Conf.*, Harbin, China, Jun. 2012, pp. 1718–1723.

[135] Y. Ye and K. W. E. Cheng, "A family of single-stage switched-capacitor–inductor PWM converters," *IEEE Trans. Power Electron.*, vol. 28, no. 11, pp. 5196–5205, Nov. 2013.

[136] Y. Tang, T. Wang, and D. Fu, "Multicell switched-inductor/switched-capacitor combined active-network converters," *IEEE Trans. Power Electron.*, vol. 30, no. 4, pp. 2063–2072, Apr. 2015.

[137] K. W. E. Cheng and Y.-M. Ye, "Duality approach to the study of switched-inductor power converters and its higher-order variations," *IET Power Electron.*, vol. 8, no. 4, pp. 489–496, Apr. 2015.

[138] Y. Tang, D. Fu, T. Wang, and Z. Xu, "Hybrid switched-inductor converters for high step-up conversion," *IEEE Trans. Ind. Electron.*, vol. 62, no. 3, pp. 1480–1490, Mar. 2015.

[139] H. Liu and F. Li, "A novel high step-up converter with a quasi-active switched-inductor structure for renewable energy systems," *IEEE Trans. Power Electron.*, vol. 31, no. 7, pp. 5030–5039, Jul. 2016.

[140] Z. H. Shi, S. L. Ho, and K. W. E. Cheng, "Static performance and parasitic analysis of tapped-inductor converters," *IET Power Electron.*, vol. 7, no. 2, pp. 366–375, Feb. 2014.

[141] B. W. Williams, "Unified synthesis of tapped-inductor DC-to-DC converters," *IEEE Trans. Power Electron.*, vol. 29, no. 10, pp. 5370–5383, Oct. 2014.

[142] D. A. Grant, Y. Darroman, and J. Suter, "Synthesis of tapped-inductor switched-mode converters," *IEEE Trans. Power Electron.*, vol. 22, no. 5, pp. 1964–1969, Sep. 2007.

[143] Q. Zhao and F. C. Lee, "High-efficiency, high step-up DC-DC converters," *IEEE Trans. Power Electron.*, vol. 18, no. 1, pp. 65–73, Jan. 2003.

[144] W. Li and X. He, "Review of nonisolated high-step-up DC/DC converters in photovoltaic grid-connected applications," *IEEE Trans. Ind. Electron.*, vol. 58, no. 4, pp. 1239–1250, Apr. 2011.

[145] R. J. Wai and R. Y. Duan, "High-efficiency DC/DC converter with high voltage gain," *IEE Proc.-Electr. Power Appl.*, vol. 152, no. 4, pp. 793–802, Jul. 2005.

[146] W. Yu, C. Hutchens, J.-S. Lai, J. Zhang, G. Lisi, A. Djabbari, G. Smith, and T. Hegarty, "High efficiency converter with charge pump and coupled inductor for wide input photovoltaic AC module applications," in *Proc. IEEE Energy Convers. Congr. Expo.*, San Jose, CA, USA, Sep. 2009, pp. 3895–3900.

[147] T. J. Liang and K. C. Tseng, "Analysis of integrated boost-flyback step-up converter," *IEE Proc.-Electr. Power Appl.*, vol. 152, no. 2, pp. 217–225, Mar. 2005.

[148] K.-B. Park, G.-W. Moon, and M.-J. Youn, "High step-up boost converter integrated with a transformer-assisted auxiliary circuit employing quasi-resonant operation," *IEEE Trans. Power Electron.*, vol. 27, no. 4, pp. 1974–1984, Apr. 2012.

[149] N. Zhang, D. Sutanto, D. Qiu, K. M. Muttaqi, and B. Zhang, "High-voltage-gain quadratic boost converter with voltage multiplier," *IET Power Electron.*, vol. 8, no. 12, pp. 2511–2519, Dec. 2015.

[150] K. Yao, M. Ye, M. Xu, and F. Lee, "Tapped-inductor buck converter for high-step-down DC-DC conversion," *IEEE Trans. Power Electron.*, vol. 20, no. 4, pp. 775–780, Jul. 2005.

[151] Y.-P. Hsieh, J.-F. Chen, T.-J. Liang, and L.-S. Yang, "Novel high step-up DC–DC converter for distributed generation system," *IEEE Trans. Ind. Electron.*, vol. 60, no. 4, pp. 1473–1482, Apr. 2013.

[152] S. Chen, T. Liang, L. Yang, and J. Chen, "A cascaded high step-up DC–DC converter with single switch for microsource applications," *IEEE Trans. Power Electron.*, vol. 26, no. 4, pp. 1146–1153, Apr. 2011.

[153] Y. P. Siwakoti, F. Blaabjerg, P. C. Loh, and G. E. Town, "High-voltage boost quasi-Z-source isolated DC/DC converter," *IET Power Electron.*, vol. 7, no. 9, pp. 2387–2395, Sep. 2014.

[154] Y. P. Siwakoti, F. Blaabjerg, and P. Chiang Loh, "Quasi-Y-Source boost DC–DC converter," *IEEE Trans. Power Electron.*, vol. 30, no. 12, pp. 6514–6519, Dec. 2015.

[155] Y. P. Siwakoti, P. Chiang Loh, F. Blaabjerg, and G. E. Town, "Y-source impedance network," *IEEE Trans. Power Electron.*, vol. 29, no. 7, pp. 3250–3254, Jul. 2014.

[156] Y. P. Siwakoti, F. Blaabjerg, P. C. Loh, and G. E. Town, "Magnetically coupled high-gain Y-source isolated DC/DC converter," *IET Power Electron.*, vol. 7, no. 11, pp. 2817–2824, Nov. 2014.

[157] J.-J. Chen, B.-H. Hwang, C.-M. Kung, W.-Y. Tai, and Y.-S. Hwang, "A new single-inductor quadratic buck converter using average-current-mode control without slope-compensation," in *Proc. 5th IEEE Conf. Ind. Electron. Appl.*, Taichung, Taiwan, Jun. 2010, pp. 1082–1087.

[158] N. Kondrath and M. Kazimierczuk, "Analysis and design of common-diode tapped-inductor PWM buck converter in CCM," in *Proc. Conf. Elect. Manuf. Coil Winding Conf.*, Nashville, TN, USA, Sep. 2009, pp. 29–30.

[159] X. Guo, C. Huang, Y. Xu, and W. Lin, "The nonlinear control of tapped inductor buck converter based on port-controlled Hamiltonian model," in *Proc. IEEE 33rd Int. Telecommun. Energy Conf. (INTELEC)*, Amsterdam, The Netherlands, Oct. 2011, pp. 1–8.

[160] K. Nishijima, K. Abe, D. Ishida, T. Nakano, T. Nabeshima, T. Sato, and K. Harada, "A novel tapped-inductor buck converter for divided power distribution system," in *Proc. 37th IEEE Power Electron. Spec. Conf.*, Jeju, South Korea, Jun. 2006, pp. 1–6.

[161] D. Wang, X. He, and R. Zhao, "ZVT interleaved boost converters with built-in voltage doubler and current auto-balance characteristic," *IEEE Trans. Power Electron.*, vol. 23, no. 6, pp. 2847–2854, Nov. 2008.

[162] W. Li, Y. Zhao, Y. Deng, and X. He, "Interleaved converter with voltage multiplier cell for high step-up and high-efficiency conversion," *IEEE Trans. Power Electron.*, vol. 25, no. 9, pp. 2397–2408, Sep. 2010.

[163] W. Li, W. Li, M. Ma, Y. Deng, and X. He, "A non-isolated high step-up converter with built-in transformer derived from its isolated counterpart," in *Proc. 36th Annu. Conf. IEEE Ind. Electron. Soc. (IECON)*, Glendale, AZ, USA, Nov. 2010, pp. 3173–3178.

[164] W. Li and X. He, "An interleaved winding-coupled boost converter with passive lossless clamp circuits," *IEEE Trans. Power Electron.*, vol. 22, no. 4, pp. 1499–1507, Jul. 2007.

[165] L. Weichen, L. Chushan, L. Wuhua, and H. Xiangning, "Interleaved high step-up ZVT converter with built-in transformer voltage doubler cell for distributed PV generation system," *IEEE Trans. Power Electron.*, vol. 28, no. 1, pp. 300–313, Jan. 2013.

[166] Y. Berkovich and B. Axelrod, "Steep conversion ratio buck converter based on a switched coupled-inductor cell," in *Proc. SPEEDAM*, Pisa, Italy, Jun. 2010, pp. 1094–1098.

[167] S. Tseng and C. Hsu, "Interleaved step-up converter with a single-capacitor snubber for PV energy conversion applications," *Int. J. Elect. Power Energy Syst.*, vol. 53, pp. 909–922, Dec. 2013.

[168] O. Pelan, N. Muntean, O. Cornea, and F. Blaabjerg, "High voltage conversion ratio, switched C & L cells, step-down DC-DC converter," in *Proc. IEEE Energy Convers. Congr. Expo.*, Denver, CO, USA, Sep. 2013, pp. 5580–5585.

[169] S. Ario Wibowo, Z. Ting, M. Kono, T. Taura, Y. Kobori, and H. Kobayashi, "Analysis of coupled inductors for low-ripple fast-response buck converter," in *Proc. IEEE Asia Pacific Conf. Circuits Syst. (APCCAS)*, Macao, China, Nov. 2008, pp. 1860–1863.

[170] G. Zhu, B. A. McDonald, and K. Wang, "Modeling and analysis of coupled inductors in power converters," *IEEE Trans. Power Electron.*, vol. 26, no. 5, pp. 1355–1363, May 2011.

[171] A. Ikriannikov and T. Schmid, "Magnetically coupled buck converters," in *Proc. IEEE Energy Convers. Congr. Expo.*, Denver, CO, USA, Sep. 2013, pp. 4948–4954.

[172] L. F. Costa, S. A. Mussa, and I. Barbi, "Multilevel buck DC-DC converter for high voltage application," in *Proc. 10th IEEE/IAS Int. Conf. Ind. Appl.*, Fortaleza, Brazil, Nov. 2012, pp. 1–8.

[173] J. Paulo Robles Balestero, F. Lessa Tofoli, G. Victor Torrico-Bascopé, and F. José Mendes de Seixas, "A DC–DC converter based on the three-state switching cell for high current and voltage step-down applications," *IEEE Trans. Power Electron.*, vol. 28, no. 1, pp. 398–407, Jan. 2013.

[174] F. Luo and H. Ye, *Advanced DC-DC Converters*, 2nd ed. Boca Raton, FL, USA: CRC Press, Dec. 2016.

[175] F. Luo, H. Ye, and M. H. Rashid, "DC/DC conversion techniques and nine series Luo-converters," in *Power electronics handbook Devices, Circuits and Applications*. Amsterdam, The Netherlands: Elsevier, 2011.

[176] F. L. Luo, "Re-lift converter: Design, test, simulation and stability analysis," *IEE Proc.-Electr. Power Appl.*, vol. 145, no. 4, pp. 315–325, Jul. 1998.

[177] F. L. Luo, "Negative output Luo-Converters: Voltage lift technique," *IEE Proc. Electr. Power Appl.*, vol. 146, no. 2, pp. 208–224, Mar. 1999.

[178] F. Lin Luo, "Six self-lift DC-DC converters, voltage lift technique," *IEEE Trans. Ind. Electron.*, vol. 48, no. 6, pp. 1268–1272, Dec. 2001.

[179] M. S. Bhaskar, R. Al-Ammari, M. Meraj, A. Iqbal, and S. Padmanaban, "Modified multilevel buck–boost converter with equal voltage across each capacitor: Analysis and experimental investigations," *IET Power Electron.*, vol. 12, no. 13, pp. 3318–3330, Jun. 2019.

[180] L. Müller and J. W. Kimball, "High gain DC–DC converter based on the Cockcroft–Walton multiplier," *IEEE Trans. Power Electron.*, vol. 31, no. 9, pp. 6405–6415, Sep. 2016.

[181] A. Iqbal, M. Sagar Bhaskar, M. Meraj, and S. Padmanaban, "DC-transformer modelling, analysis and comparison of the experimental investigation of a non-inverting and non-isolated nx multilevel boost converter (Nx MBC) for low to high DC voltage applications," *IEEE Access*, vol. 6, pp. 70935–70951, 2018.

[182] W. Bin and K. Smedley, "A family of two-switch boosting switched-capacitor converters," *IEEE Trans. Power Electron.*, vol. 30, no. 10, pp. 5413–5424, Oct. 2015.

[183] Y. J. A. Alcazar, D. de Souza Oliveira, F. L. Tofoli, and R. P. Torrico-Bascope, "DC–DC nonisolated boost converter based on the three-state switching cell and voltage multiplier cells," *IEEE Trans. Ind. Electron.*, vol. 60, no. 10, pp. 4438–4449, Oct. 2013.

[184] J. Rosas-Caro, J. Mayo-Maldonado, R. Cabrera, A. Rodriguez, S. Nacu, and R. Castillo-Ibarra, "A family of DC-DC multiplier converters," *Advance*, to be published. [Online]. Available: http://www.engineeringletters.com/issues_v19/issue_1/EL_19_1_10.pdf

[185] M. S. B. Ranjana, N. SreeramulaReddy, and R. K. P. Kumar, "A novel non-isolated switched inductor floating output DC-DC multi-level boost converter for fuelcell applications," in *Proc. IEEE Students' Conf. Electr., Electron. Comput. Sci.*, Bhopal, India, Mar. 2014, pp. 1–5.

[186] M. S. B. Ranjana, N. S. Reddy, and R. K. P. Kumar, "A novel high gain floating output DC-DC multilevel boost converter for fuelcell applications," in *Proc. Int. Conf. Circuits, Power Comput. Technol. (ICCPCT)*, Nagarcoil, India, Mar. 2014, pp. 291–295.

[187] M. Sagar Bhaskar Ranjana, N. SreeramulaReddy, and R. Kusala Pavan Kumar, "A novel sepic based dual output DC-DC converter for solar applications," in *Proc. Power Energy Syst., Towards Sustain. Energy*, Bangalore, India, Mar. 2014, pp. 1–5.

[188] P. K. Maroti, M. S. B. Ranjana, and D. K. Prabhakar, "A novel high gain switched inductor multilevel buck-boost DC-DC converter for solar applications," in *Proc. IEEE 2nd Int. Conf. Electr. Energy Syst. (ICEES)*, Chennai, India, Jan. 2014, pp. 152–156.

[189] C. A. Villarreal-Hernandez, J. C. Mayo-Maldonado, J. E. Valdez-Resendiz, and J. C. Rosas-Caro, "Modeling and control of an interleaved DC-DC multilevel boost converter," in *Proc. IEEE 18th Workshop Control Modeling Power Electron. (COMPEL)*, Stanford, CA, USA, Jul. 2017, pp. 1–6.

[190] J. C. Rosas-Caro, J. Mayo-Maldonado, J. Valdez, R. Salas-Cabrera, A. Rodriguez, E. Salas-Cabrera, H. Cisneros-Villegas, and J. Gonzalez-Hernandez, "Multiplier SEPIC converter," in *Proc. 21st Int. Conf. Elect. Commun. Comput.*, Cholula, Mexico, Feb./Mar. 2011, pp. 233–238.

[191] S. B. Mahajan, P. Sanjeevikumar, O. Ojo, M. Rivera, and R. M. Kulkarni, "Non-isolated and inverting nx multilevel boost converter for photovoltaic DC link applications," in *Proc. IEEE Int. Conf. Automatica (ICA-ACCA)*, Curico, Chile, Oct. 2016, pp. 1–8.

[192] M. Mousa, M. Ahmed, and M. Orabi, "A switched inductor multilevel boost converter," in *Proc. IEEE Int. Conf. Power Energy*, Kuala Lumpur, Malaysia, Nov. 2010, pp. 819–823.

[193] M. S. Bhaskar, S. Padmanaban, F. Blaabjerg, O. Ojo, S. Seshagiri, and R. Kulkarni, "Inverting Nx and 2Nx non-isolated multilevel boost converter for renewable energy applications," in *Proc. 4th IET Clean Energy Technol. Conf. (CEAT)*, Kuala Lumpur, Malaysia, Nov. 2016, pp. 1–8.

[194] M. S. Bhaskar, R. M. Kulkarni, S. Padmanaban, P. Siano, and F. Blaabjerg, "Hybrid non-isolated and non inverting nx interleaved DC-DC multilevel boost converter for renewable energy applications," in *Proc. IEEE 16th Int. Conf. Environ. Electr. Eng. (EEEIC)*, Florence, Italy, Jun. 2016, pp. 1–6.

[195] M. S. Bhaskar, P. Sanjeevikumar, F. Blaabjerg, V. Fedák, M. Cernat, and R. M. Kulkarni, "Non isolated and non-invertingCockcroft-Walton multiplier based hybrid 2Nx interleaved boost converterfor renewable energy applications," in *Proc. IEEE Int. Power Electron. Motion Control Conf. (PEMC)*, Varna, Bulgaria, Sep. 2016, pp. 146–151.

[196] M. S. Bhaskar, S. Padmanaban, F. Blaabjerg, L. E. Norum, and A. H. Ertas, "4Nx non-isolated and non-inverting hybrid interleaved multilevel boost converter based on VLSIm cell and cockcroft walton voltage multiplier for renewable energy applications," in *Proc. IEEE Int. Conf. Power Electron., Drives Energy Syst. (PEDES)*, Trivandrum, India, Dec. 2016, pp. 1–6.

[197] S. B. Mahajan, P. Sanjeevikumar, P. Wheeler, F. Blaabjerg, M. Rivera, and R. Kulkarni, "X-Y converter family: A new breed of buck boost converter for high step-up renewable energy applications," in *Proc. IEEE Int. Conf. Automatica (ICA-ACCA)*, Curico, Chile, Oct. 2016, pp. 1–8.

[198] M. S. Bhaskar, S. Padmanaban, R. Kulkarni, F. Blaabjerg, S. Seshagiri, and A. Hajizadeh, "Novel LY converter topologies for high gain transfer ratio-a new breed of XY family," in *Proc. 4th IET Clean Energy Technol. Conf. (CEAT)*, Kuala Lumpur, Malaysia, Nov. 2016, pp. 1–8.

[199] M. S. Bhaskar, S. Padmanaban, A. Iqbal, M. Meraj, A. Howeldar, and J. Kamuruzzaman, "L-L converter for fuel cell vehicular power train applications: Hardware implementation of primary member of X-Y converter family," in *Proc. IEEE Int. Conf. Power Electron., Drives Energy Syst. (PEDES)*, Chennai, India, Dec. 2018, pp. 1–6.

[200] M. S. Bhaskar, P. Sanjeevikumar, J. B. Holm-Nielsen, J. K. Pedersen, and Z. Leonowicz, "2L-2L converter: Switched inductor based high voltage step-up converter for fuel cell vehicular applications," in *Proc. IEEE Int. Conf. Environ. Electr. Eng. IEEE Ind. Commercial Power Syst. Eur. (EEEIC/I&CPS Europe)*, Genova, Italy, Jun. 2019, pp. 1–6.

[201] P. K. Maroti, S. Padmanaban, M. S. Bhaskar, F. Blaabjerg, V. K. Ramachandaramurthy, P. Siano, and V. Fedak, "A novel 2L-Y DC-DC converter topologies for high conversion ratio renewable application," in *Proc. IEEE Conf. Energy Convers. (CENCON)*, Kuala Lumpur, Malaysia, Oct. 2017, pp. 323–328.

[202] M. S. Bhaskar, S. Padmanaban, P. K. Maroti, V. Fedak, F. Blaabjerg, and V. K. Ramachandaramurthy, "New 2LC-Y DC-DC converter topologies for high-voltage/low-current renewable applications: New members of X-Y converter family," in *Proc. 19th Int. Conf. Electr. Drives Power Electron. (EDPE)*, Dubrovnik, Croatia, Oct. 2017, pp. 139–146.

[203] M. S. Bhaskar, S. Padmanaban, P. Wheeler, F. Blaabjerg, and P. Siano, "A new voltage doubler based DC-DC 2LC$_m$-Y power converter topologies for high-voltage/low-current renewable energy applications," in *Proc. IEEE Transp. Electrific. Conf. Expo (ITEC)*, Long Beach, CA, USA, Jun. 2018, pp. 1–6.

[204] M. S. Bhaskar, S. Padmanaban, V. Fedak, F. Blaabjerg, P. W. Wheeler, and V. K. Ramachandaramurthy, "L-L multilevel boost converter topology for renewable energy applications: A new series voltage multiplier L-L converter of XY family," in *Proc. 19th Int. Conf. Electr. Drives Power Electron. (EDPE)*, Dubrovnik, Croatia, Oct. 2017, pp. 133–138.

[205] M. S. Bhaskar, P. Sanjeevikumar, F. Blaabjerg, J. B. Holm-Nielsen, and D. M. Ionel, "L-L and L-2L multilevel boost converter topologies with voltage multiplier with L-L and L-2L converter of XY familiy," in *Proc. IEEE 59th Int. Sci. Conf. Power Electr. Eng. Riga Tech. Univ. (RTUCON)*, Riga, Latvia, Nov. 2018, pp. 1–6.

[206] M. S. Bhaskar, M. Meraj, A. Iqbal, R. Al-ammari, and S. Padmanaban, "New DC-DC multilevel configurations of 2L-Y boost converters with high voltage conversion ratio for renewable energy applications," in *Proc. IEEE 28th Int. Symp. Ind. Electron. (ISIE)*, Vancouver, BC, Canada, Jun. 2019, pp. 2527–2532.

[207] S. Sadaf, N. A. Al-Emadi, A. Iqbal, M. S. Bhaskar, and M. Meraj, "New high gain 2LC-Y Multilevel-Boost-Converter (2LC-Y MBC) topologies for renewable energy conversion: Members of X-Y converter family," in *Proc. IEEE 28th Int. Symp. Ind. Electron. (ISIE)*, Vancouver, BC, Canada, Jun. 2019, pp. 2647–2652.

[208] S. Padmanaban, M. S. Bhaskar, F. Blaabjerg, and Y. Yang, "A new DC-DC multilevel breed of XY converter family for renewable energy applications: LY multilevel structured boost converter," in *Proc. 44th Annu. Conf. IEEE Ind. Electron. Soc. (IECON)*, Washington, DC, USA, Oct. 2018, pp. 6110–6115.

[209] M. S. Bhaskar, P. Sanjeevikumar, J. K. Pedersen, J. Bo Holm-Nielsen, and Z. Leonowicz, "XL Converters- new series of high gain DC-DC converters for renewable energy conversion," in *Proc. IEEE Int. Conf. Environ. Electr. Eng. IEEE Ind. Commercial Power Syst. Eur. (EEEIC/I&CPS Europe)*, Genova, Italy, Jun. 2019, pp. 1–6.

[210] M. S. Bhaskar, L. Ben-Brahim, A. Iqbal, S. Padmanaban, M. Meraj, and S. Rahman, "Hardware implementation of a new single input double output L-L converter for high voltage auxiliary loads in fuel-cell vehicles," in *Proc. IEEE Appl. Power Electron. Conf. Expo. (APEC)*, Long Beach, CA, USA, Mar. 2019, pp. 1595–1600.

[211] M. S. Bhaskar, S. Padmanaban, and J. B. Holm-Nielsen, "Double stage double output DC–DC converters for high voltage loads in fuel cell vehicles," *Energies*, vol. 12, no. 19, p. 3681, Jan. 2019.

[212] K. M. Tan, V. K. Ramachandaramurthy, and J. Y. Yong, "Three-phase bidirectional electric vehicle charger for vehicle to grid operation and grid voltage regulation," in *Proc. IEEE Transp. Electrific. Conf. Expo, Asia–Pacific (ITEC Asia–Pacific)*, Busan, South Korea, Jun. 2016, pp. 7–12.

[213] J. Y. Yong, V. K. Ramachandaramurthy, K. M. Tan, and J. Selvaraj, "Experimental validation of a three-phase off-board electric vehicle charger with new power grid voltage control," *IEEE Trans. Smart Grid*, vol. 9, no. 4, pp. 2703–2713, Jul. 2018.

MAHAJAN SAGAR BHASKAR (Senior Member, IEEE) received the bachelor's degree in electronics and telecommunication engineering from the University of Mumbai, Mumbai, India, in 2011, the master's degree in power electronics and drives from VIT University, India, in 2014, and the Ph.D. degree in electrical and electronic engineering from the University of Johannesburg, South Africa, in 2019. He is currently with the Renewable Energy Laboratory, Department of Communications and Networks Engineering, College of Engineering, Prince Sultan University, Riyadh, Saudi Arabia. He has published scientific papers in the field of power electronics, with the particular reference to XY converter family, multilevel DC/DC and DC/AC converter, and high gain converter. He has authored over 100 scientific papers and has received the Best Paper Research Paper Awards from the IEEE-CENCON'19, IEEE-ICCPCT'14, IET-CEAT'16, and ETAEERE'16 sponsored *Lecture Notes in Electrical Engineering* (Springer). He is a Senior Member of the IEEE Industrial Electronics; Power Electronics; Industrial Application; and Power and Energy, Robotics and Automation; Vehicular Technology Societies; Young Professionals; as well as various IEEE Councils and Technical Communities. He is a reviewer member of various international journals and conferences, including the IEEE and IET. He received the IEEE Access award "Reviewer of Month" in January 2019, for his valuable and thorough feedback on manuscripts, and for his quick turnaround on reviews.

VIGNA K. RAMACHANDARAMURTHY (Senior Member, IEEE) received the bachelor's degree in electrical and electronics engineering from the University of Manchester Institute of Science and Technology (UMIST), U.K., in 1998, under the Malaysian Government scholarship, and the Ph.D. degree in electrical engineering from the Institute of Science and Technology, The University of Manchester, U.K., in 2001. He is currently a Professor with the Institute of Power Engineering, Universiti Tenaga Nasional, Malaysia. He is also the Principal Consultant for Malaysia's most prominent electrical utility, Tenaga Nasional Berhad, and has completed over 250 projects in renewable energy. He has also developed several technical guidelines for distributed generation in Malaysia. His areas of interests include power systems-related studies, renewable energy, energy storage; power quality, electric vehicle, and rural electrification. He joined the Malaysian electrical utility, Tenaga Nasional Berhad in 2002, as an Electrical Engineer. In 2005, he moved to Universiti Tenaga Nasional (UNITEN), where he is currently a Professor with the Institute of Power Engineering. He has received many awards for research and leadership. In 2008, he received the "Institution of Engineering and Technology (IET) Mike Sargeant Award" in London. The award is given to a young professional who is judged to have made significant achievements in career over several years globally. In 2009, he received the prestigious Institution of Engineers Malaysia (IEM) Young Engineers Award. He was also a recipient of the Best Researcher Award for few consecutive years in the College of Engineering and UNITEN. He has also won several gold medals at the International Invention Competition. His achievement has led to him being appointed as the Chief Judge at the National Schools Robotics Competition and at the World Young Inventors Exhibition in conjunction with ITEX, a leading invention exhibition in Asia. He is also in the Editorial Board/Associate Editor of the *IET Smart Grid*, IET RPG, IEEE Smart Grid, and IEEE Access. He is also a Chartered Engineer registered with the Engineering Council of U.K., and a Professional Engineer registered with the Board of Engineers, Malaysia.

SANJEEVIKUMAR PADMANABAN (Senior Member, IEEE) received the bachelor's degree in electrical engineering from the University of Madras, Chennai, India, in 2002, the master's degree (Hons.) in electrical engineering from Pondicherry University, Puducherry, India, in 2006, and the Ph.D. degree in electrical engineering from the University of Bologna, Bologna, Italy, in 2012.

He was an Associate Professor at VIT University from 2012 to 2013. In 2013, he joined the National Institute of Technology, India, as a Faculty Member. In 2014, he was invited as a Visiting Researcher at the Department of Electrical Engineering, Qatar University, Doha, Qatar, funded by the Qatar National Research Foundation (Government of Qatar). He continued his research activities with the Dublin Institute of Technology, Dublin, Ireland, in 2014. Furthermore, he served an Associate Professor with the Department of Electrical and Electronics Engineering, University of Johannesburg, Johannesburg, South Africa, from 2016 to 2018. Since 2018, he has been a Faculty Member with the Department of Energy Technology, Aalborg University, Esbjerg, Denmark. He has authored more than 300 scientific papers. He was a recipient of the Best Paper cum Most Excellence Research Paper Award from IET-SEISCON'13, IET-CEAT'16, IEEE-EECSI'19, IEEE-CENCON'19, and five best paper awards from ETAEERE'16 sponsored Lecture Notes in Electrical Engineering (Springer). He is a Fellow of the Institution of Engineers, India; the Institution of Electronics and Telecommunication Engineers, India; and the Institution of Engineering and Technology, U.K. He is an Editor/Associate Editor/Editorial Board for refereed journals, in particular the IEEE SYSTEMS JOURNAL, IEEE TRANSACTION ON INDUSTRY APPLICATIONS, IEEE ACCESS, *IET Power Electronics*, *IET Electronics Letters*, and *International Transactions on Electrical Energy Systems* (Wiley), Subject Editorial Board Member of *Energy Sources – Energies Journal*, MDPI, and the Subject Editor for the *IET Renewable Power Generation*, *IET Generation, Transmission and Distribution*, and *FACTS* journal (Canada).

FREDE BLAABJERG (Fellow, IEEE) received the Ph.D. degree in electrical engineering from Aalborg University, in 1995.

He was with ABB-Scandia, Randers, Denmark, from 1987 to 1988. He became an Assistant Professor in 1992, an Associate Professor in 1996, and a Full Professor of power electronics and drives in 1998. Since 2017, he has been a Villum Investigator. He is an honoris causa at the University Politehnica Timisoara (UPT), Romania, and also at Tallinn Technical University (TTU), Estonia. His current research interests include power electronics and its applications such as in wind turbines, PV systems, reliability, harmonics, and adjustable speed drives. He has published more than 600 journal papers in the fields of power electronics and its applications. He is the coauthor of four monographs and an editor of ten books in power electronics and its applications.

Dr. Blaabjerg has received 32 IEEE Prize Paper Awards, the IEEE PELS Distinguished Service Award in 2009, the EPE-PEMC Council Award in 2010, the IEEE William E. Newell Power Electronics Award 2014, the Villum Kann Rasmussen Research Award 2014, the Global Energy Prize in 2019, and the 2020 IEEE Edison Medal. He has been a Distinguished Lecturer of the IEEE Power Electronics Society (2005–2007) and the IEEE Industry Applications Society (2010–2011) as well as (2017–2018). From 2019 to 2020, he had served as the President of the IEEE Power Electronics Society. Moreover, he is the Vice-President of the Danish Academy of Technical Sciences. He is nominated by Thomson Reuters (2014–2019) as among the 250 most cited researchers in Engineering across the world. In 2017, he became Honoris Causa at UPT. He was the Editor-in-Chief of the IEEE TRANSACTIONS ON POWER ELECTRONICS from 2006 to 2012.
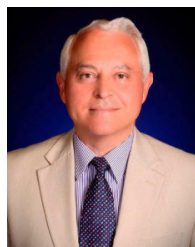
DAN M. IONEL (Fellow, IEEE) received the M.Eng. and Ph.D. degrees in electrical engineering from the Polytechnic University of Bucharest, Bucharest, Romania. His doctoral program included a Leverhulme Visiting Fellowship with the University of Bath, Bath, U.K. He was a Postdoctoral Researcher with the SPEED Laboratory, University of Glasgow, Glasgow, U.K. He worked in the industry, most recently as a Chief Engineer for Regal Beloit Corp., Grafton, WI, USA, and, before that, as the Chief Scientist for Vestas Wind Turbines. Concurrently, he was also a Visiting and Research Professor with the University of Wisconsin and Marquette University, Milwaukee, WI, USA. He is currently a Professor of electrical engineering and the L. Stanley Pigman Chair in Power with the University of Kentucky, Lexington, KY, USA, where he is also the Director of the Power and Energy Institute of Kentucky and of the SPARK Laboratory. He has authored and coauthored more than 30 patents, two books, and more than 200 technical papers, including five that received IEEE awards. He has contributed to technology developments with long-lasting industrial impact. He was the Inaugural Chair of the IEEE Industry Applications Society Renewable and Sustainable Energy Conversion Systems Committee and an Editor for the IEEE TRANSACTIONS ON SUSTAINABLE ENERGY. He is the Editor-in-Chief of the *Electric Power Components and Systems Journal*, the Past Chair of the IEEE Power and Energy Society Electric Motor Subcommittee and of the IEEE WG 1812, and was the General Chair of the IEEE 2017 Anniversary Edition of the International Conference on Electrical Machines and Drives.

MASSIMO MITOLO (Fellow, IEEE) received the Ph.D. degree in electrical engineering from the University of Napoli Federico II, Italy, in 1990. He is currently a Full Professor of Electrical Engineering with Irvine Valley College, Irvine, CA, USA, and a Senior Consultant in Electric Power Engineering with Engineering Systems Inc., ESi. He has authored more than 118 journal articles and books such as *Electrical Safety of Low-Voltage Systems* (McGraw-Hill, 2009) and *Laboratory Manual for Introduction to Electronics: A Basic Approach* (Pearson, 2013). His research interests include the analysis and grounding of power systems and electrical safety engineering. He was a recipient of numerous recognitions and best paper awards, including the IEEE-I&CPS Ralph H. Lee Department Prize Paper Award, the IEEE-I&CPS 2015 Department Achievement Award, and the IEEE Region 6 Outstanding Engineer Award. He is currently the Deputy Editor-in-Chief of the IEEE TRANSACTIONS ON INDUSTRY APPLICATIONS. He is active within the Industrial and Commercial Power Systems Department of the IEEE Industry Applications Society (IAS) in numerous committees and working groups. He also serves as an Associate Editor for the IEEE IAS TRANSACTIONS. He is a registered Professional Engineer in the State of California and in Italy.

DHAFER ALMAKHLES (Senior Member, IEEE) received the B.E. degree in electrical engineering from the King Fahd University of Petroleum and Minerals, Dhahran, Saudi Arabia, in 2006, and the master's degree (Hons.) and the Ph.D. degree from The University of Auckland, New Zealand, in 2011 and 2016, respectively. Since 2016, he has been with Prince Sultan University, Saudi Arabia, where he is currently the Chairman of the Communications and Networks Engineering Department and the Director of the Science and Technology Unit. He is the Leader for Renewable Energy Laboratory, Prince Sultan University. He has authored many published articles in the area of control systems. He served as a reviewer for many journals, including the IEEE TRANSACTIONS ON FUZZY SYSTEMS, *Control of Network Systems*, *Industrial Electronics*, *Control Systems Technology*, the IEEE CONTROL SYSTEMS LETTERS, and *International Journal of Control*.

● ● ●